AD _____

TWENTY-EIGHTH QUARTERLY REPORT

to Sponsors of

The Institute for the Study of Metals

THE UNIVERSITY OF CHICAGO

FOR PRIVATE CIRCULATION ONLY

MARCH 1953

TWENTY-EIGHTH QUARTERLY REPORT

to *Sponsors* of

The Institute for the Study of Metals

THE UNIVERSITY OF CHICAGO

FOR PRIVATE CIRCULATION ONLY

MARCH 1953

* * *

Acknowledgment is made to the following organizations for their sponsorship of the Institute for the Study of Metals as a whole:

Aluminum Company of America
Aluminium Laboratories, Ltd.
American Can Company
Bethlehem Steel Company
Copper and Brass Research Association
Crane Company
E. I. DuPont de Nemours and Company
General Electric Company
General Motors Corporation
Inland Steel Company
International Harvester Company
Motorola, Inc.
Pittsburgh Plate Glass Company
Standard Oil Company (Indiana)
Standard Oil Development Company of New Jersey
Union Carbide and Carbon Corporation
United States Steel Corporation
Westinghouse Electric Corporation

Acknowledgment is also made to the following:

The U. S. Office of Naval Research for sponsorship of a program on the deformation of metals [Contract No. N-6ori-IV, NR 019 302 and War Department Contract No. TB4-2] and on high pressure research [Contract No. N-6ori-20-XX];

The U. S. Air Research and Development Command for their support of our metal surface reaction research [Contract No. AF33(038)-6534] and of our boron in steel program [Contract No. AF18(600)-12];

The U. S. Atomic Energy Commission for their support of research on graphite [Contract No. AT(1101)-96];

The U. S. Army Ordnance Department for their support of research on grain boundaries [Contract No. DA-11-022-ORD-834].

CONTENTS

I

SUPERCONDUCTING SILICIDES AND GERMANIDES

George F. Hardy and John K. Hulm
Submitted to Physical Review

While investigating the occurrence of superconductivity among the silicides and germanides of Group IV, V, and VI transition metals, we have recently observed that the compound V_3Si becomes superconducting at about 17°K, apparently the highest temperature at which the phenomenon has so far been observed.* This compound and twenty-nine other silicides and germanides were prepared by sintering compressed pellets consisting of appropriate mixtures of the powdered elements for several hours in an atmosphere of purified helium at 1500°C (silicides) or 1000°C (germanides). Additional specimens which were prepared by melting the compressed pellets in an argon arc furnace gave essentially the same X-ray and superconducting results as those prepared by sintering. The presence of superconductivity was detected by ballistic measurement of the magnetic induction of the specimens in a magnetic field of a few oersteds; the transition temperatures quoted are those for the mid-point of the transition extrapolated to zero field.

The following compounds became superconducting at the temperatures given in parenthesis: V_3Si (17.0°K), V_3Ge (6.0°K), Mo_3Si (1.30°K), Mo_3Ge (1.43°K), $MoSi_{0.7}$ (1.34°K), $MoGe_{0.7}$ (1.20°K), $WSi_{0.7}$ (2.84°K), $ThSi_2$ (3.16°K). On the other hand, compounds which did not show superconductivity at temperatures just below 1.2°K were: Ti_5Si_3, Ti_5Ge_3, TiSi, $TiSi_2$, $TiGe_2$, Zr_4Si, Zr_2Si, Zr_3Si_2, Zr_4Si_3, Zr_6Si_5, ZrSi, $ZrSi_2$, VSi_2, $NbSi_{0.6}$, $NbSi_2$, $TaSi_2$, Cr_3Si, Cr_3Si_2, CrSi, $CrSi_2$, WSi_2, $MoSi_2$. It will be noted that in the isomorphous series V_3Si, V_3Ge, Mo_3Si, Mo_3Ge, and Cr_3Si, which have a cubic structure with atomic positions similar to those in β tungsten, only the chromium compound remained normal down to 1.2°K.

The transition temperature and breadth of transition of V_3Si were found to be rather sensitive to variations in impurity content of the specimens. The purest samples were prepared from vanadium supplied by The Electro Metallurgical Company in which the main impurities were about 0.1% of iron and manganese. In these samples the transition temperatures ranged from about 16.5° to 17°K, the sharpest transition being that of an arc furnace specimen which passed from a completely normal to a completely superconducting state between 17.1° and 16.8°K. On the other hand, both sintered and arc furnace specimens of V_3Si prepared from vanadium containing about 1% of

* Although Aschermann, Friederich, Justi, and Kramer, Physik. Z. 42, 349 (1941) reported superconductivity in niobium nitride at temperatures above 17°K, the more recent work of Horn, F. H., and Ziegler, W. T., J. Am. Chem. Soc. 69, 2762 (1947) and Rögener, H., Z. Physik 132, 446 (1952) indicates that the transition point for this compound is approximately 15°K.

iron as its major impurity showed superconducting transitions close to 14.5°K with breadths of more than 1°K. This appreciable drop in transition temperature in the presence of 1% Fe suggests that even for our purest samples, containing about 0.1% Fe, the transition temperatures probably lie a few tenths of a degree below the correct value for spectroscopically pure V_3Si.

Finally, in an effort to produce superconductivity above 17°K, we replaced a portion of the vanadium or silicon in V_3Si by neighboring elements in the periodic system. The effect of replacing one-tenth of the vanadium by either Ti, Zr, Nb, Mo, Cr, or Ru, or one-tenth of the silicon by either B, C, Al, or Ge was to depress the transition temperature by amounts ranging from a few tenths to more than ten degrees below that of control specimens of pure V_3Si. Carbon and boron produced the smallest effect, but it must be remarked that although the whole series of specimens was prepared by arc furnace melting, completely homogeneous solid solutions were not formed in all cases.

A detailed account of this work will be published later.

II

A THERMODYNAMIC STUDY OF THE EQUILIBRIUM

$2\ Cu(s) + H_2S(g) = Cu_2S\ (\gamma) + H_2(g)$

Alfred A. Brooks*
Submitted to Journal of Physical Chemistry

Abstract

The equilibrium $2\ Cu(s) + H_2S(g) = Cu_2S(\gamma) + H_2(g)$ has been investigated between 342°C and 1037°C by a recirculating technique with particular effort to eliminate the effects of thermal diffusion.

Introduction

Several authors have investigated the equilibrium between copper, hydrogen sulfide, hydrogen and cuprous sulfide. A flow method was used by Jellinek and Zakowski,[1] Britzke and Kapustinsky,[2] and by Sudo[3] to investigate the solid Cu-Cu_2S system. Sano[4] and Cox[5] used a circulating method. Schuhmann and Moles[6] investigated the region of liquid copper sulphides by a flow method. The results are not in particularly good agreement and some of the data[5] show bad scattering. The flow method has the disadvantages that at low flow rates the effects of thermal diffusion are not negligible and at high flow rates equilibrium is not well established. The circulation method has the advantage that eventually equilibrium must be reached but has the disadvantage of producing relatively small samples. In addition, with some pump designs the linear flow rate may be so slow that thermal diffusion is an important error. In the present study an attempt was made to eliminate some of these disadvantages.

Experimental

Apparatus

A schematic sketch of the apparatus is shown in Figure 1. Variations in the entrance area and in the pumping rate were sufficient to change the linear velocity of the entrace gas from 67 to 6.7 cm/sec and that of the exit gas from 23 to 11 cm/sec. A differential thermocouple was placed beside the Pt-PtRh measuring thermocouple and in the charge crucible. Changes in pumping rate from 10 cc/sec to 0 cc/sec gave rise to temperature differences which were random and were not greater than 1°C at furnace temperatures between 300°C and 1000°C.

Temperatures were determined by means of a thermocouple constructed of thermocouple-grade platinum and platinum-10% rhodium with an L & N Type K Potentiometer to measure emf's. The thermocouple was calibrated by determining the cooling curves of pure metals (Ag, CuAg, Al, Zn). The errors in temperature measurement are estimated to be less than 1°C.

* Present address: Standard Oil Company of Indiana, Whiting, Ind.

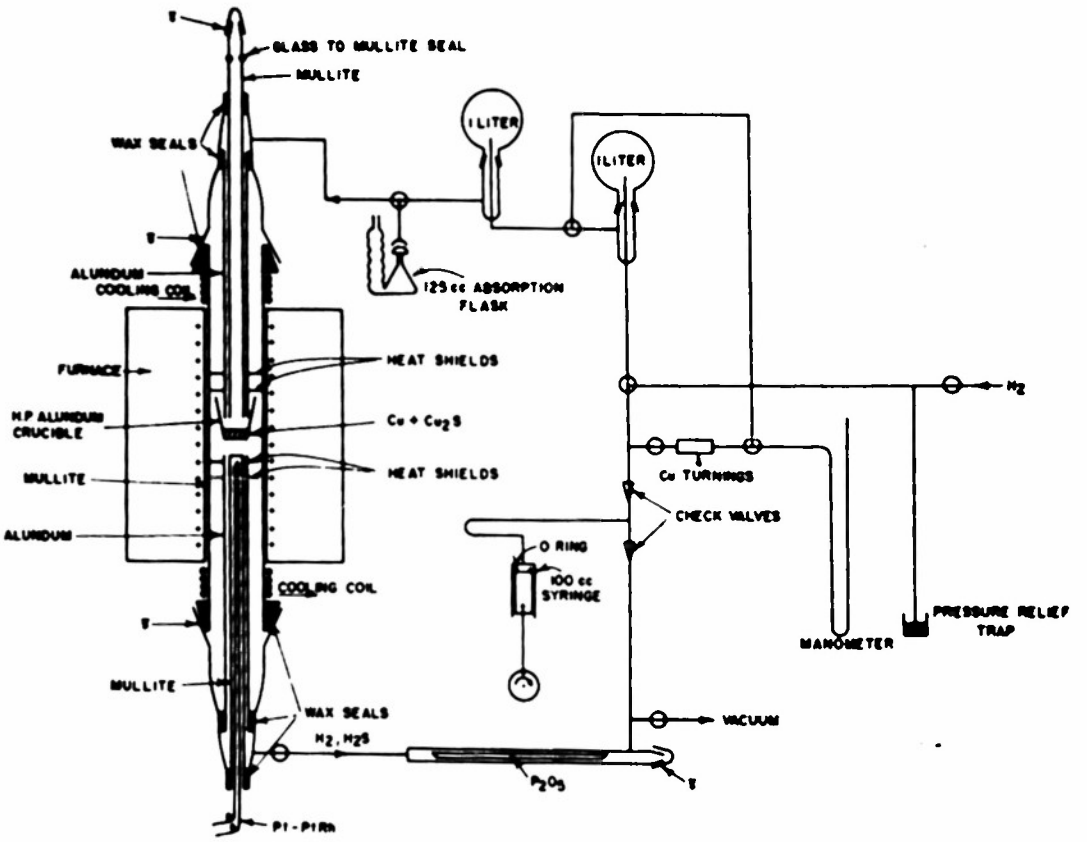

Figure 1. Schematic diagram of apparatus.

Procedure

The crucible was charged with about 30 g of Cu_2S and 30 g of Cu. Purified hydrogen was then admitted to the evacuated and leak-free system until the pressure was slightly over one atmosphere. The circulating pump was then started and the gas circulated from 12 to 120 hours, depending upon the temperature. The gas was kept anhydrous by passage over P_2O_5. The equilibrium conditions were approached from both high and low H_2S/H_2 ratios and when equilibrium was reached the gas sample was flushed from the calibrated sample volume (0.3-2 l) by a stream of pure hydrogen into a KOCl solution.

Chemicals

Cuprous sulfide was prepared by heating redistilled C.P. sulfur and C.P. copper together in an evacuated, sealed quartz tube at 700°C for 20 hours. The hydrogen was purified by passing it over charcoal cooled to the hydrogen triple point. After the runs were completed, the mixture of copper and cuprous sulfide had a total analysis (Cu + S) of 99.85% and showed 0.09% metallic impurities by spectrographic analysis.

Analytical Method

The method of Dunicz and Rosenqvist[7] was used to analyze the gaseous mixture for H_2S. The method was entirely satisfactory when precautions were taken to wash adsorbed H_2S from the walls of the absorbing flask and

gave results reproducible to 0.03 ml of 0.01 N thiosulfate solution. This represents an accuracy of $\pm$ 0.1% to $\pm$ 1% over the entire range of H_2S concentrations.

The measurements of the sample volume, temperature, and pressure allowed the calculation of the H_2S/H_2 ratio.

Results

The results are summarized in Table I, columns 1 and 2. The method of

TABLE 1

Summary of Data

T °C	$[H_2S]/[H_2]$ x 10^4	Σ	T °C	$[H_2S]/[H_2]$ x 10^4	Σ
1037.3	22.16	10.888	572.0	2.881	9.447
1036.0	22.09	10.884	554.4	2.612	9.376
831.1	11.70	10.410	486.0	1.499	9.011
828.4	11.38	10.395	461.2	1.048	8.806
720.4	7.171	10.064	441.8	.910	8.705
664.0	5.291	9.854	404.9	.593	8.442
660.6	5.126	9.835	378.7	.435	8.243
658.2	5.010	9.819	361.7	.349	8.108
636.8	4.609	9.755	342.0	.261	7.933

Randall[8] and the following heat capacity (C_p) equations

$H_2(g)$: $6.9469 - 0.1999 \times 10^{-3} T + 4.808 \times 10^{-7} T^2$ (See Ref. 9)

$H_2S(g)$: $6.864 + 3.852 \times 10^{-3} T + 7.85 \times 10^{-7} T^2 - 6.34 \times 10^{-10} T^3$ (See Ref. 10)

Cu(s): $5.522 + 1.324 \times 10^{-3} T$ (See Ref. 11)

$Cu_2S(\gamma)$: 20.2 (See Ref. 12)

give rise to the expressions:

$$\Delta C_p = \alpha + \beta T + \gamma T^2 + \delta T^3$$

$$\Delta H_o^o/T + I = \epsilon R \Sigma = -R \ln K + \alpha \ln T + \beta T/2 + \gamma T^2/6 + \delta T^3/12 \quad (1)$$

where

$\alpha = 9.239$ $\quad \delta = 6.34 \times 10^{-10}$

$\beta = -6.700 \times 10^{-3}$ $\quad R = 1.9872$ cal/mol

$\gamma = -3.04 \times 10^{-7}$ $\quad \epsilon = \log 10$

The Σ 's calculated from the above are shown in Table I, column 3. All the Σ 's except that at 342°C (which lies below a phase transition[13]) were treated by the method of least squares and yield

$$H_o^o = -15,736 \pm 35\ (.225)\ \text{calories/mol}$$

$$I = 61.854 \pm .046\ (.07\%\ \text{calories/deg. mol}$$

where the errors are given as probable errors.[14] The deviations in Σ show no trend nor any correlation with the flow rate or the direction of approach to equilibrium. Table II shows the thermodynamic values derived from the

TABLE II

Standard Thermodynamic Values

	$2\ Cu + H_2S \quad Cu_2S + H_2$		$2\ Cu + S(r) = CuS(\alpha)$ 298.16°C		
	700 °K	298.16 °K	Present	Sudo[3]	N.B.S.[a]
ΔF^o cal/mol	-13,166	-13,300	-21,198	-21,290	-20,600
ΔH^o cal/mol	-10,907	-15,155	-19,970	-19,940	-19,000
ΔS^o cal/mol - °C	3.23	- 6.22	4.11	4.53	5.37

[a] National Bureau of Standards "Selected Values of Chemical Thermo dynamic Properties," Washington, D. C., 1949.

above constants at 700°K, and, the values corrected to 298.16°K, with the tabular data of Kelly.[13] Combining these values with data of Evans and Wagman[15] for $H_2(g) + S(r) = H_2S(g)$ results in the values given in Table II for $2\ Cu(s) + S(r) = Cu_2S(\alpha)$.

Discussion

The graph of Figure 2 shows the more recent data for the reaction. The data of Schuhmann and Moles and that of Sudo, both taken by the flow technique, appear to be consistent, assuming no great change in slope between 1067°C and 1105°C. The data of Cox, et al, taken by a circulation technique agree with Schuhmann and Moles above 1105°C and about equally well with Sudo and the present work below 1067°C. The present data lie about 10% below that of Sudo. The substitution of Sudo's data into equation 1 yields the following values:

$$\Delta H_o^o = -15,888 \pm 477\ (3.0\%)$$

$$I = 62.174 \pm 0.473\ (.76\%).$$

The corresponding values for the present work lie well within the above probable errors, the difference for ΔH_o^o being less than 1%.

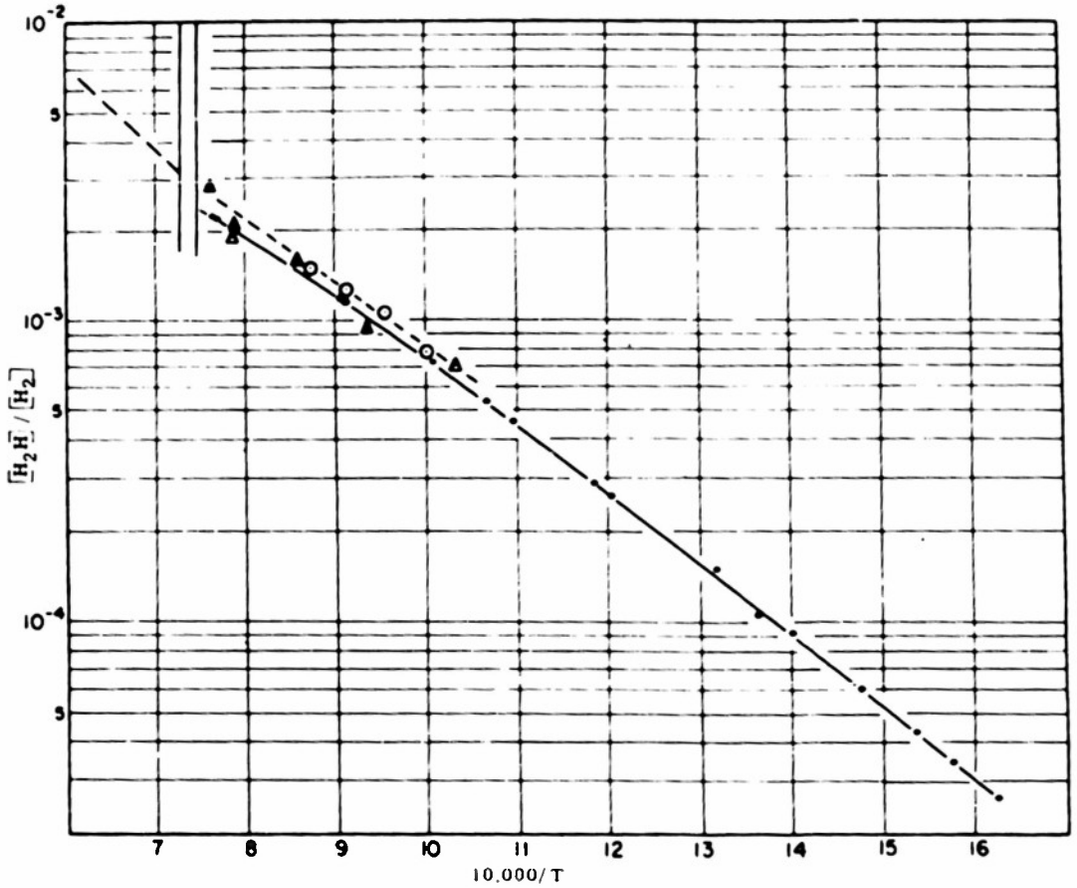

Figure 2. Summary of recent data (Schuhmann and Moles ---, Sudo ⊖--⊖--, Cox, et al, ΔΔ, Present ————).

The data of Sudo extrapolated along the same path as the present data give rise to a heat of formation of Cu_2S at 298.16°K which differs from the present data by .76%. The value given by the Bureau of Standards disagrees with that of Sudo and the present work by about 5 per cent, which is greater than the probable errors.

The author feels that the 10 per cent difference in the equilibrium constants between the present work and that of Sudo is due to the failure of the flow method to give equilibrium values. Emmett and Shultz[16] found that thermal diffusion effects were negligible with hydrogen-water mixtures at flow rates of 10-18 cm/sec; but at .27-.40 cm/sec the errors introduced were between 20-30 per cent. The present method employs flow rates which should eliminate the thermal diffusion effects. The composition of the exit gas of a single-pass flow system will vary in a complicated manner depending upon the flow rate, the rate of thermal diffusion, the rate of reaction, and the design of the reactor bed, and it seems difficult to evaluate the extrapolation of the data to zero flow rate in the absence of specific knowledge of the effects of these variables. In the case of a recirculating system, thermal diffusion is the only interfering effect and this can be simply determined.

The present work does not support the conclusion of Hirahara[17] that a phase transition occurs in Cu_2S at 470°C.

Acknowledgments

The author wishes to acknowledge the many helpful suggestions of Drs. T. Rosenqvist and N. H. Nachtrieb.

References

1. K. Jellinek and J. Zakowski, Z. anorg. allgem. Chem., 142, 1 (1925).
2. E. V. Britzke and A. F. Kapustinsky, Z. anorg. allgem. Chem., 205, 171 (1932).
3. K. Sudo, Sci. Rep. R.I.T.U., A 2, 513 (1950).
4. Sano, Nippon-Kinsoku-Gakkaishi, 3, 718 (1939).
5. E. M. Cox, et al., J. Metals, 1, Trans., 185, 27 (1949).
6. R. Schuhmann and O. W. Moles, J. Metals, 3, Trans., 191, 235 (1951).
7. B. L. Dunicz and T. Rosenqvist, Anal. Chem., 24, 404 (1952).
8. M. Randall, J. Chem. Ed., 8, 1062 (1931).
9. H. M. Spenser and J. L. Justice, J. Am. Chem. Soc., 56, 2311 (1934).
10. H. M. Spenser, J. Am. Chem. Soc., 67, 1859 (1945).
11. J. M. Jaeger, Proc. Acad. Sci. Amsterdam, 35, 772 (1934).
12. W. P. White, J. Am. Chem. Soc., 55, 1047 (1933).
13. K. K. Kelley, Bur. of Mines Bull. #476 (1949).
14. H. Margenau and G. M. Murphy, "The Mathematics of Physics and Chemistry," Van Nostrand, N. Y., 1943, p. 502.
15. W. H. Evans and D. D. Wagman, NBS Report #1037 (1951).
16. P. H. Emmett and J. F. Shultz, J. Am. Chem. Soc., 55, 1376 (1933).
17. E. Hirahara, J. Phys. Soc. (Japan), 6, 422 (1951).

III

THE ADSORPTION OF GASES AT HIGH SATURATIONS: I. THE ADSORPTION OF NITROGEN, ARGON, AND OXYGEN

Raymond Bowers
To be published in the Philosophical Magazine

Abstract

The adsorption of argon, nitrogen, and oxygen on an aluminum foil has been determined by a gravimetric method. The purpose of the investigation was to obtain data at high saturations for comparison with the Frenkel-Halsey-Hill equation describing multilayer adsorption. The isotherms obtained indicate that this equation is obeyed closely for the three gases. Apparent deviations in the case of argon and oxygen can be ascribed to anomalous packing in the first few atomic layers and allowance can be made for this effect. The verification is discussed in terms of the theoretical basis for the equation. Data is also given for the cross-sections of the argon and oxygen molecules in the first atomic layer. It is suggested that these cross sections are considerably greater than values calculated from the corresponding bulk density. The magnitude of the standard nitrogen cross section is also discussed.

Introduction

From a theoretical point of view, there are two regions of an adsorption isotherm which are of particular interest. These regions comprise, firstly, that at very low saturation, where the first few atomic layers are being formed, and, secondly, the region at very high saturation, where the transition from multi-molecular layers to the liquid phase is taking place. Although there exists no comprehensive theory of adsorption describing the growth of the adsorbed layers over the entire pressure range, important theoretical calculations have been made which appear to be satisfactory within the two regions mentioned above. The physical difference between these two regions is best described in terms of the binding forces involved. At low saturations, the forces between adsorbed molecule and the adsorbing wall dominate the process, while near saturation, the forces between the molecules in the adsorbed layers become the most important.

The formation of the first few adsorbed layers has been described by a number of theories, of which the most successful is that of Brunauer, Emmet, and Teller (1938); however, it is generally admitted that a number of crude approximations must be made in order to solve the equations describing the adsorption process. For example, it is assumed that the number of molecules adsorbed over a given site is independent of the numbers on adjacent sites. In other words, lateral interactions between molecules in the adsorbed layers are neglected. Furthermore, the energy of adsorption of all but the first layer is assumed to be equal to the energy of liquefaction, so that only the first layer is considered to be significantly different from the liquid.

A number of attempts have been made to introduce refinements into the B.E.T. theory (e.g., Brunauer, Deming, Deming, and Teller, 1940; Cassel, 1944), but a satisfactory solution for the complete adsorption isotherm has not been obtained because of the mathematical difficulties encountered when a more realistic model is assumed (Hill, 1952).

As a result of these difficulties, the region of high saturation is of special interest. Here the number of layers is high enough for anomalous properties of the first layer to be relatively unimportant. It is therefore possible to make predictions of the form of the isotherm without having recourse to the type of approximation necessary for any solution of the low saturation problem. Calculations for this region have been made by Frenkel (1946), Halsey (1948), Hill (1949), and McMillan and Teller (1951). They suggested that, approaching saturation, the isotherm should follow the relation:

$$- \ln p/p_o = \frac{K}{\nu^3} \qquad (1)$$

where ν is the number of layers adsorbed at a pressure p, and p_o is the saturated vapor pressure. K is a constant of proportionality determined by molecular forces, as will be discussed later. Actually, Halsey proposed a more general form:

$$- \ln p/p_o = \frac{K}{\nu^s}$$

without specifying the index s explicitly.

Equation (1) has a simple physical basis. It is derived by assuming that the van der Waals forces between an adsorbed atom and the adsorbing wall fall off as the cube of the distance. The specific form of (1) results from equating the difference in the differential Gibbs free energy of the adsorbed phase and the bulk liquid, $\mu - \mu_l = kT \ln p/p_o$, to the corresponding change in potential energy due to the van der Waals forces. It is possible to allow for the influence of the interactions within the adsorbed layer as well as the attraction due to the wall. The calculation of Hill (see McMillan and Teller, 1951) gives the following form for the constant of proportionality in (1):

$$K = \frac{\pi}{6} \rho_1^4 d_{11}^6 \sigma_1^3 \frac{\varepsilon_{11}}{kT} \left(\frac{\rho_2 d_{12}^6 \varepsilon_{12}}{\rho_1 d_{11}^6 \varepsilon_{11}} - 1 \right) \qquad (2)$$

where ρ is the molecular number density, d_{ij} the equilibrium distance between a pair of molecules of types i and j, ε_{ij} is the potential energy of such a pair at the distance d_{ij}, and σ is the effective molecular cross section. The subscripts 1 and 2 refer to the adsorbate and adsorbent respectively. McMillan and Teller have shown that this constant is approximately

$$K = \frac{\pi}{6} \frac{\varepsilon_{11}}{kT} \left(\frac{\varepsilon_{12}}{\varepsilon_{11}} - 1 \right) \qquad (3)$$

It is therefore possible to correlate the magnitude of adsorption at high saturations with the molecular forces involved.

Further approximation enables us to express K in terms of the measured energies of adsorption. McMillan and Teller have shown that $\varepsilon_{12} - \varepsilon_{11}$ is of the order of $\frac{1}{N}(E_1 - E_\ell)$, where E_1 is the energy of

adsorption of the first layer, E_ℓ is the energy of liquefaction, and N is Avagadro's number. $(E_1 - E_\ell)$ is a quantity appearing explicitly in the equation of Brunauer, Emmet, and Teller and can be derived from the intercept of the B.E.T. plot of $\frac{p}{(p_o - p)V}$ against p/p_o. (V is the volume adsorbed at the pressure p). Thus we take for our final approximation:

$$K = \frac{\pi}{6RT} (E_1 - E_\ell) \qquad (3a)$$

Owing to the fundamental basis and essential simplicity of this relation, experimental tests of its validity are of particular interest. The data usually quoted as supporting these conclusions are those of Harkins and Jura (1944) who measured the adsorption of nitrogen and of water on anatase (powdered TiO_2). This data showed that equations (1) and (3) are followed quite closely, although Halsey (1948) deduces that an exponent of ν equal to 2.67 instead of 3 describes the data more accurately. Halsey considers this deviation from the cubic law to be important and has asserted that the empirical value of the exponent of ν in Equation (1) "has no simple relation to the power in the expression for London forces." From the work of Drain and Morrison (1952), it appears that the exponent may even be as low as 2 for argon adsorbed on rutile.

In the case of more complicated systems, it is evident from the work of Boyd and Livingston (1942) that for adsorption of water on graphite, and propyl alcohol on anatase and barium sulphate, large deviations occur from the Frenkel-Halsey-Hill relation. This is to be expected, since the derivation of Equation (1) is only valid for adsorbed systems with spherical fields and this simplification may not be satisfactory for complicated systems where orientation effects in the surface layer are possible. The data of Boyd and Livingston are insufficient for an exact determination of the deviation.

There are two reasons why further work on this high saturation region was desirable. In the first place, it is not easy to determine the number of adsorbed layers at high saturations using the volumetric method of previous workers, since the dead space corrections become large and deviations from the ideal gas law make them difficult to calculate. Secondly, it is desirable to observe adsorption on surfaces which are better defined than that of a fine powder such as anatase, in which capillary condensation may produce serious errors, especially near saturation. McMillan (1947) has shown that many of the deviations from the ideal B.E.T. isotherm can be explained quantitatively in terms of surface heterogeneity, thus emphasizing the importance of the character of the surface.

For these reasons a determination of the adsorption at high saturations for a number of gases has been undertaken. The measurements were carried out using nitrogen, argon, and oxygen as adsorbate gases and aluminum foil of low roughness factor as an adsorbent. Measurements have also been made with helium and these results will be described in the next paper (Bowers, 1953). Due to the unique properties of helium at low temperatures, its adsorption is of interest for reasons beyond those being considered in this paper.

The adsorption was determined gravimetrically, using a microbalance similar to that described by Gulbransen (1944) and more recently by Rhodin

(1950). The principle of the method is simply that of determining the increase in weight of the specimen as adsorbed layers form on it. This method has the important advantage that at high saturations there are no corrections to be applied to the observed weight of the adsorbed layer. Furthermore, it is possible to use a relatively small specimen with a small roughness factor for this determination.

Method

The microbalance used in this determination was very similar in design to that described by Rhodin (1950), having in particular the same symmetrical construction in order to avoid buoyancy corrections. The apparatus was primarily designed for experiments on helium adsorption at liquid helium temperatures, but by filling the liquid helium dewars with liquid argon, nitrogen, or oxygen, the specimen and counterweight could readily be maintained at various temperatures between 77 and 90°K, determined by the boiling points of the respective gases. The arrangement is shown schematically in Figure 1. The specimen of aluminum foil and the aluminum counterweight,

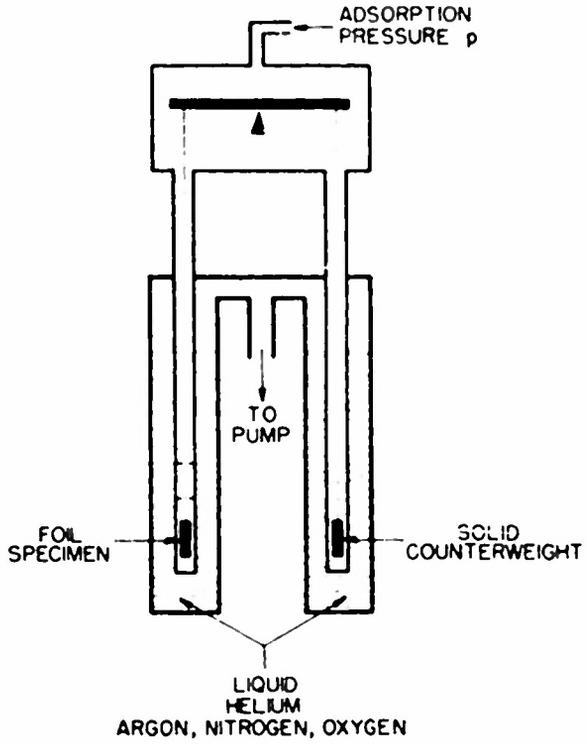

Figure 1. Schematic diagram of apparatus.

balanced to 10^{-5} gm, are supported from the arm of the balance by Kovar wires of .002" diameter. They are suspended inside tubes of 1/2" diameter which lead into two separate dewar vessels as shown in Figure 1.

The specimen of aluminum foil was wound into a loose coil; it had a geometrical area of 306 sq cm and weighed 1/2 gram. The counterweight was cylindrical and had a surface area of 2 sq cm. Thus the adsorption measured refers to the difference in area between specimen and counter-

weight equal to 304 sq cm. The specimen was degassed initially at 350°C for 12 hours, the pressure in the specimen chamber being 2×10^{-6} mm of mercury. This was done with the specimen in its final position in the cryostat and subsequent contamination was avoided by keeping the chamber evacuated to 2×10^{-6} mm between experiments. Presumably, there is a layer of chemisorbed oxygen on the aluminum, which is not removed in the degassing.

Elaborate shock mounting was used in order to prevent vibration reaching the balance system. Much of the complexity in the apparatus is necessary only for the adsorption work with liquid helium; accordingly, the details of the microbalance and associated cryogenic equipment will not be described here. There is one aspect of the arrangement which differs from similar apparatus of other workers. When working with nitrogen, argon, and oxygen, it was found desirable to place these liquids not only in the dewars represented in Figure 1, but also in dewars which enclosed the ones shown. These outer dewars are essential for providing nitrogen temperature shielding of the inner dewars when liquid helium is being used, but their use with the other gases results in a quiescent liquid in the inner vessels and this reduces spurious movement of the balance. The pumping tube shown in Figure 1 is only used with helium, since delayed boiling in the other liquefied gases renders precise temperature control impossible during pumping.

Results

Adsorption of Nitrogen

In Figure 2 is shown an isotherm for nitrogen at 77.4°K and in Figure 3

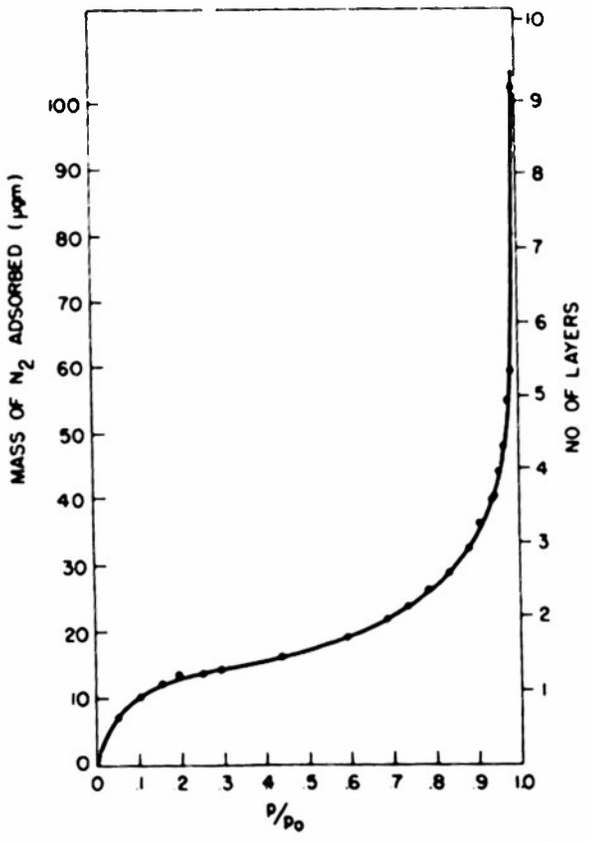

Figure 2. Nitrogen isotherm at 77.4°K.

the corresponding B.E.T. plot (Brunauer, Emmet, and Teller, 1938) which indicates a satisfactory agreement between theory and experiment between theory and experiment between 5 and 30 per cent saturation. The effective

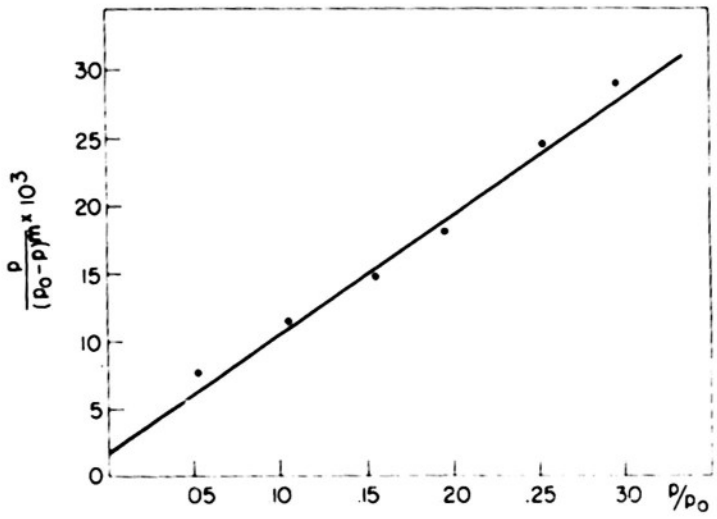

Figure 3. The B.E.T. plot for nitrogen at 77.4°K. (In the figure, m is the mass adsorbed in gm.)

area of the foil determined from this B.E.T. diagram was 388 sq cm as compared with the geometrical area of 304 sq cm. This implies a surface roughness factor of 1.3. In the calculation of the surface area, the cross section of the nitrogen molecule was taken to be 16.2 sq Å (Emmet, 1948; Harkins, 1952, p. 227). Thus the specimen of aluminum foil could be considered relatively smooth from the point of view of adsorption, since this roughness factor is small. From the B.E.T. plot it was calculated that a completed monolayer on the specimen weighed 11.1×10^{-6} gm; the number of layers could therefore be determined to a precision of at least one-tenth of a layer.

We shall now turn to an analysis of this data. In Figure 4 we show a

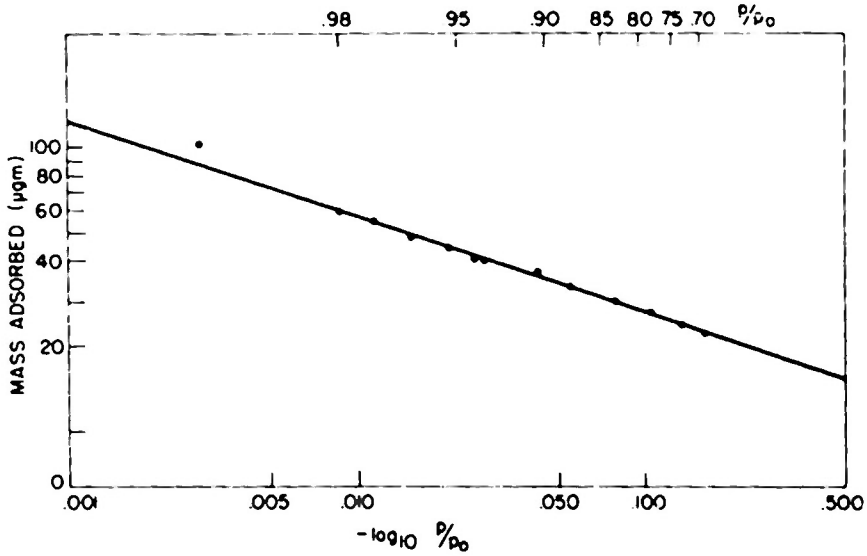

Figure 4.

graph of loglog p/p_o against log (mass adsorbed). This graph should be a straight line, the slope giving the exponent of ν in the Frenkel-Halsey-Hill relation, assuming the number of layers is proportional to the mass adsorbed. The slope of this straight line was found to be 3.0 as predicted by Frenkel and Hill. One notices that there is one point, corresponding to 99.3 per cent saturation, which lies above the line, suggesting that in this very high saturation region the number of layers is increasing at a more rapid rate than given by the cubic relation. However, since the isotherm is extremely steep in this region, one cannot say with certainty that this deviation does not arise from experimental error. Nevertheless, it does seem possible that at the highest saturations the number of layers is indeed increasing faster than the cubic law would require. It is difficult to specify the exact meaning of such an increase, because even though the roughness factor of the aluminum foil is small, some form of capillary condensation may be influencing the total weight of the specimen so near the saturation point. It is probably significant that one can see this tendency to a more rapid growth in the number of layers at a lower saturation, of the order of 96 per cent, in the data of Harkins and Jura on anatase, where capillary condensation is more likely to occur. Apart from capillary effects, the influence of surface tension and gravity on the adsorbed film may have to be reconsidered at these high coverages.

In Figure 5 we have plotted log p/p_o against $1/\nu^3$ in order to determine K, the constant of proportionality in Equation (1). The agreement between experiment and theory is most striking when plotted in this manner. The value of the constant K for nitrogen was found to be 3.10.

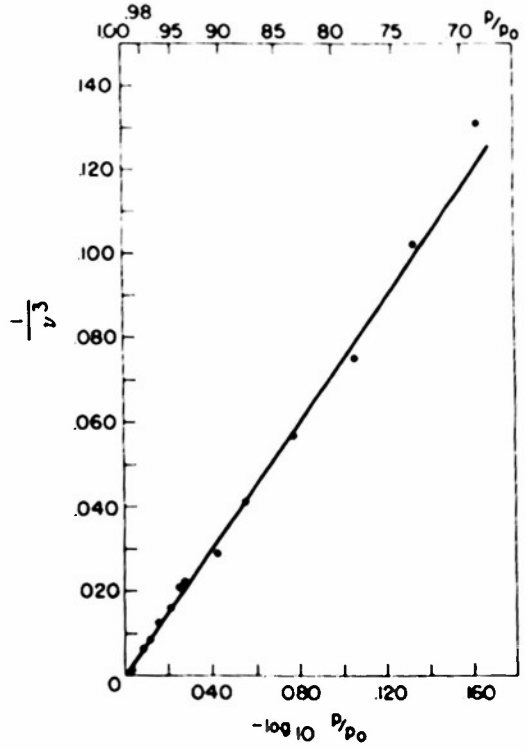

Figure 5.

We may compare the empirical value with the approximate equation (3a). Substituting $E_1 - E_\ell = 800$ cal/mole (Brunauer, 1945, p. 157) in this equation, we obtain $K \simeq 2.7$ at 77°K. This is very close to the observed value of 3.1 mentioned above. This degree of agreement may be fortuitous, since an order of magnitude is all that McMillan and Teller claim for their method of estimating K.

Summing up the results for nitrogen, it seems that the Frenkel-Halsey-Hill relation is followed very closely; the proportionality between log p/p_o and $1/\nu^3$ is established and the constant K has the correct order of magnitude.

The Adsorption of Oxygen

The adsorption of oxygen has been measured at 77.4°K and 89.7°K. The two isotherms were found to be similar in character, and in Figure 6 we show the data for 77.4°K. Adsorption and desorption points are shown in this figure.

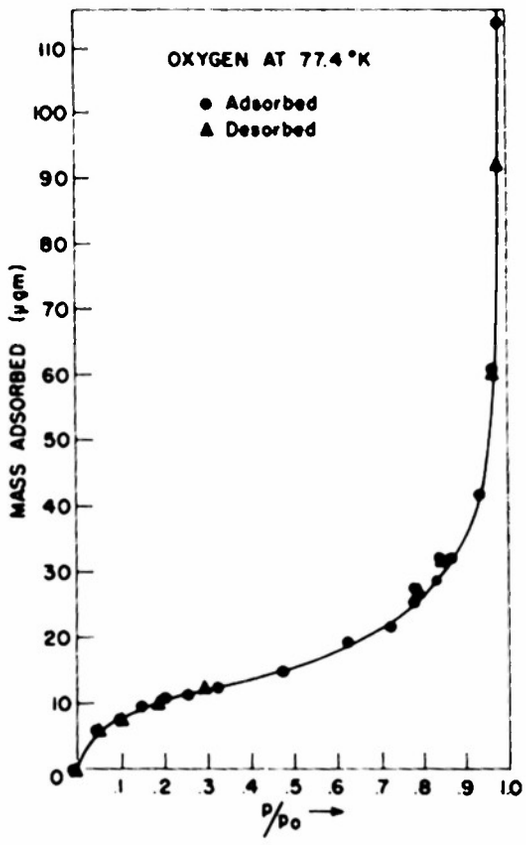

Figure 6. Oxygen isotherm.

There is no evidence of significant hysteresis in the data. This is to be expected, since hysteresis in adsorption is usually ascribed to cracks and pores in the surface of the adsorbent (Zsigmondy, 1911; McBain, 1935).

The B.E.T. plot was found to be a straight line between 5 per cent and 25 per cent saturation. The weight of the first layer was found to be 10.1 μgm at 77.4°K and 9.05 μgm at 89.7°K. Assuming the area for adsorption is 388 sq cm, as determined from the nitrogen isotherm, these values imply

a cross-section for the oxygen molecule in the first layer which is greater than that calculated from the bulk liquid density (Brunauer, 1945, p. 287). The area per molecule in the first layer was found to be 20.3 sq Å at 77.4°K and 22.7 sq Å at 89.7°K as compared with a value of 14.2 sq Å calculated from the bulk liquid density at 89°K. The existence of anomalous densities in the first few layers is well known in the adsorption of gases (Beebe, Beckwith, and Honig, 1945; Davis, DeWitt, and Emmet, 1947; Emmet, 1948), although the values for the cross-sections found in this experiment for oxygen seem higher than those of other workers.

The existence of the anomalous first layer introduces a further problem in the comparison of our results with the Frenkel-Halsey-Hill equation. We must allow for the varying density of the layers in computing the number of layers, from our measured values of the mass adsorbed. In the case of nitrogen, previous work has shown that the first layer is not anomalous, so that it has become a standard gas for area determinations (Harkins and Jura, 1944); this means that we could take the number of layers as proportional to the mass adsorbed. It is instructive to see how the variation in layer density affects the evaluation of our data, because this factor may be responsible for apparent deviations from the Frenkel-Halsey-Hill relation.

In Figure 7 we show a graph of log v against loglog p/p_o for data obtained at 89.7°K. In computing the points for curve I, we have assumed that

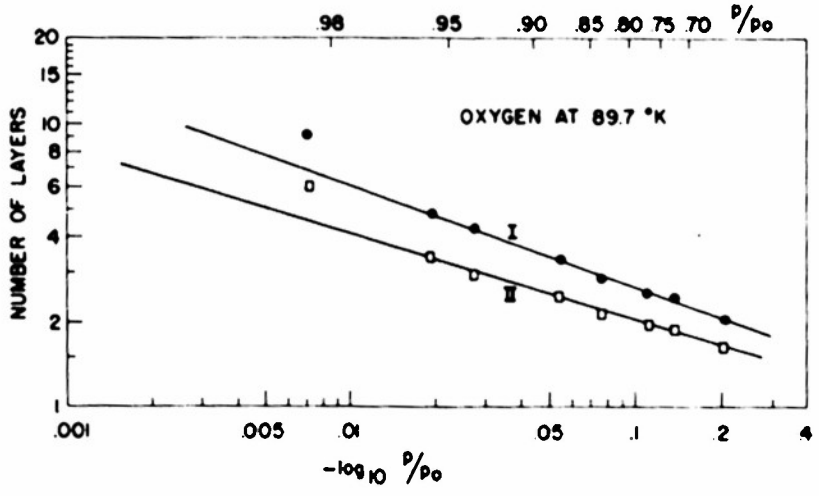

Figure 7.

all the layers have the same density as the first layer. The inverse slope of this line (which should equal the exponent of v in Equation (1)) was found to be 2.78. The points on curve II have been computed, assuming that only the first layer has the anomalous density determined from the B.E.T. plot, while all the rest have the bulk liquid density. The inverse slope of this line is 3.34. It is quite clear that the assumptions underlying the computation of these two curves are unrealistic; neither can be accepted physically. However, the errors involved are in opposite directions and the real physical picture must lie between the two assumptions. The situation in the adsorbed film must involve a gradual change from the low density of the first layer

to the liquid density in the outermost layers. It is interesting to see that one assumption yields an exponent slightly greater than 3, while the second yields one which is slightly less than 3. Since a realistic distribution of density would give a line in between the two shown in Figure 7, an exponent of 3 cannot be far wrong.

The value of K computed from the experimental results is 4.5 for points on curve I and 2.7 for those on curve II. These values have the correct order of magnitude as calculated from Equation (3a). At the highest saturations, greater than about 98 per cent, the number of layers again appear to be greater than expected from the cubic law.

The isotherm obtained at 77.4°K for oxygen presents features which are very similar to the 89.7°K isotherm. Plotting the results as for curves I and II of Figure 7, we obtain inverse slopes of 2.7 and 3.1 respectively. The corresponding values for K are 6.4 and 2.9. (In comparing these values for K, it should be remembered that K determines the cube of the number of layers; hence the evaluation of K is subject to 3 times the errors in the basic isotherm.)

Thus the results for oxygen exhibit two features. They indicate the existence of a packing in the first adsorbed layer which is significantly less than that calculated from the bulk density. They also indicate that if this anomalous packing is taken into account in a realistic manner, the isotherm at high saturation is described by Equation (1).

The Adsorption of Argon

Isotherms for argon have been determined at 77.4°K and 87.5°K. At the saturation vapor pressure, argon is solid at 77.4°K and liquid at 87.5°K. The isotherm at 77.4°K is therefore the only one involving solid layers which we have investigated.

The data for 87.5°K are shown in Figure 8. This isotherm exhibits features which are similar to the oxygen isotherms. The weight of the first layer was calculated to be 10.3 μgm. This implies a cross-section at the argon atom in the first layer equal to 24.8 sq Å, as compared with a value of 14.3 sq Å calculated from the bulk liquid density. This disparity is even greater than that observed for oxygen; it is similar in magnitude to that observed by Beebe, Beckwith, and Honig (1945) for the krypton monolayer. Thus in analyzing the data at high saturations we are faced with the same situation presented by the oxygen results because of the anomalous first layer. In Figure 9 we show a graph of $\log \nu$ plotted against loglog p/p_o, computing ν in the same way as for Figure 7. The assumption of a uniform layer density equal to that in the first layer (curve I) gives a value of 2.78 for the exponent of ν in Equation (1). The assumption of a layer density given by the bulk liquid density in all but the first layer (curve II) gives 3.13 for this exponent. Again we may assume that the real physical situation is one involving the gradual change throughout the first few layers from the anomalous first layer packing to that calculated from bulk liquid density. Such a physical model would lead to a curve between I and II of Figure 9 and at the highest saturations would be approximately a straight line whose inverse slope must be close to 3.0.

In Figure 10 we show the data plotted on the form of $1/\nu^3$ against $-\log p/p_o$; ν was calculated as for curve II in Figure 9. The purpose of this plot is merely to show how closely the highest saturation data is represented by the cubic law in spite of the fact that an exponent of 3.12 should

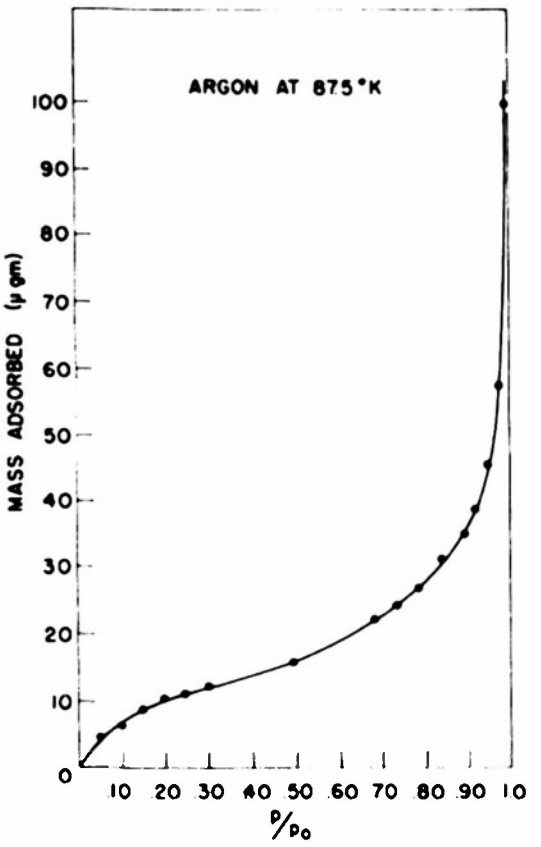

Figure 8. Argon isotherm.

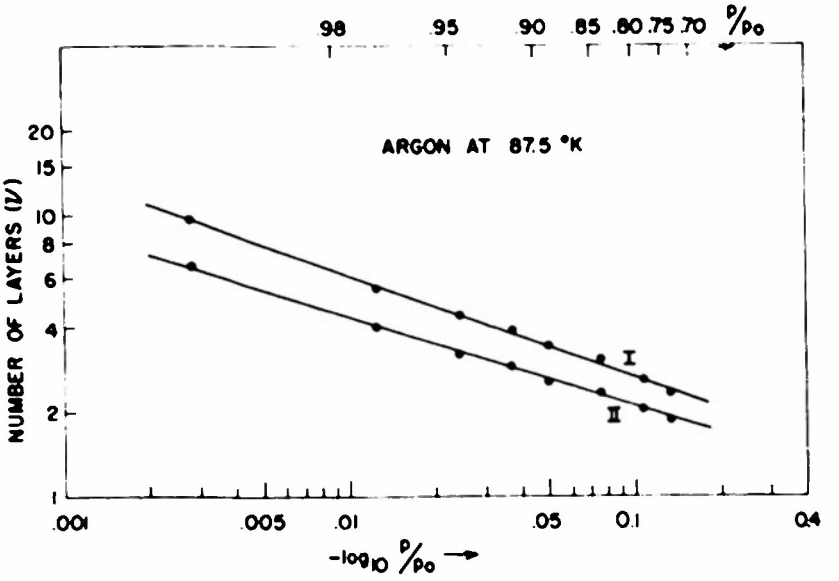

Figure 9.

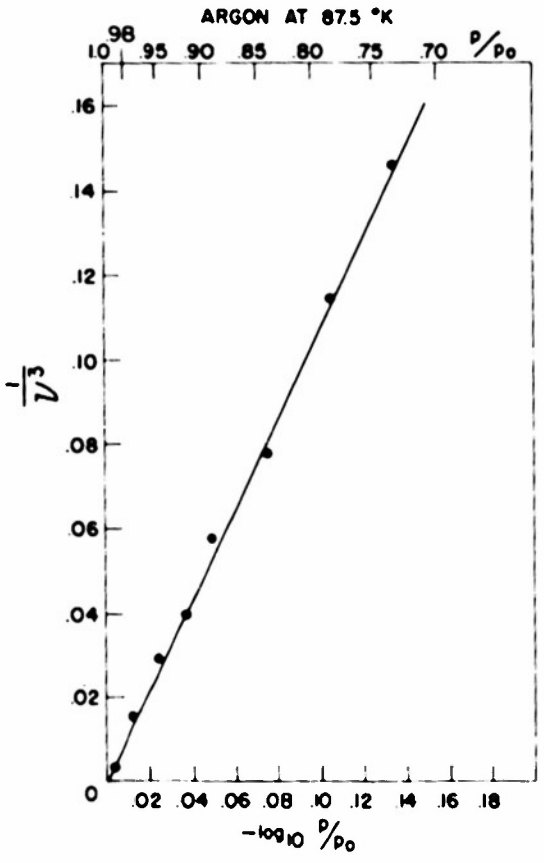

Figure 10.

provide the best general fit. It emphasizes the question of whether we should consider small deviations from the power 3 to be significant, as has been done by Halsey (1948).

The value of K was found to be 4.7 for the points on curve II of Figure 9 and 2.2 for the points on curve I. These values are of the correct order as calculated from Equation (3a).

The isotherm for argon at 77.4°K is shown in Figure 11. The value taken for p_o is that appropriate to the solid phase at 77.4°K. Considerable difficulty was encountered when measuring the adsorption at high saturations in this case. It is not certain that equilibrium was finally attained; heat transfer between the specimen and the gas seemed to be very slow. The isotherm has two interesting aspects. Firstly, the cross-section of the argon atom in the first layer is again greater than one can calculate from the density of solid argon; the figures are 17.9 sq Å and 12.9 sq Å, respectively. Secondly, the isotherm appears to meet the $p/p_o = 1$ axis at a finite value in the region of 3.5 layers. The adsorption at high saturations of solid layers is little understood, but the latter effect has been observed before with other gases, for example, carbon dioxide (Brunauer and Emmet, 1937) and krypton (Beebe, Beckwith, and Honig, 1945). As the result of this effect, the data at the high saturations cannot be represented by a power law similar to Equation (1).

Frequently the isotherm for solid layers is plotted with a p_o appropriate

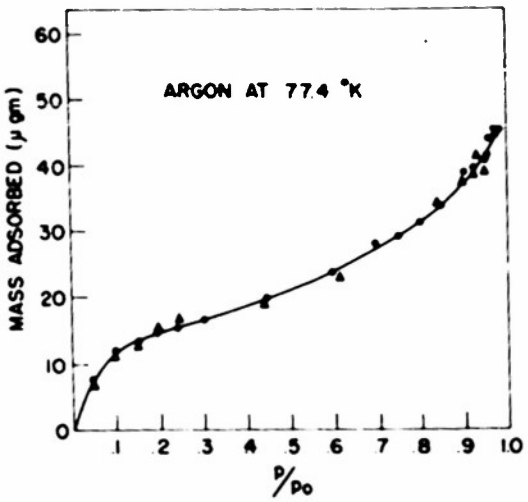

Figure 11. Argon isotherm.

to the supercooled liquid (David, DeWitt, and Emmet, 1947) which is larger than the solid value for a given temperature. In the case of argon at 77°K, the difference between the two saturated values is 15 per cent (Clark, et al, 1951). However, if the data are plotted with respect to this liquid p_o, the highest saturation obtained experimentally is 85 per cent, so that the data are insufficient for a test of Equation (1).

Discussion

The results presented in this paper suggest that Equation (1) is accurate in describing the adsorption of nitrogen, oxygen, and argon at the highest saturations and at temperatures where the layers can be considered to be "liquid." The apparent deviation in the case of oxygen and argon may be ascribed to anomalous structure of the first few layers. The only serious deviations appear in the region of 99 per cent saturation; however, it is difficult to determine the isotherm precisely so close to saturation.

The relation verified is based particularly on the following assumptions:

(a) The van der Waals forces involved vary as $1/r^3$ (London, 1930);

(b) The distance of an adsorbed molecule in the outer layer from the wall may be taken proportional to the number of layers.

For the interaction of a neutral molecule with the metallic wall, calculations of Lennard-Jones (1932), Bardeen (1940), and Margenau and Pollard (1941) all yield a $1/r^3$ dependence for the forces involved. They differ only in calculations of the size of the force. Until the K of Equation (1) can be estimated more precisely than by Equation (3a), we are not able to make a comparison between our data and the calculations mentioned. Prosen and Sachs (1942) have made a direct quantum mechanical calculation of the interaction between a neutral molecule and a metallic wall, using perturbation theory. They propose that the potential energy varies as $\frac{\log R}{R^2}$ when electron degeneracy is taken into account. Of course, the interaction between neutral molecules and the non-conducting adsorbed film still varies as $1/r^3$. The introduction of this potential into an equation similar to (1) would

lead to deviations from the cubic law if its influence were significant compared with interactions between adsorbate molecules. However, it is almost certain that the treatment of Prosen and Sachs is not valid for the distances from the wall found in multilayer adsorption and should only be applied to limited aspects of monolayer adsorption. It breaks down at short distances where the wave functions of neutral atom and metallic electrons overlap and also at large distances where the electron coulomb interactions cannot be properly treated. Thus assumption (a) seems justified.

Halsey (1948) has criticized assumption (b). He points out that one should not take the distance of an adsorbed molecule in the outer layer as proportional to the number of layers, because the actual distance involved is not continuously varying, but is a step function with values which are appropriate to integral numbers of layers. However, this view is based on a rather idealized picture of the adsorbed layers and the validity of the criticism may be less when we consider the statistical nature of what we call "the number of layers." The verification of Equation (1) for the simple systems described in this paper indicates that assumption (b) does not introduce serious error.

In the course of this work it has been necessary to determine the density of the first adsorbed layers for nitrogen, oxygen, and argon on the specimen of aluminum. Unfortunately, the values we give for the cross-sections of argon and oxygen are relative to the nitrogen cross-section. If the nitrogen first layer is normal, as appears to be the case from other workers (Harkins and Jura, 1944), then the first layers of oxygen and argon are significantly less dense than the outer layers calculated from the appropriate bulk density. The differences in density we obtain are larger than the comparable values of other workers (Emmet, 1948). Considering the work of Beebe, Beckwith, and Honig (1945) on krypton, which yielded a disparity of similar magnitude, it is clear that the first layer packing of the isotherm is not adequately understood.

With regard to the nitrogen first layer, Davis, DeWitt, and Emmet (1947) state the following: ". . . it is well to keep in mind the present status of area determination by nitrogen and to ask particularly whether or not it is possible that the cross sectional area assigned to the nitrogen molecule may be too low. The most convincing answer to this question will be obtained when and if someone measures the surface area of a metal foil or ribbon using nitrogen as an adsorbate. Only if one then obtains too low a roughness factor for such surfaces, will one be able to conclude with certainty that the usual value of 16.2 sq A per molecule is too small. The experiment of Harkins and Jura (1944) is not absolutely conclusive." The value of 1.3 for the roughness factor of the aluminum foil determined in the present investigation seems reasonable and lends support to the assumption of the normal 16.2 sq A for nitrogen.

Acknowledgments

Grateful acknowledgment is due to Professors E. A. Long and L. Meyer for their constant advice and encouragement. My thanks are also due Dr. J. R. Arnold, of the Institute for Nuclear Studies, for his helpful interest.

References

Bardeen, J., 1940, Phys. Rev. 58, 727.

Beebe, R. A., Beckwith, J. B., and Honig, J. M., 1945, J. Am. Chem. Soc. 67, 1554.

Bowers, R., 1953, Phil. Mag. (refers to following paper).

Boyd, G. E., and Livingston, H. K., 1942, J. Am. Chem. Soc. 64, 2383.

Brunauer, S., 1945, The Adsorption of Gases and Vapors, Oxford University Press.

Brunauer, S., Deming, L. S., Deming, W. E., and Teller, E., 1940, J. Am. Chem. Soc. 62, 1723.

Brunauer, S., and Emmet, P. H., 1937, J. Am. Chem. Soc. 59, 2682.

Brunauer, S., Emmet, P. H., and Teller, E., 1938, J. Am. Chem. Soc. 60, 309.

Cassel, H. M., 1944, J. Phys. Chem. 48, 195.

Clark, A. M., Din, F., Robb, J., Michaels, A., Wassenaar, T., and Zwieterling, T. N., 1951, Physica 17, 876.

Davis, R. T., DeWitt, T. W., and Emmet, P. H., 1947, J. Am. Chem. Soc. 51, 1237.

Drain, L. E., and Morrison, J. A., 1952, Trans. Farad. Soc. 48, 840.

Emmet, P. H., 1948, Advances in Catalysis, Vol. I, Academic Press, N. Y.

Frenkel, J., 1946, Kinetic Theory of Liquids, Oxford Univ. Press., p. 332.

Gulbransen, E. A., 1944, Rev. Sci. Instr. 15, 201.

Halsey, G. D., 1948, J. Chem. Phys. 16, 931.

Harkins, W. D., 1952, The Physical Chemistry of Surface Films, Reinhold Publishing Corp., N. Y.

Harkins, W. D., and Jura, G., 1944, J. Am. Chem. Soc. 66, 1362 & 1366.

Hill, T. L., 1946, J. Chem. Phys. 14, 263 & 441; 1947, Ibid, 15, 767; 1949, Ibid, 17, 580 and 668; 1952, Advances in Catalysis, Vol. IV, Academic Press, N. Y., p. 225.

Lennard-Jones, J. E., 1932, Trans. Farad. Soc. 28, 333.

Margenau, H., and Pollard, W. G., 1941, Phys. Rev. 60, 128.

McBain, J. W., 1935, J. Am. Chem. Soc. 57, 669.

McMillan, W. G., 1947, J. Chem. Phys. 15, 390.

McMillan, W. G., and Teller, E., 1951, J. Chem. Phys. 19, 25.

Prosen, E. J. R., and Sachs, R. G., 1942, Phys. Rev. 61, 65.

Rhodin, T. N., 1950, J. Am. Chem. Soc. 72, 4343.

Zsigmondy, R., 1911, Zeit. anorg. Chem., 71, 356.

IV

THE ADSORPTION OF GASES AT HIGH SATURATIONS: II. THE THICKNESS OF THE UNSATURATED HELIUM FILM

Raymond Bowers
To be published in the Philosophical Magazine

Abstract

The adsorption of helium on an aluminum foil has been measured between 1.8°K and 4.2°K. The principal interest was in the form of an isotherm close to saturation. The maximum thickness observed for the adsorbed layer at the highest saturations (greater than 99.9 per cent) was twenty atomic layers below the λ-point and ten layers above the λ-point. These values for the unsaturated film are compared with existing data for the thickness of the saturated helium II film. The data are also compared with the Frenkel-Halsey-Hill equation for multilayer adsorption and the calculations of Band on the adsorption of a Bose-Einstein gas.

Introduction

It is well known that when any solid surface is in contact with liquid helium II or its vapor, a thick film is formed which possesses unique transport properties (Daunt and Mendelssohn, 1939). Estimates of the thickness of the film above the liquid vary from 50 to 150 atoms (Jackson, 1953). Recently attention has been drawn to the fact that even in the comparatively thin adsorbed layers, characteristic of pressures below the saturated vapor pressure, superfluidity is observed when the temperature is reduced below 2.19°K. Long and Meyer (1950) showed that this peculiar mobility could be observed whenever the number of layers exceeded the first statistical layer. More recently, considerable work has been done on the magnitude of the mobility to be found in these thin layers (Bowers, Brewer, and Mendelssohn, 1951; Long and Meyer, 1952a & b). In these experiments one measures the mass transfer directly or its contribution to the heat flow through the film. These total flows involve a product of the linear velocity of the flow and the thickness of the film, as well as ρ_n/ρ_s (the relative concentration of normal and superfluid components in the flowing film). One of the striking features of the data available is that the total superflow, even at 95 per cent saturation, is still very much smaller (less than 10 per cent) than that in the saturated film. It is of considerable interest to determine whether this is merely a consequence of the much smaller film thickness involved in the unsaturated case, or whether the other factors determining the flow are also different in the two cases.

In order to separate the variation of the velocity and ρ_n/ρ_s from the measured transport property, it is necessary to know the variation of the thickness of this film with pressure. Essentially, this requires an accurate determination of the adsorption isotherm. There is available a considerable amount of data on the isotherm up to about 90 per cent saturation (e.g.,

Keesom and Schweers, 1941; Frederikse and Gorter, 1950; Schaeffer, Smith, and Wendell, 1949; Strauss, 1952) and, on the whole, the agreement between the results of different workers appears to be satisfactory. However, much less is known about the form of the isotherm at the highest saturation. The isotherms determined by Kistemaker (1947) and Long and Meyer (1949) are the only ones which give measured points close to saturation. Long and Meyer found that the thickness of the film is of the order of 7 to 8 layers at 90 per cent saturation, as observed by the earlier workers. However, with helium II the adsorption at saturations higher than 90 per cent was found to be anomalously high, the isotherm rising very rapidly close to saturation to a measured value of 160 atomic layers. This effect was not observed above the λ-point. In Kistemaker's original paper, he calculated about 30 layers for a similar limit, but a re-evaluation of his data (Frederikse, 1950) indicates a film several times thicker than the 30 layers stated. The observation by Long and Meyer and by Kistemaker of a very thick film close to, but definitely below, the saturation pressure is of considerable importance, since it has direct bearing on the problem of whether the thick helium II film is formed from the vapor, or whether contact with the liquid is necessary for its formation (Mendelssohn, 1946). If we assume that they are observing the formation of the thick helium II film normally characteristic of saturation conditions, there is a large disparity between their values and the most recent direct determinations of the thickness of the saturated film (Burge and Jackson, 1951; Hensaw and Jackson, 1951). The latter workers have obtained thicknesses which are less than a third of the 160 atoms recorded by Long and Meyer.

The form of the helium isotherm at high saturation is of interest from another point of view. One may ask whether the Frenkel-Halsey-Hill relation, described in the preceding paper (Bowers, 1953), is valid for helium adsorption. This law was actually derived on a classical basis, using the $1/r^3$ van der Waals force. If the cubic law is found to be valid, it would mean that quantum phenomena influence the magnitude of the forces involved, but not their dependence on the effective distance. On the other hand, quantum effects such as Bose-Einstein degeneracy, might dominate the picture to such a degree that the simple cubic law is no longer valid. The influence of the gravitational field on the Bose-Einstein condensation is also a factor that may influence the adsorption considerably (Lamb and Nordsieck, 1941; Becker, 1950; Liebfried, 1950; Halpern, 1952a & b). Calculations on the influence of degeneracy on helium adsorption have been made by Temperley (1949) and Band (1951).

This paper describes a determination of the helium isotherm by a gravimetric method. The work has been undertaken for the following reasons:

(1) To investigate the high saturation region in greater detail in order to obtain data which are sufficient for a test of the cubic law.

(2) To investigate the disparity between the values reported by Kistemaker and by Long and Meyer for the thickness of the film and the comparable values due to Jackson and co-workers.

(3) To provide a basis for a gravimetric determination of the thickness of the helium II film under saturated conditions.

Method

The apparatus and specimen used in this experiment were the same as used for the nitrogen, oxygen, and argon work described in the preceding paper. The microbalance and associated low temperature system will be described in detail elsewhere.

The two helium baths (see Figure 1, preceding paper) were pumped through a common pumping tube, keeping the same temperature in both. Furthermore, care was taken to keep the helium levels in these two dewars at the same height. The vapor pressure of the helium in the dewars is the p_o of the isotherm; the value of p is the pressure in the tubes containing the specimen and counterweight. The specimen and counterweight space could be evacuated to 5×10^{-7} mm Hg when liquid helium was in the dewars. During a determination of the isotherm, the vapor pressure p_o in the helium dewars was held constant to 0.1 mm of oil (octoil-S). The pressure inside the specimen chamber was changed by adding purified helium gas and, as in the earlier experiments, the deflection of the balance beam was observed as the adsorbed layers increase the weight of the specimen. Two radiation shields, with orifices of 1 mm, were mounted above the specimen. Both shields were in good thermal contact with the outer helium bath.

In spite of the elaborate shock mounting of the apparatus, a slight residual disturbance was noticeable when the helium was being pumped. This presented a difficulty only when a zero reading was being taken with the specimen space evacuated; the presence of even a small amount of gas in the specimen space provided enough damping of the balance for complete stability. Accordingly, all the isotherms below 4.2°K are measured from an arbitrary starting point at about 15 per cent saturation, and in computing the total number of adsorbed layers, it is necessary to allow for the gas already adsorbed at this initial saturation. Such a correction can be made quite accurately, using the data of other workers, because at 15 per cent saturation we are in the region of the completed monolayer where the isotherm has a small slope. Since no difficulty of a similar nature was encountered when using liquid nitrogen, oxygen, and argon at their boiling points, the disturbance presumably originated in the pumping system. A zero reading was obtained for helium at 4.2°K.

Results

Isotherms have been determined at the following temperatures: 1.644, 1.829, 2.050, 2.132, 3.012, 4.198°K. In Figure 1 is shown an isotherm for helium II determined at 1.829°K. The left-hand ordinate gives the mass of helium adsorbed, while the right-hand ordinate gives the equivalent number of statistical layers. For layers other than the first two, the weight of the layer is calculated assuming a normal liquid density, taking the effective area of the specimen as 388 sq cm as determined by the nitrogen isotherm described in the preceding paper. We allow for the fact that the density in the first and second layers is significantly higher than successive layers by the following method: We have assumed that the density in the first layer is 3.6 times that for liquid packing (Schaeffer, Smith, and Wendell, 1949; Long and Meyer, 1949; Gorter and Frederikse, 1950; Strauss, 1952), while the second layer is arbitrarily taken to be half as dense as the first. It can be seen that the right-hand ordinate in Figure 1 has a scale which allows

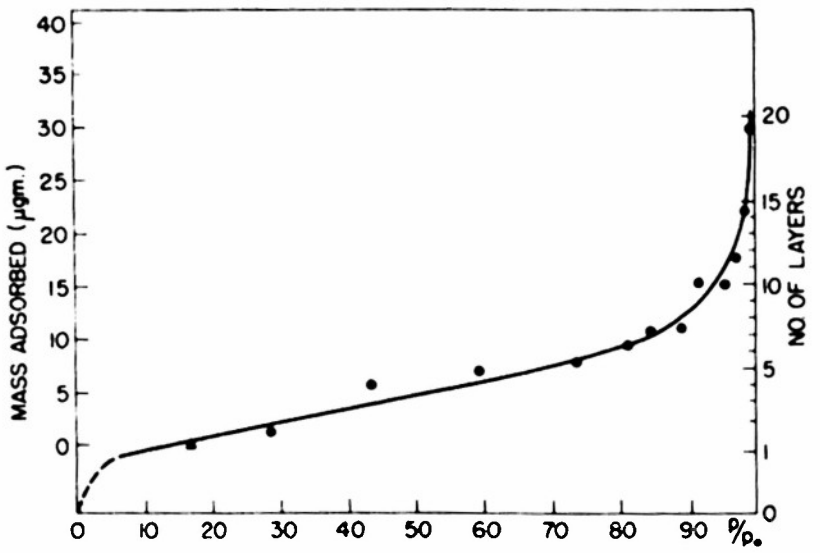

Figure 1. Helium isotherm at 1.829°K. The symbol ▲ denotes the arbitrary starting point mentioned in the text.

for these closely-packed layers.

In Figure 2 we have a similar isotherm at 2.132°K, including in this curve some values for the coverage obtained by desorption from 99.25 per cent saturation. It can be seen that there is no significant hysteresis, as was the case for oxygen with the same specimen (see preceding paper, Bowers, 1953).

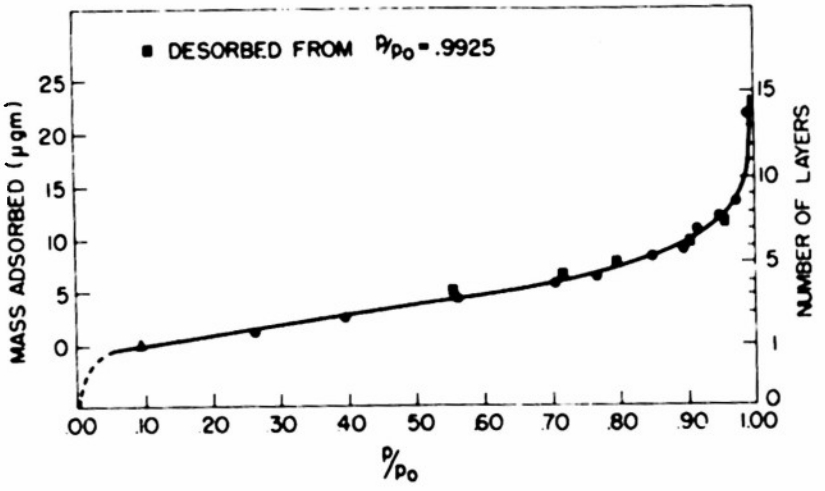

Figure 2. Helium isotherm at 2.132°K.

As a final example of a measured isotherm, we show in Figure 3 the data for 4.197°K. Two isotherms have been obtained above the λ -point, at 3.02°K and 4.20°K. It is much more difficult to obtain accurate isotherms in the helium I range. The bubbling of the liquid helium I and the simultaneous difficulty in controlling temperature make the balance less stable. Furthermore, the total number of layers found above the λ -point is

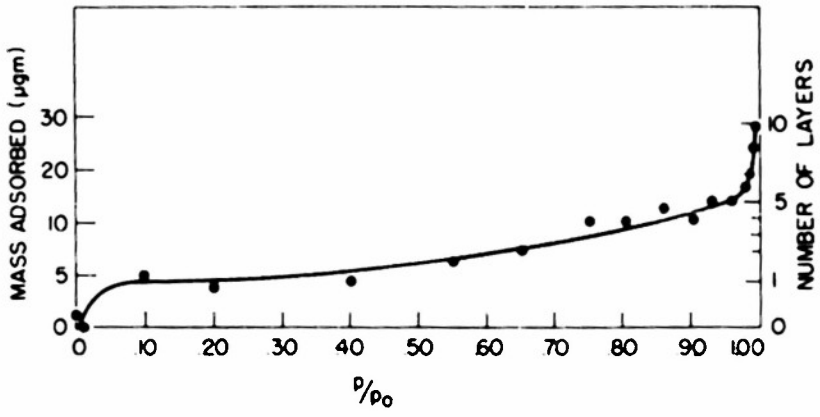

Figure 3. Helium isotherm at 4.197°K.

considerably less than the number observed below the λ -point for the same saturation. The maximum number of layers observed above the λ -point was ten at 99.91 per cent saturation, for the 4.2° isotherm.

Discussion

The results presented above will be considered from two points of view. First we shall consider their relation to the formation of a very thick film at saturation and, secondly, we shall consider to what extent the adsorption at high saturation is compatible with a law of the type proposed by Frenkel, Halsey, and Hill outlined in the introduction to the preceding paper. With regard to the formation of a thick film at saturation in helium II, it can be seen that there is no sign of a 160-layer film even at saturations as high as 99.92 per cent. However, the isotherm is very steep in this region and it is difficult to put a definite upper limit on the number of layers which one could obtain, but in no case were films thicker than 20 atoms observed. Furthermore, it may be said provisionally that we have not been able to obtain films thicker than 40 or 50 layers even with the bulk liquid helium II present, providing the specimen is in contact with the vapor alone as opposed to being in direct contact with the liquid. (See Mendelssohn, 1946.) (Work on the film associated with the bulk liquid is still in progress and requires further clarification.)

These results seem to contradict those of Kistemaker and of Long and Meyer, which yielded a film about 160 atoms thick near saturation. Our results are in better agreement with those of Jackson and co-workers. One explanation of the disparity with the results of Long and Meyer may be found in capillary condensation, since they used tightly-packed rouge as an adsorbent. However, the fact that Long and Meyer did not find a similar thick film above the λ -point is evidence against capillary condensation.

There is another possible explanation for the disparity involving the dependence of the helium II film thickness on the height above the bulk liquid. It is well known that the thickness of the film varies rapidly with the height above the bulk liquid level for heights less than a few millimeters (Burge and Jackson, 1951). Any bulk liquid introduced into a tightly-packed powder, such as the rouge, would be dispersed throughout the rouge by the large surface tension forces in the very small channels, and if we imagine a helium II film being formed from this dispersed liquid, it is clear that

the film on the grains will have a thickness characteristic of a "height" of the order of the grain size. Since this effective height is extremely small, we should expect the thickness to be considerably greater than the value obtained in experiments such as those of Burge and Jackson, where a height of order of the centimeters is involved. Thus, even if a correction could be made for the presence of bulk liquid in an adsorption experiment at saturation, it seems reasonable to expect a film thickness for the fine powder greater than that obtained in other determinations. This is, of course, largely an academic point, since such a correction for the presence of bulk liquid is almost impossible to make.

None of the arguments presented above can be used in order to explain the disparity between our values and those of Kistemaker. He measured the adsorption of helium in a glass system designed so as to virtually eliminate the possibility of capillary condensation. At the present time no reasonable explanation of this disparity presents itself. The thickness of the film very near saturation should be extremely sensitive to the temperature of the specimen with respect to its surroundings and the disparity may indicate that the temperature of the specimen was higher in our case. This is mentioned because it is definitely easier to shield the specimen in the volumetric methods of Kistemaker and of Long and Meyer than in the present investigation. However, considering the radiation shields used in the present work, this mechanism for the disparity remains unlikely.

We have already mentioned in the introduction to this paper the fact that the total superflow observed in these adsorbed layers is very much smaller than that in the saturated film. Our isotherms and those of previous workers indicate that this is largely due to the smaller thickness of the adsorbed layers as compared with the film at saturation. However, there is a spread of about 50 to 150 atoms in the existing values for the thickness of the saturated film (Jackson, 1953), so that it is not possible to analyze this aspect of the isotherms in any detail. If the saturated film is 50 atoms thick, the reduced thickness of the adsorbed film at 95 per cent saturation would result in a direct reduction of superflow to about 20 per cent of its value in the saturated film; a saturated film 100 atoms thick would make this figure 10 per cent.

Leaving the question of the relation to the bulk liquid film, we shall now consider the over-all magnitude of the adsorption observed. Our data are in general agreement with the previous work of Gorter and Frederikse (1950), Kistemaker (1947), Long and Meyer (1949) (except as mentioned above), and Strauss (1953). Generally speaking, helium forms a larger number of layers above about 70 per cent saturation than one finds with other gases (cf. preceding paper, Bowers, 1953) when the temperature is below the λ -point.

In order to compare our data with the equation of Frenkel-Halsey-Hill (Equation 1 of the preceding paper) we have plotted in Figure 4 a graph of loglog p/p_o against $1/\nu^3$ for three different temperatures. As in the previous notation, ν is the number of layers. It is clear that the data illustrated can be described by the relation

$$-\ln \frac{p}{p_o} = \frac{K}{\nu^3}$$

where K varies with temperature, and this seems to be true of all the

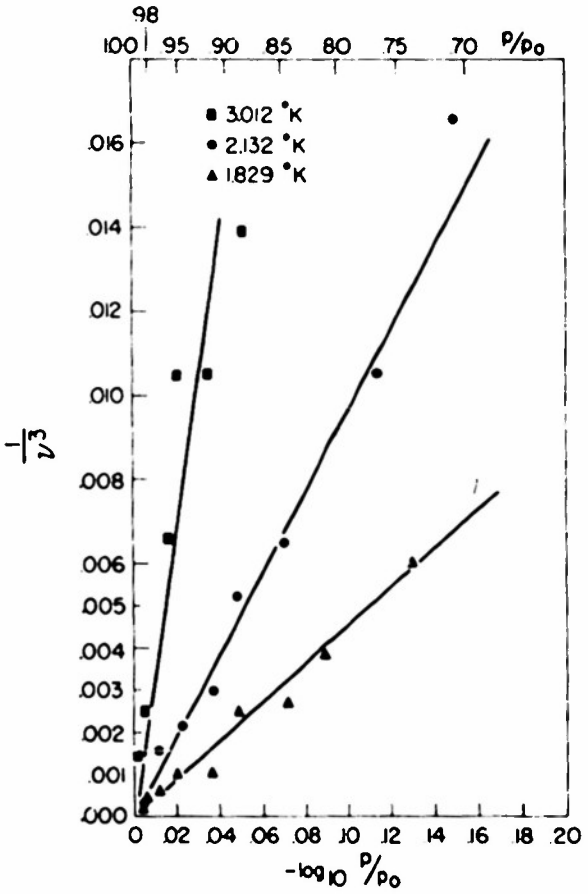

Figure 4.

isotherms obtained. The very striking way in which the data at 3.02°K fit on a straight line is to some extent accidental, since this degree of agreement exceeds the experimental precision for isotherms above the λ -point. However, taking errors above the λ -point into account, it seems as though the relation is consistent with the data between 1.8°K and 4.2°K. The variation of the constant of proportionality K with 1/T is shown in Figure 5. It must be remembered that the value of K determines the cube of the number of layers, hence its determination is subject to 3 times the errors inherent in the original measurement of the isotherm. The variation of K in the helium II region from 60 at 1.64°K to 24 at 2.13°K involves only a difference of 35 per cent in a number of layers. Hence the points in Figure 5 should be taken to illustrate the definite rise in K in going through the λ -point, but they are not accurate enough to give the exact functional dependence of K on temperature. (In Figure 5 a straight line has been drawn through the helium I region because this is the variation predicted by theory.)

In the preceding paper, estimates of K have been made using the approximation:

$$K = \frac{\pi}{6RT}(E_1 - E_\ell)$$

where E_1 is the energy of adsorption in the first layer and E_ℓ is the energy

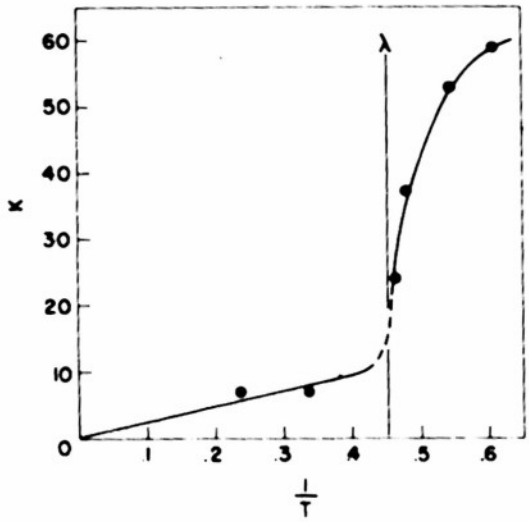

Figure 5. The variation of K with 1/T.

of liquefaction. A difficulty arises in the application of this formula to helium adsorption because $E_1 - E_\ell$ varies considerably with coverage throughout the first layer (Keesom and Schweers, 1941). If we obtain $E_1 - E_\ell$ from the B.E.T. plot, as in the preceding paper, we obtain a value appropriate to the completed first layer which has an anomalously high density. The B.E.T. plot of Schaeffer, Smith, and Wendell (1945) yields about 25 cal/mole for $E_1 - E_\ell$. However, the data of Keesom and Schweers (1941) show that $E_1 - E_\ell$ is at least 80 cal/mole at the lowest coverages and one could justify taking even higher values on the basis of the anomalous high density of the completed first layer. Taking $E_1 - E_\ell = 25$ cal/mole, we obtain $K \simeq 3$, while an assumption of 80 cal/mole yields $K \simeq 10$. It is important to emphasize that these values for K represent no more than a guess. Firstly, the value taken for $E_1 - E_\ell$ is arbitrary. Secondly, on more fundamental grounds, we cannot expect a formula derived classically to explain helium II adsorption which is probably influenced considerably by the Bose-Einstein degeneracy. Apart from statistics, we have allowed for the anomalous first layer in computing the total number of layers by assigning a particular high density to this layer, but we have not considered the possibility of a co-operative effect between the first and subsequent layers which would render the treatment of Hill and Frenkel inapplicable.

The experimental data are best described by a $K = 7$ in the helium I region; this is not too far from the estimates made above. In the helium II region it is clear that the experimental K is considerably larger than the estimates. The data show that K is not proportional to 1/T, but this is not surprising because of the λ-transition. Summing up the observations, it is found that the Frenkel-Halsey-Hill equation describes the variation of the number of layers with pressure quite well for a given temperature; the variation with temperature is complicated by the λ-transition which invalidates the application of their formula.

Recently Band (1951) has provided another method for the comparison of our results with theory. He has calculated the form of an isotherm for a degenerate Bose-Einstein system, taking various powers in the force between

the adsorbate gas and the solid adsorbent. In Figure 6 we compare his predictions with our data. In this figure are shown 6 isotherms and 3 calculated curves of Band. The various dotted lines correspond to n = 2, 2.5, and 3, where n is the exponent in the attractive field potential proportional to $1/r^n$. It appears that the curve with n = 2 fits the data most successfully. Band's formula implies that the isotherm is independent of temperature for a fixed value of n and clearly this is an approximation in the case of helium.

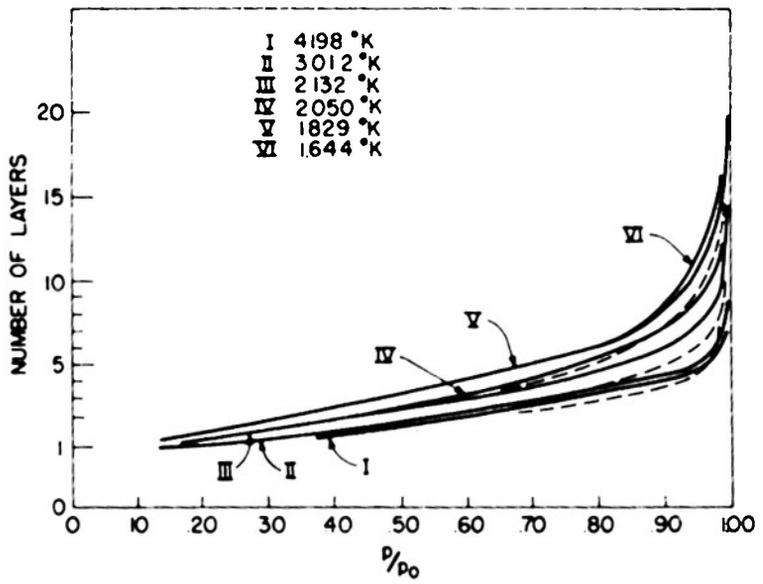

Figure 6. The solid lines are the isotherms determined in the present investigation. The broken lines represent the calculation of Band with n = 2, 2.5, and 3; the highest broken line refers to n = 2 and the lowest to n = 3.

It is difficult at the present time to choose between the equation of Frenkel-Halsey-Hill and the equation of Band as representing the most reasonable picture of helium adsorption. The agreement with the data in the case of the former suggests that a binding potential energy proportional to the inverse cube of the distance is applicable to helium at low temperatures, but the magnitude of these forces may be very different in the helium II region from that which one could calculate classically. On the other hand the description given by Band, although based on the important degeneracy, has one feature which is difficult to understand physically. As mentioned above, the best fit between his formula and the adsorption data is given when a binding potential between the adsorbate gas molecule and the combined wall and helium film varies as the inverse square of the distance involved. It is not easy to see the significance of such a law of force (see discussion in preceding paper, Bowers, 1953). Such a formulation may be compared with the calculation of Bijl, de Boer, and Michels (1941) on the influence of zero-point energy in a thick film of helium. However, this calculation has been criticized by Mott (1949) because their potential term in $1/r^2$, which results from the zero-point energy, would not exist if lateral interactions in the film were taken into account. Temperley (1949) has

also calculated quantum-mechanically the binding energy of a gas molecule with a wall and adsorbed layer. He considered the approximation of a very thick adsorbed layer. This calculation yields an energy with terms in $1/r^2$ and $1/r^4$. However, the term in $1/r^2$ is very much smaller than the term in $1/r^4$, so that this cannot be considered an interpretation of the Band formula.

The influence of the zero point energy is obviously important in calculating the magnitude of the adsorption of helium, but one can see from the large change in K in the region of the λ -point that zero point energy alone cannot explain the disparity between a classical treatment of the problem, such as that of Frenkel and Hill, and the observed isotherms. It would be interesting to see if one could calculate its influence on K; no calculation exists at the present time on this point.

Conclusion

The isotherms obtained with helium possess the following features: first, there appears to be no evidence with helium II for a film greater than about 20 atoms thick below the saturation pressure. Secondly, the over-all magnitude appears to be best described by a relation derived from a van der Waals force varying as the inverse cube of distance. The results can also be described reasonably successfully by Band's formula for the adsorption of a degenerate Bose-Einstein system. In this case it is necessary to assume that the force of interaction between a gas molecule and the wall varies as the inverse square of the distance.

Acknowledgments

I wish to thank Professors E. A. Long and L. Meyer for their continued interest in this work. Many aspects of this investigation have originated in their suggestions.

References

Band, W., 1951, J. Chem. Phys. 19, 435.
Becker, R., 1950, Z. Physik 128, 120.
Bijl, A., de Boer, J., and Michels, A., 1941, Physica 8, 655.
Bowers, R., 1953, Phil. Mag. (refers to preceding paper).
Bowers, R., Brewer, D. F., and Mendelssohn, K., 1951, Phil. Mag. 42, 1445.
Burge, E. J., and Jackson, L. C., 1951, Proc. Roy. Soc. A 205, 270.
Daunt, J. G., and Mendelssohn, K., 1939, Proc. Roy. Soc. A 170, 423.
Frederikse, H. P. R., 1949, Physica 15, 860.
Frederikse, H. P. R., 1950, Thesis, Leiden, p. 60.
Gorter, C. J., and Frederikse, H. P. R., 1950, Physica 16, 403.
Halpern, O., 1952a, Phys. Rev. 86, 126; 1952b, Ibid, 87, 520.
Henshaw, D. G., and Jackson, L. C., 1951, Proc. Int. Conf. on Low Temp., Oxford, p. 65.
Jackson, L. C., 1953, Phil. Mag. Suppl. (in press).
Keesom, W. H., and Schweers, J., 1941, Physica 8, 1020 & 1032.
Kistemaker, J., 1947, Physica 13, 81.
Lamb, W., and Nordsieck, A., 1941, Phys. Rev. 59, 677.
Liebfried, G., 1950, Z. Physik 128, 133.
Long, E. A., and Meyer, L., 1949, Phys. Rev. 76, 440; 1950, Ibid, 79, 1031; 1952a, Ibid, 85, 1030; 1952b, Ibid, 87, 153; 1953, Phil. Mag. Suppl. (in press).

Mendelssohn, K., 1946, Proc. Int. Conf. on Low Temp, Cambridge, p. 41.
Mott, N. F., 1949, Phil. Mag. 40, 61.
Schaeffer, W. D., Smith, W. R., and Wendell, C. B., 1949, J. Am. Chem. Soc. 71, 863.
Strauss, A. J., 1953, Thesis, Chicago (Reviewed in Long and Meyer, 1953).
Temperley, H. N. V., 1949, Proc. Roy. Soc. A 198, 438.

V

THERMOCHEMISTRY AND THE THERMODYNAMIC PROPERTIES OF SUBSTANCES*

J. W. Stout

To be published in Annual Review of Physical Chemistry, 1953

Although the general thermodynamic principles and the techniques of measurement of what are called thermodynamic properties have been well established for many years, the field of thermochemistry and the thermodynamic properties of substances continues to attract many investigators. In addition to the importance of free energy and heat data for the investigation of the stability of chemical compounds and equilibrium in chemical reactions, the use of thermodynamic methods is a valuable tool in understanding many diverse phenomena. Because of limitations of space it has not been possible to include in this review all topics of thermodynamic interest. No survey is given of work on adsorption and the thermodynamics of surfaces, on solutions, on bond energies, or on isotopic equilibria. Work in some of these fields is reviewed elsewhere in this volume.

Physical Constants and Tabulations of Data

A committee of the National Research Council [Rossini et al[1]] has considered and selected best values of the fundamental constants needed in physical chemistry. The Bureau of Standards circular, "Selected Values of Chemical Thermodynamic Properties," compiled under the direction of Rossini & Wagman,[2] has now been issued in a bound volume. This work, which runs to 1268 pages, is a critical selection of best, and internally self-consistent, values of thermodynamic properties for all chemical substances except carbon compounds containing more than two carbon atoms. The tables of Series I list the heat of formation at 0°K, and heat and free energy of formation, entropy and heat capacity at 298.16°K. In Series II are given values of pressure, temperature, ΔH, ΔS, and ΔC_p for processes of solid transition, fusion, vaporization and sublimation. Complete literature references are given. The tables of Series III, which list the thermodynamic properties at a number of temperatures, are not included in the bound volume and have appeared only as loose sheets without references.

Data of State for Gases, Liquids and Solids

For some time Beattie and co-workers at M.I.T. and Michels and co-workers at the University of Amsterdam have been making accurate pressure-volume-temperature measurements on gases. In the year 1952 data on several substances were reported from each of these laboratories. Beattie, Douslin & Levine[3] have investigated the compressibility of gaseous neo-pentane from its critical temperature (160.6°C) to 275°C and at densities

* The survey of the literature pertaining to this review was concluded in December, 1952.

of from one to seven moles per liter. Similar measurements on n-pentane were made by Beattie, Levine & Douslin.[4] In each case the constants of the Beattie-Bridgeman equation of state and values of the second virial coefficient were calculated from the experimental data. Beattie, Brierly & Barriault[5,6] have made compressibility measurements on gaseous krypton at temperatures from 0 to 300°C and at densities from one to ten moles per liter. It was found that values of the second virial coefficient calculated from these data agreed with those predicted by a Lennard-Jones interatomic potential function with a sixth-power attractive term and a twelfth-power repulsive term. The two parameters in the Lennard-Jones potential were chosen to give the best fit to the observed second virial coefficients. The experimental values of the third virial coefficient were, however, about twice as large as those calculated.

Michels et al[7] report compressibility data on CH_3F from 0 to 150°C and at pressures up to 150 atm. Data for CO over the same temperature range and at pressures up to 3000 atm are given by Michels et al.[8] In both cases values of internal energy, entropy and heat capacity, derived from the compressibility data combined with heat capacities of the low pressure gas, are tabulated. An extensive summary of the thermodynamic properties of nitrogen in the temperature range from -125 to 150°C and at pressures up to 6000 atm has been given by Lunbeck, Michels & Wolkers.[9] Hamann & Pearse[10] have measured second virial coefficients of CH_3Br, CH_3Cl, CH_3F and cyclopropane. They find that the results may be fitted by a 6-12 Lennard-Jones potential function and do not require the use of a non-spherically symmetrical potential as might be expected for permanent dipoles. They conclude that the molecular rotation causes a polar molecule to behave like a sphere. Other values of second virial coefficients are: Korvezee,[11] C_6H_6; Francis et al,[12] C_6H_6; Fox & Lambert,[13] mixed organic vapors; Casado, Massie & Whytlaw-Gray,[14] $(C_2H_5)_2O$, CCl_4, CS_2 and perfluoromethylcyclohexane. The last named authors were principally interested in the limiting PV product at zero pressure for molecular weight determination, but from the slope of PV versus P a value of the second virial coefficient may be obtained. It is interesting to note that for acetone at 22°C, even in the range of 20 to 150 mm pressure, there is a serious curvature in the graph of PV versus P, indicating that the gas imperfection in this gas cannot be adequately represented by a single virial coefficient.

Theoretical Calculations of Equation of State

Fickett & Wood[15] have made numerical calculations of the Lennard-Jones and Devonshire equation of state in the region of high temperatures and densities. Hamann[16] has calculated corrections to this equation of state by quantizing the translational motion within individual molecular cages. By comparison with experimental data he finds that this procedure overcorrects for quantum effects. Roe, Epstein & Powers[17] and Epstein & Hibbert[18] calculate second virial coefficients for a 6-9 Lennard-Jones potential and Epstein[19] derives an asymptotic form valid at low temperatures for a 6-s potential, where s, the coefficient of the repulsive term, may be arbitrarily chosen. No correction is made for quantum effects. Cottrell & Paterson[20] have calculated an equation of state applicable to gases at densities comparable to solid densities and at high temperatures. Mayer & Careri[21] have discussed equation of state computations at high densities. They suggest a logical computation method which involves making exact calculations of the

Helmholtz free energy for the non-equilibrium system and then finding the equilibrium state by minimizing this free energy at constant volume and temperature. The method resembles the cell method of Lennard-Jones and Devonshire, but with cells of variable size, and is numerically easier and more exact than previous applications of the cell method. Himpan[22] has proposed a new empirical equation of state.

Critical Phenomena

A very interesting series of Canadian papers has clarified the experimental situation regarding the "flat top" in liquid-vapor coexistence curves at the critical point. It is found experimentally that the temperature at which the liquid-vapor meniscus is seen to disappear in a long vertical tube is the same throughout an appreciable range of overall density. This has been interpreted as indicating that there does not exist a unique critical temperature and density, a question of considerable theoretical interest. Because of the very large isothermal compressibilities in the critical region, however, a fluid which has a unique critical temperature will in a gravitational field exhibit large equilibrium density gradients. For a given overall density there will be a certain height in the tube which at the critical temperature has the correct critical density and at this position the meniscus will disappear. For other densities the correct critical density will be reached at a different position in the tube, but the disappearance of the meniscus will still occur at the critical temperature. Thus in a long vertical tube the critical temperature will seem, because of the gravity effect, to be constant over a wide range of density. Weinberger & Schneider[23] observed that in a vertical tube 19 cm long there was an appreciable horizontal portion in the curve of temperature versus overall density for xenon in the critical region, but when the tube was laid on its side so that its height was 1.2 cm the flat-top portion was not detectable. Using a radioactive tracer technique, these authors[24] have also investigated the equilibrium density gradients in a vertical tube of xenon near its critical temperature and find a considerable density gradient consistent with the calculated effect of gravity. Murray & Mason[25] have investigated by means of light scattering the density gradients near the critical temperature of ethane and conclude that the observed gradients can explain the flat portion of the liquid-vapor coexistence curve. Weinberger, Habgood & Schneider[26] have measured isotherms of xenon in a short bomb and agree that gravitational effects are capable of explaining the whole of the flat-top width of observed coexistence curves. Zimm[27] has pointed out that the experimental data of Rowden & Rice[28] on the two-liquid system aniline-cyclohexane are as consistent with a coexistence curve cubic in the composition difference from the maximum as with the flat-topped curve proposed by the authors.

Using a correlation liquid model, Goldstein[29] has shown theoretically that for a normal monatomic liquid there is at the critical temperature a condensation in the space of relative momenta somewhat analogous to the condensation of a Bose-Einstein fluid in ordinary momentum space. Alder & Jura[30] have reconsidered the old question of the possibility of a solid-gas critical temperature. They calculate that a critical point should exist for solid helium at about 90°K and 29,000 atm pressure.

Anderson et al[31] report experimental critical constants of OF_2.

Transitions in Solids

Stephenson, Blue & Stout[32] report low temperature heat capacity

measurements on NH_4Cl and ND_4Cl. In both compounds the entropy change associated with the gradual transition is about R ln 2, indicating that the transition is from an ordered low temperature state to a high temperature state in which each ammonium ion may occupy two positions of nearly equal energy. The crystal structure as determined from neutron diffraction measurements by Levy & Peterson[33] confirms this interpretation. Stephenson, Landers & Cole[34] have found that the gradual transition near 231°K in NH_4I is similar to that in NH_4Cl, but the heat capacity data indicate that above the first order transition occurring at 257°K, corresponding to a change from the CsCl to the NaCl lattice, the ammonium ions are rotating. Transition temperatures of solid solutions of NH_4Cl and NH_4Br and a new transition in NH_4Br are reported by Stephenson & Adams.[35] Kondo & Oda[36] have made dilatometric and thermal measurements of two phase transformations in barium dicalcium n-butyrate and Powles[37] has given a general theoretical discussion of the phase changes in the solid hydrogen halides. The papers and discussions of the 1948 Cornell symposium on phase transformations in solids have been published in book form.[38] The articles in this monograph, written by leading authorities, provide an excellent summary of both the theoretical and experimental knowledge about phase transformations.

Vapor Pressures, Heats of Vaporization and Fusion

Additional references on vapor pressures and heats of fusion, transition and vaporization will be found in the section on Heat Capacities, Heat Contents and Entropies, since accurate measurement of these quantities is often made in an entropy determination. References to papers primarily concerned with vapor pressure are (a) Elements: Michels, Wassenaar & Zwietering,[39] Kr; Brooks,[40] Te and Se; Edwards, Johnston & Blackburn,[41] Mo; Gulbransen & Andrew,[42] Cr; Searcy,[43] Ge. (b) Inorganic compounds: Burns & Dainton,[44] NOCl; Schnizlein et al,[45] OF_2; Schäfer and co-workers,[46,47,48] $FeCl_2$, $CoCl_2$, $NbCl_5$; Junkins and co-workers,[49,50] NbF_5 and TeF_4; Jolly & Latimer,[51] GeI_4; Shapiro,[52] ThO_2. (c) Organic compounds: Michels, Wassenaar & Zwietering,[53] CO; Allen, Everett & Penney,[54] C_6H_6; Edwards,[55] tetranitromethane; Day with Felsing,[56] 3-methylpentane (also liquid compressibility); Milton & Oliver,[57] n-hexadecafluoroheptane (also critical constants); Stiles & Cady,[58] perfluoro-n-hexane and perfluoro-2-methylpentane. In most cases, heats of vaporization are calculated from the vapor pressure data. In cases where the free energy of the gas can be calculated from molecular data and that of the solid from thermal data and the third law of thermodynamics, a value of the enthalpy of vaporization may be obtained from each vapor pressure point. The constancy of the values of ΔH_o^o obtained over a range of temperatures is a sensitive test of the consistency of the data and, if there is no significant trend in the values, a much more precise value for the heat of vaporization may be obtained than is possible from the slope of a log P versus 1/T curve. For example, in the case of molybdenum[41] the mean deviation in the value (155.55 kcal) of ΔH_o^o was 0.19 kcal.

The question of the vapor pressure and heat of vaporization of graphite remains unsettled. Doehaerd, Goldfinger & Waelbroeck[59,60] have made measurements of evaporation rates from a crucible in which the ratio of evaporating area to orifice was 24,000. They obtain a heat of vaporization consistent with the spectroscopic value of 141 kcal and conclude that the

sticking coefficient of C atoms is very low and that consequently the value of 170 kcal obtained by Brewer, Giles & Jenkins[61] for the heat of vaporization is too high. This conclusion has been questioned by Brewer[62] who emphasizes the importance of volatile impurities in graphite which give a high vapor pressure and consequently a low heat of vaporization. Farber & Darnell[63] report measurements of the evaporation rate from a graphite filament, but in the absence of knowledge of the sticking coefficient cannot determine the vapor pressure.

Brown[64] discusses vapor pressure curves and the Hildebrand rule, and Simons & Hickman[65] suggest empirical equations correlating energy of vaporization with polarizability.

The heat of fusion of lithium has been measured by Kilner.[66]

Heat Capacities, Heat Contents and Entropies

Jura & Pitzer[67] discuss theoretically the specific heat of small particles at low temperatures. For the case of cubes of aluminum, 100 Å on an edge, the contribution of the translation and rotation of the crystals, which is independent of temperature, is, below 3°K, larger than the vibrational heat capacity. Law[68] also discusses the surface contribution to the heat capacity of solids.

Inorganic Substances

Values of low temperature heat capacities, heat contents and third law entropies are: Hu & Johnston,[69] CuBr; Adams & Johnston,[70] β-Ga_2O_3; Oliver & Grisard,[71] BrF_3 (also vapor pressure data); Todd & Coughlin,[72] TiS_2 (also high temperature heat content data); Todd & Lorenson,[73] Ba_2TiO_4 Sr_2TiO_4 and an equimolal solid solution; Todd,[74] Mg_2TiO_4 and $Mg_2Ti_2O_5$; Todd & Lorenson,[75] $BaTiO_3$, $SrTiO_3$ and a solid solution; Jones, Gordon & Long,[76] U, UO_2 and UO_3; Rubin & Giauque,[77] H_2SO_4, $H_2SO_4 \cdot H_2O$ and $H_2SO_4 \cdot 2H_2O$ (also heat of fusion); Kunzler & Giauque,[78] $H_2SO_4 \cdot 3H_2O$ glass and crystals (also heat of fusion); Busey & Giauque,[79] $NiCl_2$. UO_2 and $NiCl_2$ exhibit peaks in heat capacity at low temperatures, almost certainly associated with an antiferromagnetic ordering of the atomic magnetic moments. Unlike crystalline ice, crystals of sulfuric acid and its mono-, di- and tri-hydrate all approach an ordered state of zero entropy at low temperatures. The disorder in sulfuric acid trihydrate glass at 0°K corresponds to 5.9 e.u. The ferroelectric material $BaTiO_3$ shows small peaks in heat capacity at temperatures corresponding to anomalies in dielectric behavior, but the corresponding anomalous entropy changes are less than 0.1 e.u., showing that there is no appreciable change in order. Friedberg[80] has measured heat capacities of the antiferromagnetic material $CuCl_2 \cdot 2H_2O$ between 1.5 and 20°K. There is a maximum in heat capacity at 4.31°K and at this temperature the vibrational heat capacity is so small that accurate correction may be made for it. About one-third of the total magnetic entropy of R ln 2 appears at temperatures above the heat capacity maximum. Measurements of the heat capacity of $CuSO_4 \cdot 5H_2O$ between 0.25 and 3°K, as well as the isentropic change in temperature and intensity of magnetization with magnetic field, are reported by Geballe & Giauque.[81] There is an anomaly in the heat capacity curve with maxima near 1.3°K. About half of the total magnetic entropy of R ln 2 is lost at a temperature of 0.25° and below this temperature the heat capacity is rising again. The detailed shape

of the heat capacity curve is very unusual and cannot be explained by any existing theories of antiferromagnetism or crystalline field splitting.

Organic Substances

The thermodynamics laboratory of the Bureau of Mines station at Bartlesville, Oklahoma has contributed a number of important papers. The group there, which was originally established under the direction of the late Hugh M. Huffman, is making precise thermodynamic measurements on a number of prototype organic compounds in order to establish a large body of data from which generalizations may be made concerning reactions of interest to the petroleum industry. Measurements are made of low temperature heat capacities, heats of transition, fusion and vaporization, and vapor pressures. The gas imperfection is estimated from the Clapeyron equation, $dP/dT = \Delta H/(T \Delta V)$, using experimental values of the heat of vaporization and vapor pressure. In some cases measurements are made of vapor heat capacities and the isothermal change of heat capacity with pressure is used, through the thermodynamic relation $(\partial C_p/\partial P)_T = -T(d^2B/dT^2)$, to correlate the second virial coefficients, B, over a range of temperature. The molecular constants of the gaseous molecules are estimated (some new infra-red data is reported). The third law entropy and vapor heat capacities are used to fix unobservable vibrational frequencies and barriers hindering internal rotation. The thermodynamic functions $(F^o - H^o_o)/T$, $(H^o - H^o_o)$, S^o and $C_p{}^o$ of the gaseous molecules are tabulated up to 1000 or 1500°K. Some measurements of heats of formation are reported. Papers appearing in 1952 are: Scott et al,[82] 2,2,3,3-tetramethylbutane; [83] 3,4-dithiahexane; Guthrie et al,[84] thiacyclopropane; McCullough et al,[85] ethanethiol; Finke et al,[86] 1-pentanethiol; Scott et al,[87] 3-thiapentane; Guthrie et al,[88] furan; Hubbard et al,[89] thiacyclopentane. Other measurements of heat capacities and entropies are: Stephenson & Berets,[90] melamine and dicyandiamide; Furukawa, McCoskey & King,[91] polytetrafluoroethylene. Pomerantz[92] describes the synthesis and physical properties of n-heptane for use as a calorimetric standard[93] for heat capacity.

Metals

Douglas et al[94] have measured heat capacities of potassium and sodium-potassium alloys in the range 0-800°C. Measurements of heat capacity in the range from 15°K to room temperature are: Busey & Giauque,[95] Ni; Geballe & Giauque,[96] Au; Adams, Johnston & Kerr,[97] Ga (including heat of fusion); Clusius & Schachinger,[98] Co. Hill & Parkinson[99] have measured low temperature heat capacities of Ge and grey Sn, and Pearlman & Keesom[100] report data for Si. The deviations from the Debye curve of the heat capacities of the isomorphous structures diamond, Si, Ge and grey Sn are similar in that all show a minimum in the apparent Debye Θ at temperatures slightly below one-tenth of the high temperature Θ-value. Even on a reduced scale of temperature, however, there are important quantitative differences between the four curves.

Considerable work has appeared on the heat capacity of metals in the temperature range of liquid helium. At these temperatures the vibrational heat capacity, which varies as T^3, has become small enough so that the electronic heat capacity, which is proportional to the temperature, is an appreciable fraction of the total. In the expression $C(\text{electronic}) = \gamma T$ for the heat capacity due to electronic excitation, the coefficient γ is proportional to the

density of electronic energy states at the top of the Fermi surface. In the transition metals γ is high because of the high density of states in the unfilled d-bands. Calorimetric measurements from which values of γ have been obtained include: Clement & Quinnell,[101] In; [102] Pb; Brown, Zemansky & Boorse,[103] Nb; Horowitz et al,[104] Pb; Keesom & Pearlman,[105] Ag; Estermann, Friedberg & Goldman,[106,107] Cu, Mg, Ti, Zr, Cr. Of particular interest are the results on chromium, which has an electronic heat capacity much smaller than the neighboring elements of the first transition series. Values of $\gamma \times 10^4$ in cal $deg^{-2} mole^{-1}$ are Ti, 8.0; V, 15; Cr, 3.8; Min, 42; Cu, 1.80. The low value found for the density of electronic states in chromium would be expected on Zener's[108] theory of ferromagnetism which predicts that the spins of the d-electrons in chromium are ordered in an antiferromagnetic fashion. In such a case the d-band will be split into two halves, with the lower half completely filled and the upper half empty. The contribution to the electronic heat capacity will then be due only to excitation of electrons in s and p bands. However, theoretical calculation of band shapes by Slater[109] and by Fletcher & Wohlfarth[110] indicate that even without an antiferromagnetic ordering the density of states is small near the middle of the d-band and the observed value for chromium is consistent with their calculations.

From measurements of critical magnetic field curves for superconductors one can deduce the difference in heat capacity between normal and superconducting states, provided the magnetic transition is reversible. Since no term linear in temperature has been observed in the heat capacity of a superconducting metal, the linear term in the difference is identified with the electronic heat capacity of the normal metal. The values so deduced are in fair agreement with those obtained calorimetrically except in the case of the "hard" superconductors which have high melting points. Wexler & Corak,[111] by special attention to purity and thermal treatment, have obtained samples of vanadium with nearly reversible magnetic properties and conclude that the source of the disagreement lies in irreversibility in the magnetic properties caused by internal strains and impurities. Other values of γ deduced from magnetic data are given by Goodman,[112] Al, Cd, Ga, Zn, Ru, Os; Smith & Daunt,[113] Cd, Zr, Hf, Ti; Stout & Guttman,[114,115] In-Tl solid solutions and MgTl; Love, Callen & Nix,[116] In-Tl solid solutions. In the case of the In-Tl alloys the magnetic transitions are reversible in the dilute solutions, but become less so as the concentration of thallium increases. γ changes little with composition as one might expect from the similarity in electronic structure of In and Tl. Although the transition temperatures of superconducting isotopes vary inversely as the square root of the isotopic mass, there is no change in the electronic heat capacity of the normal metal. Measurements on Sn isotopes are reported by Maxwell[117] and on Hg and Sn by Reynolds, Serin & Nesbitt.[118] The electronic heat capacities of metals in the superconducting state are discussed by Worley, Zemansky & Boorse[119] and by Maxwell.[120] Thermodynamic discussions of the destruction of superconductivity by a magnetic field are given by Garfunkel,[121] Pippard[122] and Marcus.[123]

Heat Capacities of Gases

The calorimetric techniques now available permit very accurate measurement of gaseous heat capacities. The isothermal variation of heat capacity with pressure furnishes valuable information on the equation of state and the value of the heat capacity at zero pressure, C_p^o, is a check on the value

calculated from molecular data and, in cases where there is uncertainty in vibrational frequency assignment or barriers hindering internal rotation, permits the evaluation of these quantities. Masi & Petkof[124] have measured the heat capacity of CO_2 and O_2. The values extrapolated to zero pressure agreed within 0.1% with values of C_p^o calculated from spectroscopic data. (An error of 0.2 to 0.3% in the published spectroscopic values of C_p^o was discovered and corrected.) Calorimetric measurements of the heat capacity of CO_2 up to pressures of 200 atm and from 20 to 40°C are reported by Michels & Strijland.[125] From measurements on CF_2Cl_2 Masi[126] has revised the frequency assignment and recalculated the thermodynamic functions of the ideal gas. He also gives an equation of state consistent with the gaseous heat capacity measurements. McCullough, Pennington & Waddington[127] have measured the heat capacity of water vapor. They use their data to get expressions for the second and third virial coefficients. Barrow[128] has measured vapor heat capacities of C_2H_5OH. As in the case of CH_3OH, there are serious deviations from ideal gas behavior. Using a frequency assignment based on new infra-red measurements, Barrow finds agreement with gaseous heat capacity and third law entropy data with a potential hindering rotation of 3300 cal for the CH_3 group and 800 cal for the OH group. The considerably different assignment of Ito[129] was made without the advantage of the accurate heat capacity data.

Heats and Free Energies of Reaction

Heats of Formation and Combustion

Calorimetric determinations of heats of formation, based mainly on measurements of heat of combustion are (a) Inorganic compounds: Holley, Huber & Meierkord,[130] In_2O_3;[131] ThO_2, UO_2, U_3O_8; Huber & Holley,[132] Nd_2O_3; Humphrey & King,[133] low-quartz and low-cristobalite; Humphrey, King & Kelley,[134] FeO; Koerner & Daniels,[135] NO and P_2O_3; Quarterman & Primak,[136] KC_4. (b) Organic compounds: Nelson & Jessup,[137] ethylenimine; Aston, Rock & Isserow,[138] methylhydrazine and symmetrical and unsymmetrical dimethylhydrazine; Hubbard et al,[139] tropolone (for which the resonance energy is estimated); Cotton & Wilkinson,[140] ferrocene; Bender & Farber,[141] anthracene transannular peroxide and dianthracene; Carson, Carson & Wilmshurst,[142] mercury dimethyl, diethyl and diphenyl; Mortimer, Pritchard & Skinner,[143] various mercury alkyls; Nelson, Jessup & Roberts,[144] copolymers of butadiene and styrene; Gilpin and Winkler,[145] RDX (trimethylenetrinitramine); Breitenbach, Derkosch & Wessely,[146] amino acids and polypeptides. The results of the last-named authors suggest that, in contrast to the first polymers of glycine, the condensation of amino acids to form high molecular weight polypeptides may be exothermic.

Heats of Reaction and of Solution

Lacher and co-workers[147,148] have measured calorimetrically the heat of hydrobromination in the vapor phase of butene-1, cis-butene-2 and trans-butene-2, and the heat of the gaseous reaction $B_2H_6 + 6Cl_2 = 2BCl_3 + 6HCl$. From the data on the butenes, heats of isomerization are calculated. Jolly & Latimer[149] have measured the heat of the reaction $GeI_2(s) + I_3^- + 3H_2O = H_2GeO_3(aq) + 4H^+ + 5I^-$. Bender & Biermann[150] report heats of neutralization of HCl and NaOH at high concentrations. From calorimetric determinations of the heat of hydrolysis, Van Artsdalen & Dworkin[151]

compute the heat of formation of B-trichloroborazole and in a similar fashion Charnley, Skinner & Smith[152] obtain heats of formation of methyl, ethyl, n-propyl and n-butyl esters of boric acid. Measurements of heats of solution and heats of formation calculated therefrom are: Westrum & Eyring,[153] Np in HCl and ΔH_f of $NpCl_3$ and $NpCl_4$; Spedding & Miller,[154] Ce and Nd and their trichlorides in HCl and ΔH_f $CeCl_3$ and $NdCl_3$; King,[155] ΔH_f $MnSiO_3$ and Fe_2SiO_4 from solution in HF; Logan, Bush & Rogers,[156] ΔH_f of Co (II) and Ni (II) pyridinated cyanates and thiocyanates from solution in HCl; Eyring, Lohr & Cunningham,[157] some oxides of Am and Pr in HCl; Evans & Richards,[158] ΔH_f $GeBr_4(\ell)$ and $GeI_4(s)$ from solution in NaOH; Li & Gregory[159] $FeCl_2$, $FeCl_3$, $FeBr_2$, $FeBr_3$, $FeBrCl_2$ in H_2O. Katzin and co-workers[160,161] have measured heats of solution of hydrates of uranyl nitrate and of cobalt nitrate in water and a number of organic solvents. From the data they calculate heats of hydration and the binding energies of water and other ligands.

Free Energy and Heat Data from Equilibrium Measurements

Jolly & Latimer[50,162] have measured equilibria in the reactions $2GeI_2(s) = Ge(s) + GeI_4(g)$ and $GeO_2(s) + Ge(s) = 2GeO(g)$. They calculate values of ΔF^o, ΔH^o and ΔS^o. Koch, Broido & Cunningham[163] report similar data for the reaction $LaCl_3(s) + H_2O(g) = LaOCl(s) + 2HCl(g)$. Schäfer and co-workers[46,47,48] have investigated equilibria in the reactions $FeCl_2(g) + H_2 = Fe(\gamma, s) + 2HCl(g)$, $2CoCl_2(g) + Cl_2(g) = 2CoCl_3(g)$ and $2NbCl_4(s) = NbCl_3(s) + NbCl_5(g)$. Chiche[164] has measured equilibrium pressures in the copper-oxygen system and Wunderlich[165] has investigated the thermodynamics of the decomposition of pyrite. Altman & Adelman[166] report measurements on the equilibrium $N_2H_4 \cdot H_2O(g) = N_2H_4(g) + H_2O(g)$. The vapor phase association of carboxylic acids has been investigated by Taylor & Bruton[167] and by Lundin, Harris & Nash.[168,169] They find that, contrary to earlier results, the heat of dimerization does not vary much with the nature of the paraffin chain, but there is considerable variation in the entropy change. Doescher[170] and Wise[171] report equilibrium data on the dissociation of F_2. Kistiakowsky, Knight & Malin[172] from measurements on detonation velocities of cyanogen-oxygen mixtures, and Thomas, Gaydon & Brewer[173] from flame temperature measurements agree that the dissociation energy of N_2 is 9.76 e.v.

Thermodynamic Properties from Electrochemical Cell Measurements

Values of free energies (and sometimes heats) of formation deduced from electromotive force data are: Suzuki,[174,175] AgN_3, TlN_3, TlCNS; Koerber & De Vries,[176] PbF_2, HgF_2 and CuF_2. The standard potential of the half-reaction GeO (brown) + $H_2O = GeO_2 + 2H^+ + 2e^-$ and the free energy difference of the yellow and brown forms of GeO is given by Jolly & Latimer.[177] Connick & Hurley[178] give potentials for the couples $RuO_4^=$ - RuO_4^- and $RuO_2 \cdot xH_2O$ - RuO_4^-. Jolly[179] summarizes data on ionic heats, free energies and entropies in liquid ammonia. From cell measurements Hachtrieb & Fryxell[180] show that the anomalous distribution coefficient of $FeCl_3$ between aqueous HCl and isopropyl ether is due to an abnormally low activity coefficient of $FeCl_3$ in the ether phase.

Miscellaneous

Ramberg[181] reviews the data on heats of formation from the oxides of oxysalts of mineralogical importance and shows the trends with position in

the periodic table. Hart[182] examines the periodicity of chemical thermodynamic functions and finds that correlation with position in the periodic table is best shown if values per equivalent (rather than per mole) are used.

Statistical Calculation of Thermodynamic Properties of Gases

A number of papers has appeared presenting calculations of the thermodynamic functions $(F^o - H_o^o)/T$, $(H^o - H_o^o)$, S^o and C_p^o, of ideal gas molecules. Articles in which the calculation is made to the rigid rotator-harmonic oscillator approximation, requiring only a knowledge of the moments of inertia and the fundamental vibration frequencies, are: McDonald,[183] OD; Cleveland & Klein,[184] O_3; Stephenson & Jones,[185] NOF; Voelz,[186] GeF_4; Voelz, Meister & Cleveland,[187] SiF_4 (correction of earlier paper); Davis, Cleveland & Meister[188] CCl_2Br_2; Günthard & Kováts,[189] CH_3CN; Ferigle & Weber,[190] diacetylene. The calculations of Scheer[191] on ClF_3 are criticized by Weber & Ferigle.[192] More refined calculations in which correction is made for anharmonicity of the vibrations and for rotational stretching are given by: Evans & Wagman,[193] S, S_2, SO, SO_2, SO_3, H_2S; Cole, Farber & Elverum,[194] F, F_2, HF; Cole & Elverum,[195] ClF, BrF, IF, BrCl, ICl, IBr. In many cases use is made of existing equilibrium or thermal data to choose values of ΔH_o^o for reactions and the calculated equilibrium constants are tabulated. Waring[196] has reviewed the thermodynamic properties of formic acid. Keller & Johnston[197] calculate an approximate entropy for decaborane. Murphy & Rubin[198] point out that the experimental value for the entropy of F_2 is inconsistent with the spectroscopically calculated one and suggest that there may be an overlooked transition in the solid near 50°K. Other references to statistical calculations of thermodynamic data will be found under Heat Capacities, Heat Contents and Entropies.

Helium

The heat capacity of liquid helium has been measured by Hull, Wilkinson & Wilks[199] between 0.6 and 1.6°K and by Kramers, Wasscher & Gorter[200] between 0.25 and 1.9°K. The data are in substantial agreement. The most interesting result is that below 0.6°K the heat capacity varies as T^3 and is consistent with that expected from a Debye-like frequency spectrum of longitudinal vibrations only. Above 0.6°K the heat capacity rises much more rapidly than T^3 due to the still incompletely understood excitation process which culminates in the maximum at the lambda-point. The new low-temperature heat capacity data permit, through the use of the third law of thermodynamics, more accurate calculations of the entropy of liquid helium which are in better agreement with fountain-effect measurements than the old values. Berman & Poulter[201] have measured the volume of vapor evolved from a calorimeter containing liquid helium when a given amount of electrical energy is introduced. In order to calculate heats of vaporization from their data, it is necessary to know the gas density at the vaporization temperature and the undertainty in this quantity is the major source of error. An accurate determination of equation of state data on helium gas is badly needed in order to make precise correlation of thermodynamic data on helium. In connection with thermal conductivity measurements Webb, Wilkinson & Wilks[202] have measured the heat capacity of solid helium at three different densities.

Because of the large compressibility, there is a considerable decrease of heat capacity with pressure. Swenson[203] has reported data on the solidification curve of helium between 1.6 and 4°K by a method which involves observation of the isobaric volume change on solidification or melting. He also obtained data for the heat of fusion which agree well with those calculated from the Clausius-Clapeyron equation using the observed volume changes and values of dP/dT. If the lambda transition from liquid He I to He II is really second order, one may calculate from the Ehrenfest equations relations that must be satisfied among various higher order derivatives at the point where He I, He II and solid He are in equilibrium. The observed change in the temperature derivative of the volume change on melting agrees with the experimental value, but there is a discrepancy in the change of d^2P/dT^2 along the melting curve. Near the transition, however, dP/dT is changing rapidly and it is not sure that the discrepancy is beyond experimental error. The very surprising results on the melting curve of helium reported by Cwilong,[204] which were inconsistent with all previous data, were later found by him to be in error.

Theoretical

Ward & Wilks[205] show that second sound and the thermo-mechanical effect in helium at very low temperatures may be understood in terms of elastic collisions between phonons without the need for a two-fluid theory. Kramers[206] discusses the general question of the excitations in the liquid at higher temperatures. A molecular theory of liquid helium based on the cell model of Lennard-Jones and Devonshire is given by Prigogine & Philippot.[207] There is an important effect of the nuclear statistics on the calculated properties. Recent review articles on helium are: Atkins,[208] "Wave propagation and flow in liquid helium II;" Daunt,[209] "Properties of helium three;" Dingle,[210] "Theories of helium II."

Solutions of Helium Isotopes

The spectacular deviations from ideal solution behavior shown by mixtures of helium isotopes three and four has continued to attract investigation. Daunt & Heer[211] report equilibrium liquid-vapor concentrations for a solution about one per cent in He^3. The quantitative results are uncertain because of difficulties with the mass spectrometer analysis, but qualitatively the results are in agreement with the theory of Heer & Daunt.[212] This theory treats the solutions as a statistically independent mixture of Fermi-Dirac (He^3) and Bose-Einstein (He^4) ideal gases. The gas molecules are assumed in smoothed potential wells and there is assumed to be no volume change on mixing. The parameters are adjusted to fit the properties of He^4. The anomalous properties of the solutions arise entirely from the quantum statistics. The theory has been extended by Daunt, Tseng & Heer.[213] Sommers[214] reports a careful series of measurements on He^3 - He^4 solutions at concentrations up to 80 per cent He^3 in the vapor and at temperatures between 1.30 and 2.18°K. There are significant quantitative deviations from all theories of these solutions that have been advanced. De Boer & Gorter[215] emphasize that there is, in a solution which undergoes a second order transition, a discontinuity in the temperature coefficient of the vapor-liquid concentration ratio at the lambda-point. This was shown in a previous thermodynamic treatment[216] of second order transitions in two-component systems.

Properties of Pure He^3

Measurements of the melting pressure of He^3 have been extended down to 0.16°K by Weinstock, Abraham & Osborne.[217] Between 0.5 and 1.5°K the results may be represented by the equation $P = 26.8 + 13.1\ T^2$ atm. Below 0.5°K the observed melting pressures vary less rapidly with temperature, but this may be partly due to poor thermal equilibrium between the He^3 and the paramagnetic salt used. From the Clapeyron equation, $dP/dT = \Delta S/\Delta V$, and the melting pressure data one can conclude that, at temperatures of 0.5°K and higher, the entropy of liquid He^3 is greater than that of the solid. Since in the solid one would expect the nuclear spin entropy of R ln 2 to persist to temperatures of 0.01°K or lower, the conclusion is that at 0.5°K there is no appreciable nuclear alignment in the liquid. Pomeranchuk[218] predicted that because of the Fermi-Dirac statistics nuclear alignment would occur in the liquid at below about 1°K and the entropy would become less than R ln 2. This would cause the melting pressure to rise at lower temperatures since ΔS would change sign. No such effect has been observed. Singwi[219] showed that the vapor pressure data reported by the Argonne workers[220] could be fitted on the assumption that the liquid has the entropy calculated for an ideal Fermi-Dirac gas of mass 3 and with the density of liquid He^3. However, this model would also give a liquid entropy less than R ln 2 at 0.5°K and is inconsistent with the melting pressure data. In reviewing the situation, Weinstock, Abraham & Osborne[221] deduce an expression for the entropy of liquid He^3 consistent with both the vapor pressure and melting data and conclude that in the actual liquid nuclear alignment must occur at an appreciably lower temperature than would be predicted for an ideal Fermi-Dirac gas at the same density.

Miscellaneous Topics

Mendelssohn[222] has discussed the adiabatic magnetization of superconductors as a method of obtaining temperatures below 1°K. Although the entropy changes are small compared to those of paramagnetic salts, the relatively small magnetic fields required and the fact that the heat capacity of the normal metal rises with temperature so there is increased thermal stability at higher temperatures may make superconductors preferable for some applications. Schmitt[223] has investigated adiabatic thermal changes in barium titanate ceramic at helium temperatures. The apparent large temperature coefficient of dielectric constant in this ferroelectric material arises from a change in the ease of rotation of domains which is an irreversible process. As in a ferromagnetic substance, there is no appreciable change in entropy upon application of a field and the only thermal effects observed were due to the irreversible production of heat occurring both upon application and removal of a field. Rothstein[224] discusses the relationship betwen information as defined in communication theory and entropy. A good earlier treatment of this topic is that of Brillouin.[225] A related question is the Gibbs paradox, the classical discontinuity in the entropy of mixing of two gases which are gradually made identical. Landé[226] concludes that from the non-existence of this discontinuity one can derive the necessity for a quantum theory, although not, of course, the value of Planck's constant.

Thermodynamics of Irreversible Processes

There is continued interest in the theory of steady state processes in

which some inherently irreversible process is taking place. In many cases the logically more satisfying treatment based on the Onsager reciprocity relations leads to the same result as the classical treatment in which the irreversible part of the process was ignored. Examples are the Kelvin treatment of electromotive force and London's derivation of the fountain-effect equation in helium. In some cases, however, new relationships are predicted and it is hoped that the theoretical work will stimulate experiments in this field. Papers appearing in 1952 are: Callen,[227] thermomagnetic effects; Callen & Greene,[228] a generalization of the Nyquist electrical noise formula; Tolhoek & de Groot,[229] the first law of thermodynamics in systems with flow of matter across the boundaries; Denbigh,[230] heat of transport in binary regular solutions; Staverman,[231] membrane processes; Tyrrell & Hollis,[232] thermal diffusion potentials in non-isothermal electrolytic systems; Davies,[233] the Joule-Kelvin effect. Unlike other workers, Verschaffelt[234,235] does not use the Onsager relations, but employs a principle of superposition in discussing transport phenomena. His treatment is criticized by Overbeek & Mazur[236] and by Davies.[237]

New Methods and Apparatus

Borovik-Romanov and Strelkov[238] describe a new gas thermometer in which a pressure-sensitive diaphragm is used to minimize the dead space volume. They report measurements of the boiling points of normal and of equilibrium hydrogen. Michels, Wassenaar & Zwietering[239] describe an apparatus for measuring PVT data of gases which uses a diaphragm sensitive to one thousandth atmosphere. In measurements on dry air, a consistency of one part in a hundred thousand was obtained. Clement & Quinnell[240] and Geballe et al[241] have investigated carbon resistance thermometers for use at low temperatures. The latter investigators studied the effect of particle size and of gas adsorption. Giauque et al[242] report data on the properties of a methyl methacrylate plastic (Plexiglas) for use in calorimetric and magnetic investigations at very low temperatures.

References

1. Rossini, F. D., Gucker, F. T., Jr., Johnston, H. L., Pauling, L., and Vinal, G. W., J. Am. Chem. Soc. 74, 2699 (1952).
2. Rossini, F. D., Wagman, D. D., Evans, W. H., Levine, S., and Jaffe, I., Selected Values of Chemical Thermodynamic Properties, Natl. Bur. Standards (U. S.) Circular 500 (1952).
3. Beattie, J. A., Douslin, D. R., and Levine, S. W., J. Chem. Phys. 20, 1619 (1952).
4. Beattie, J. A., Levine, S. W., and Douslin, D. R., J. Am. Chem. Soc., 74, 4778 (1952).
5. Beattie, J. A., Brierley, J. S., and Barriault, R. J., J. Chem. Phys., 20, 1613 (1952).
6. Beattie, J. A., Brierley, J. S., and Barriault, R. J., J. Chem. Phys., 20, 1615 (1952).
7. Michels, A., Visser, A., Lunbeck, R. J., and Wolkers, G. J., Physica, 18, 114 (1952).
8. Michels, A., Lupton, J. M., Wassenaar, T., and de Graaff, W., Physica, 18, 121, 128 (1952).
9. Lunbeck, R. J., Michels, A., and Wolkers, G. J., Applied Sci. Research,

[A] 3, 197 (1952).
10. Hamann, S. D., and Pearse, J. F., Trans. Faraday Soc., 48, 101 (1952).
11. Korvezee, A. E., Rec. trav. chim., 70, 697 (1951).
12. Francis, P. G., McGlashan, M. L., Hamann, S. D., and McManamey, W. J., J. Chem. Phys. 20, 1341 (1952).
13. Fox, J. H. P., and Lambert, J. D., Proc. Roy. Soc. (London), [A] 210, 557 (1952).
14. Casado, F. L., Massie, D. S., and Whytlaw-Gray, R., Proc. Roy. Soc. (London), [A] 214, 446 (1952).
15. Fickett, W., and Wood, W. W., J. Chem. Phys., 20, 1624 (1952).
16. Hamann, S. D., Trans. Faraday Soc., 48, 303 (1952).
17. Roe, G. M., Epstein, L. F., and Powers, M. D., J. Chem. Phys., 20, 1665 (1952).
18. Epstein, L. F., and Hibbert, C. J., J. Chem. Phys. 20, 752 (1952).
19. Epstein, L. F., J. Chem. Phys. 20, 1670 (1952).
20. Cottrell, T. L., and Paterson, S., Proc. Roy. Soc. (London), [A] 213, 214 (1952)
21. Mayer, J. E., and Careri, G., J. Chem. Phys., 20, 1001 (1952).
22. Himpan, J., Compt. rend., 234, 2523 (1952); Z. Physik, 131, 17, 130 (1951).
23. Weinberger, M. A., and Schneider, W. G., Can. J. Chem., 30, 422 (1952).
24. Weinberger, M. A., and Schneider, W. G., Can. J. Chem., 30, 847 (1952).
25. Murray, F. E., and Mason, S. G., Can. J. Chem., 30, 550 (1952).
26. Weinberger, M. A., Habgood, H. W., and Schneider, W. G., Can. J. Chem., 30, 815 (1952).
27. Zimm, B. H., J. Chem. Phys., 20, 538 (1952).
28. Rowden, R. W., and Rice, O. K., J. Chem. Phys., 19, 1423 (1951).
29. Goldstein, L., Phys. Rev., 85, 35 (1952).
30. Alder, B. J., and Jura, G., J. Chem. Phys., 20, 1491 (1952).
31. Anderson, R., Schnizlein, J. G., Toole, R. C., and O'Brien, T. D., J. Phys. Chem., 56, 473 (1952).
32. Stephenson, C. C., Blue, R. W., and Stout, J. W., J. Chem. Phys., 20, 1046 (1952).
33. Levy, H. A., and Peterson, S. W., Phys. Rev., 86, 766 (1952).
34. Stephenson, C. C., Landers, L. A., and Cole, A. G., J. Chem. Phys., 20, 1044 (1952).
35. Stephenson, C. C., and Adams, H. E., J. Chem. Phys., 20, 1658 (1952).
36. Kondo, S., and Oda, T., J. Chem. Phys. 20, 1659 (1952).
37. Powles, J. G., Trans. Faraday Soc., 48, 430 (1952).
38. Smoluchowski, R., Mayer, J. E., and Weyl, W. A., Phase Transformations in Solids (Wiley, New York, 1951).
39. Michels, A., Wassenaar, T., and Zwietering, Th. N., Physica, 18, 63 (1952).
40. Brooks, L. S., J. Am. Chem. Soc., 74, 227 (1952).
41. Edwards, J. W., Johnston, H. L., and Blackburn, P. E., J. Am. Chem. Soc., 74, 1539 (1952).
42. Gulbransen, E. A., and Andrew, K. F., J. Electrochem. Soc., 99, 402 (1952).
43. Searcy, A. W., J. Am. Chem. Soc., 74, 4789 (1952).
44. Burns, W. G., and Dainton, F. W., Trans. Faraday Soc., 48, 21 (1952).
45. Schnizlein, J. G., Sheard, J. L., Toole, R. C., and O'Brien, T. D., J.

Phys. Chem., 56, 233 (1952).
46. Schäfer, H., and Krehl, K., Z. anorg. allgem. Chem., 268, 25 (1952).
47. Schäfer, H., and Krehl, K., Z. anorg. allgem. Chem., 268, 35 (1952).
48. Schäfer, H., Bayer, L., and Lehmann, H., Z. anorg. allgem. Chem., 268, 268 (1952).
49. Junkins, J. H., Farrar, R. L., Barber, E. J., and Bernhardt, H. A., J. Am. Chem. Soc., 74, 3464 (1952).
50. Junkins, J. H., Bernhardt, H. A., and Barber, E. J., J. Am. Chem. Soc., 74, 5749 (1952).
51. Jolly, W. L., and Latimer, W. M., J. Am. Chem. Soc., 74, 5754 (1952).
52. Shapiro, E., J. Am. Chem. Soc., 74, 5233 (1952).
53. Michels, A., Wassenaar, T., and Zwietering, Th. N., Physica, 18, 160 (1952).
54. Allen, P. W., Everett, D. H., and Penney, M. F., Proc. Roy. Soc. (London), [A] 212, 149 (1952).
55. Edwards, G., Trans. Faraday Soc., 48, 513 (1952).
56. Day, H. O., with Felsing, W. A., J. Am. Chem. Soc., 74, 1951 (1952).
57. Milton, H. T., and Oliver, G. D., J. Am. Chem. Soc., 74, 3951 (1952).
58. Stiles, V. E., and Cady, G. H., J. Am. Chem. Soc., 74, 3771 (1952).
59. Doehaerd, T., Goldfinger, P., and Waelbroeck, F., J. Chem. Phys., 20, 757 (1952).
60. Waelbroeck, F., J. Chem. Phys., 20, 757 (1952).
61. Brewer, L., Giles, P. W., and Jenkins, F. A., J. Chem. Phys., 16, 797 (1948).
62. Brewer, L., J. Chem. Phys. 20, 758 (1952).
63. Farber, M., and Darnell, A. J., J. Am. Chem. Soc., 74, 3941 (1952).
64. Brown, O. L. I., J. Am. Chem. Soc., 74, 6096 (1952).
65. Simons, J. H., and Hickman, J. B., J. Phys. Chem., 56, 420 (1952).
66. Kilner, S. B., J. Am. Chem. Soc., 74, 5221 (1952).
67. Jura, G., and Pitzer, K. S., J. Am. Chem. Soc., 74, 6030 (1952).
68. Law, J. T., J. Chem. Phys., 20, 1329 (1952).
69. Hu, J., and Johnston, H. L., J. Am. Chem. Soc., 74, 4771 (1952).
70. Adams, G. B., Jr. and Johnston, H. L., J. Am. Chem. Soc., 74, 4788 (1952).
71. Oliver, G. D., and Grisard, J. W., J. Am. Chem. Soc., 74, 2705 (1952).
72. Todd, S. S., and Coughlin, J. P., J. Am. Chem. Soc., 74, 525 (1952).
73. Todd, S. S., and Lorenson, R. E., J. Am. Chem. Soc., 74, 3764 (1952).
74. Todd, S. S., J. Am. Chem. Soc., 74, 4669 (1952).
75. Todd, S. S., and Lorenson, R. E., J. Am. Chem. Soc., 74, 2043 (1952).
76. Jones, W. M., Gordon, J., and Long, E. A., J. Chem. Phys., 20, 695 (1952).
77. Rubin, T. R., and Giauque, W. F., J. Am. Chem. Soc., 74, 800 (1952).
78. Kunzler, J. E., and Giauque, W. F., J. Am. Chem. Soc., 74, 797 (1952).
79. Busey, R. H., and Giauque, W. F., J. Am. Chem. Soc., 74, 4443 (1952).
80. Friedberg, S. A., Physica, 18, 714 (1952).
81. Gebaile, T. H., and Giauque, W. F., J. Am. Chem. Soc., 74, 3513 (1952).
82. Scott, D. W., Douslin, D. R., Gross, M. E., Oliver, G. D., and Huffman, H. M., J. Am. Chem. Soc., 74, 883 (1952).
83. Scott, D. W., Finke, H. L., McCullough, J. P., Gross, M. E., Pennington, R. E., and Waddington, G., J. Am. Chem. Soc., 74, 2478 (1952).
84. Guthrie, G. B., Jr., Scott, D. W., and Waddington, G., J. Am. Chem.

Soc., 74, 2795 (1952).
85. McCullough, J. P., Scott, D. W., Finke, H. L., Gross, M. E., Williamson, K. D., Pennington, R. E., Waddington, G., and Huffman, H. M., J. Am. Chem. Soc., 74, 2801 (1952).
86. Finke, H. L., Scott, D. W., Gross, M. E., Waddington, G., and Huffman, H. M., J. Am. Chem. Soc., 74, 2804 (1952).
87. Scott, D. W., Finke, H. L., Hubbard, W. N., McCullough, J. P., Oliver, G. D., Gross, M. E., Katz, C., Williamson, K. D., Waddington, G., and Huffman, H. M., J. Am. Chem. Soc., 74, 4656 (1952).
88. Guthrie, G. B., Jr., Scott, D. W., Hubbard, W. N., Katz, C., McCullough, J. P., Gross, M. E., Williamson, K. D., and Waddington, G., J. Am. Chem. Soc., 74, 4662 (1952).
89. Hubbard, W. N., Finke, H. L., Scott, D. W., McCullough, J. P., Katz, C., Gross, M. E., Messerly, J. F., Pennington, R. E., and Waddington, G., J. Am. Chem. Soc., 74, 6025 (1952).
90. Stephenson, C. C., and Berets, J. D., J. Am. Chem. Soc., 74, 882 (1952).
91. Furukawa, G. T., McCoskey, R. E., and King, G. J., J. Research Natl. Bur. Standards, 49, 273 (1952).
92. Pomerantz, P., J. Research Natl. Bur. Standards, 48, 76 (1952).
93. Chem. Eng. News, 27, 2772 (1949).
94. Douglas, T. B., Ball, A. F., Ginnings, D. C., and Davis, W. D., J. Am. Chem. Soc., 74, 2472 (1952).
95. Busey, R. H., and Giauque, W. F., J. Am. Chem. Soc., 74, 3157 (1952).
96. Geballe, T. H., and Giauque, W. F., J. Am. Chem. Soc., 74, 2368 (1952).
97. Adams, G. B., Jr., Johnston, H. L., and Kerr, E. C., J. Am. Chem. Soc., 74, 4784 (1952).
98. Clusius, K., and Schachinger, L., Z. Naturforsch., 7a, 185 (1952).
99. Hill, R. W., and Parkinson, D. E., Phil. Mag., 43, 309 (1952).
100. Pearlman, N., and Keesom, P. H., Phys. Rev., 88, 398 (1952).
101. Clement, J. R., and Quinnell, E. H., Natl. Bur. Standards (U. S.) Circular, 519 (1952), p. 89.
102. Clement, J. R., and Quinnell, E. H., Phys. Rev., 85, 502 (1952).
103. Brown, A., Zemansky, M. W., and Boorse, H. A., Phys. Rev., 86, 134 (1952).
104. Horowitz, M., Silvidi, A. A., Malaker, S. F., and Daunt, J. G., Phys. Rev., 88, 1182 (1952).
105. Keesom, P. H., and Pearlman, N., Phys. Rev., 88, 140 (1952).
106. Friedberg, S. A., Estermann, I., and Goldman, J. E., Phys. Rev., 85, 375 (1952).
107. Estermann, I., Friedberg, S. A., and Goldman, J. E., Phys. Rev., 87, 582 (1952).
108. Zener, C., Phys. Rev., 81, 440 (1951).
109. Slater, J. C., Phys. Rev., 49, 537 (1936).
110. Fletcher, G. C., and Wohlfarth, E. P., Phil. Mag., 42, 106 (1951).
111. Wexler, A., and Corak, W. S., Phys. Rev., 85, 85 (1952).
112. Goodman, B. B., Natl. Bur. Standards (U. S.) Circular 519 (1952), p. 71.
113. Smith, T. S., and Daunt, J. G., Phys. Rev., 88, 1172 (1952).
114. Stout, J. W., and Guttman, L., Phys. Rev., 88, 703 (1952).
115. Guttman, L., and Stout, J. W., Natl. Bur. Standards (U. S.) Circular 519 (1952), p. 65.
116. Love, W. F., Callen, E., and Nix, F. C., Phys. Rev., 87, 844 (1952).

117. Maxwell, E., Phys. Rev., 86, 235 (1952).
118. Reynolds, C. A., Serin, B., and Nesbitt, L. B., Natl. Bur. Standards (U. S.) Circular 519 (1952), p. 27.
119. Worley, R. D., Zemansky, M. W., and Boorse, H. A. Phys. Rev., 87, 1142 (1952).
120. Maxwell, E. Phys. Rev., 87, 1126 (1952).
121. Garfunkel, M. P., Phys. Rev., 87, 108 (1952).
122. Pippard, A. B., Phil. Mag., 43, 273 (1952).
123. Marcus, P. M., Phys. Rev., 88, 373 (1952).
124. Masi, J. F., and Petkof, B., J. Research Natl. Bur. Standards, 48, 179 (1952).
125. Michels, A., and Strijland, J., Physica, 18, 613 (1952).
126. Masi, J. F., J. Am. Chem. Soc., 74, 4738 (1952).
127. McCullough, J. P., Pennington, R. E., and Waddington, G., J. Am. Chem. Soc., 74, 4439 (1952).
128. Barrow, G. M., J. Chem. Phys., 20, 1739 (1952).
129. Ito, K., J. Chem. Phys. 20, 531 (1952).
130. Holley, C. E., Jr., Huber, E. J., Jr., and Meierkord, E. H., J. Am. Chem. Soc., 74, 1084 (1952).
131. Huber, E. J., Jr., Holley, C. E., Jr., and Meierkord, E. H., J. Am. Chem. Soc., 74, 3406 (1952).
132. Huber, E. J., Jr., and Holley, C. E., Jr., J. Am. Chem. Soc., 74, 5530 (1952).
133. Humphrey, G. L., and King, E. G., J. Am. Chem. Soc., 74, 2041 (1952).
134. Humphrey, G. L., King, E. G., and Kelley, K. K., U. S. Bur. Mines Rept. Invest. No. 4870 (1952).
135. Koerner, W. E., and Daniels, F., J. Chem. Phys., 20, 113 (1952).
136. Quarterman, L., and Primak, W., J. Am. Chem. Soc., 74, 806 (1952).
137. Nelson, R. A., and Jessup, R. S., J. Research Natl. Bur. Standards, 48, 206 (1952).
138. Aston, J. G., Rock, E. J., and Isserow, S., J. Am. Chem. Soc., 74, 2484 (1952).
139. Hubbard, W. N., Katz, C., Guthrie, G. B., Jr., and Waddington, G., J. Am. Chem. Soc., 74, 4456 (1952).
140. Cotton, F. A., and Wilkinson, G., J. Am. Chem. Soc., 74, 5764 (1952).
141. Bender, P., and Farber, J., J. Am. Chem. Soc., 74, 1450 (1952).
142. Carson, A. S., Carson, E. M., and Wilmshurst, B., Nature, 170, 320 (1952).
143. Mortimer, C. T., Pritchard, H. O., and Skinner, H. A., Trans. Faraday Soc., 48, 220 (1952).
144. Nelson, R. A., Jessup, R. S., and Roberts, D. E., J. Research Natl. Bur. Standards, 48, 275 (1952).
145. Gilpin, V., and Winkler, C. A., Can. J. Chem., 30, 743 (1952).
146. Breitenbach, J. W., Derkosch, J., and Wessely, F., Nature, 169, 922 (1952).
147. Lacher, J. R., Billings, T. J., Campion, D. E., Lea, K. R., and Park, J. D., J. Am. Chem. Soc., 74, 5291 (1952).
148. Lacher, J. R., Scruby, R. E., and Park, J. D., J. Am. Chem. Soc., 74, 5292 (1952).
149. Jolly, W. L., and Latimer, W. M., J. Am. Chem. Soc., 74, 5752 (1952).
150. Bender, P., and Biermann, W. J., J. Am. Chem. Soc., 74, 322 (1952).

151. Van Artsdalen, E. R., and Dworkin, A. S., J. Am. Chem. Soc., 74, 3401 (1952).
152. Charnley, T., Skinner, H. A., and Smith, N. B., J. Chem. Soc., 1952, 2288.
153. Westrum, E. F., Jr. and Eyring, L., J. Am. Chem. Soc., 74, 2045 (1952).
154. Spedding, F. H., and Miller, C. F., J. Am. Chem. Soc., 74, 4195 (1952).
155. King, E. G., J. Am. Chem. Soc., 74, 4446 (1952).
156. Logan, A. V., Bush, D. C., and Rogers, C. J., J. Am. Chem. Soc., 74, 4194 (1952).
157. Eyring, L., Lohr, H. R., and Cunningham, B. B., J. Am. Chem. Soc., 74, 1186 (1952).
158. Evans, D. F., and Richards, R. E., J. Chem. Soc., 1952, 1292.
159. Li, J. C. M., and Gregory, N. W., J. Am. Chem. Soc., 74, 4670 (1952).
160. Katzin, L. I., Simon, D. M., and Ferraro, J. R., J. Am. Chem. Soc., 74, 1191 (1952).
161. Katzin, L. I., and Ferraro, J. R., J. Am. Chem. Soc., 74, 6040 (1952).
162. Jolly, W. L., and Latimer, W. M., J. Am. Chem. Soc., 74, 5757 (1952).
163. Koch, C. W., Broido, A., and Cunningham, B. B., J. Am. Chem. Soc., 74, 2349 (1952).
164. Chiche, P., Ann. chimie, 7, 361 (1952).
165. Wunderlich, G., Z. Elektrochem., 56, 218 (1952).
166. Altman, D., and Adelman, B., J. Am. Chem. Soc., 74, 3742 (1952).
167. Taylor, M. D., and Bruton, J., J. Am. Chem. Soc., 74, 4151 (1952).
168. Lundin, R. E., Harris, F. E., and Nash, L. K., J. Am. Chem. Soc., 74, 743 (1952).
169. Lundin, R. E., Harris, F. E., and Nash, L. K., J. Am. Chem. Soc., 74, 4654 (1952).
170. Doescher, R. N., J. Chem. Phys., 20, 330 (1952).
171. Wise, H., J. Chem. Phys., 20, 927 (1952).
172. Kistiakowsky, G. B., Knight, H. T., and Malin, M. E., J. Chem. Phys., 20, 876 (1952).
173. Thomas, N., Gaydon, A. G., and Brewer, L., J. Chem. Phys., 20, 369 (1952).
174. Suzuki, S., J. Chem. Soc. Japan, 73, 150 (1952).
175. Suzuki, S., J. Chem. Soc. Japan, 73, 153 (1952).
176. Koerber, G. G., and De Vries, T., J. Am. Chem. Soc., 74, 5008 (1952).
177. Jolly, W. L., and Latimer, W. M., J. Am. Chem. Soc., 74, 5751 (1952).
178. Connick, R. E., and Hurley, C. R., J. Am. Chem. Soc., 74, 5012 (1952).
179. Jolly, W. L., Chem. Rev., 50, 351 (1952).
180. Nachtrieb, N. H., and Fryxell, R. E., J. Am. Chem. Soc., 74, 897 (1952).
181. Ramberg, H., J. Chem. Phys., 20, 1532 (1952).
182. Hart, D., J. Phys. Chem., 56, 202 (1952).
183. McDonald, G., J. Am. Chem. Soc., 74, 5539 (1952).
184. Cleveland, F. F., and Klein, M. J., J. Chem. Phys., 20, 337 (1952).
185. Stephenson, C. V., and Jones, E. A., J. Chem. Phys. 20, 135 (1952).
186. Voelz, F. L., J. Chem. Phys., 20, 1662 (1952).
187. Voelz, F. L., Meister, A. G., and Cleveland, F. F., J. Chem. Phys., 20, 1498 (1952).
188. Davis, A., Cleveland, F. F., and Meister, A. G., J. Chem. Phys., 20,

454 (1952).
189. Günthard, H. H., and Kováts, E., Helv. Chim. Acta, 35, 1190 (1952).
190. Ferigle, S. M., and Weber, A., J. Chem. Phys., 20, 1657 (1952).
191. Scheer, M. D., J. Chem. Phys., 20, 924 (1952).
192. Weber, A., and Ferigle, S. M., J. Chem. Phys., 20, 1497 (1952).
193. Evans, W. H., and Wagman, D. D., J. Research Natl. Bur. Standards, 48, 141 (1952).
194. Cole, L. G., Farber, M., and Elverum, G. W., Jr., J. Chem. Phys., 20, 586 (1952).
195. Cole, L. G., and Elverum, G. W., Jr., J. Chem. Phys., 20, 1543 (1952).
196. Waring, W., Chem. Revs., 51, 171 (1952).
197. Keller, W. E., and Johnston, H. L., J. Chem. Phys., 20, 1749 (1952).
198. Murphy, G. M., and Rubin, E., J. Chem. Phys., 20, 1179 (1952).
199. Hull, R. A., Wilkinson, K. R., and Wilks, J., Proc. Phys. Soc. (London), [A] 64, 379 (1951).
200. Kramers, H. C., Wasscher, J. D., and Gorter, C. J., Physica, 18, 329 (1952).
201. Berman, R., and Poulter, J., Phil. Mag., 43, 1047 (1952).
202. Webb, F. J., Wilkinson, K. R., and Wilks, J., Proc. Roy. Soc. (London) [A] 214, 546 (1952).
203. Swenson, C. A., Phys. Rev., 86, 870 (1952).
204. Cwilong, B. M., Phys. Rev., 88, 135, 1435 (1952).
205. Ward, J. C., and Wilks, J., Phil. Mag., 43, 48 (1952).
206. Kramers, H. A., Physica, 18, 653 (1952).
207. Prigogine, I., and Philippot, J., Physica, 18, 729 (1952).
208. Atkins, K. R., Advances in Physics, 1, 169 (1952).
209. Daunt, J. G., Advances in Physics, 1, 209 (1952).
210. Dingle, R. B., Advances in Physics, 1, 111 (1952).
211. Daunt, J. G., and Heer, C. V., Phys. Rev., 86, 205 (1952).
212. Heer, C. V., and Daunt, J. G., Phys. Rev., 81, 447 (1951).
213. Daunt, J. G., Tseng, T. P., and Heer, C. V., Phys. Rev., 86, 911 (1952).
214. Sommers, H. S., Jr., Phys. Rev., 88, 113 (1952).
215. Boer, J. de, and Gorter, C. J., Physica, 18, 565 (1952).
216. Stout, J. W., Phys. Rev., 74, 605 (1948).
217. Weinstock, B., Abraham, B. M., and Osborne, D. W., Phys. Rev., 85, 158 (1952).
218. Pomeranchuk, I., J. Exptl. Theoret. Phys. (U. S. S. R.), 20, 919 (1950).
219. Singwi, K. S., Phys. Rev., 87, 540 (1952).
220. Abraham, B., Osborne, D. W., and Weinstock, B., Phys. Rev., 80, 366 (1950).
221. Weinstock, B., Abraham, B. W., and Osborne, D. W., Phys. Rev., (in press).
222. Mendelssohn, K., Nature, 169, 366 (1952).
223. Schmitt, R. W., Phys. Rev., 85, 1 (1952).
224. Rothstein, J., Phys. Rev., 85, 135 (1952).
225. Brillouin, L., J. Applied Phys., 22, 334, 338 (1951).
226. Landé, A., Phys. Rev., 87, 267 (1952).
227. Callen, H. B., Phys. Rev., 85, 16 (1952).
228. Callen, H. B., and Greene, R. F., Phys. Rev., 86, 702 (1952).
229. Tolhoek, H. A., and de Groot, S. R., Physica, 18, 780 (1952).
230. Denbigh, K. G., Trans. Faraday Soc., 48, 1 (1952).

231. Staverman, A. J., Trans. Faraday Soc., 48, 176 (1952).
232. Tyrell, H. J. V., and Hollis, G. L., Trans. Faraday Soc., 48, 893 (1952).
233. Davies, R. O., Physica, 18, 270 (1952).
234. Verschaffelt, J. E., Rec. trav. chim., 71, 705 (1952).
235. Verschaffelt, J. E., Physica, 18, 43 (1952).
236. Overbeek, J. Th. G., and Mazur, P., Rec. trav. chim., 71, 717 (1952).
237. Davies, R. O., Physica, 18, 182 (1952).
238. Borovik-Romanov, A. S., and Strelkov, P. G., Doklady Akad. Nauk S. S. S. R., 83, 59 (1952).
239. Michels, A., Wassenaar, T., and Zwietering, Th. N., Physica, 18, 67 (1952).
240. Clement, J. R., and Quinnell, E. H., Rev. Sci. Instruments, 23, 213 (1952).
241. Geballe, T. H., Lyon, D. N., Whelan, J. M., and Giauque, W. F., Rev. Sci. Instruments, 23, 489 (1952).
242. Giauque, W. F., Gebelle, T. H., Lyon, D. N., and Fritz, J. J., Rev. Sci. Instruments, 23, 169 (1952).

VI

NOTE ON FIELD EMISSION

Robert Gomer
Submitted to Journal of Chemical Physics

In a recent publication on the velocity distribution of electrons in field emission and its application to the field emission microscope[1] the statement occurs that an experimental determination of this distribution would be desirable. I am indebted to Professor E. Müller for calling my attention to the fact that he has performed this experiment.[2] He also pointed out to me that very similar conclusions to those reached in my paper[1] were drawn by Richter[3] who computed this velocity distribution at $T = 0^{\circ}K$ by a somewhat different method. I wish to take this opportunity to thank Professor Müller for calling my attention to these unfortunate omissions. Also, an error occurs in my paper in that reference (9) should refer to Professor Müller's paper in Z. Naturforsch., 5a, 473 (1950) instead of to Z. Physik, 131, 136 (1951).

References

1. R. Gomer, J. Chem. Phys. 20, 1172 (1952).
2. E. W. Müller, Z. Physik, 120, 261 (1943).
3. G. Richter, Z. Physik, 119, 406 (1942).

VII

PHASE EQUILIBRIUM IN THE SYSTEM CALCITE-ARAGONITE[+]

John C. Jamieson*

Abstract

The equilibrium curve for two of the phases of $CaCO_3$, calcite-aragonite, has been determined as a function of temperature and pressure over the range 25 - 80°C and several thousand kg/cm^2, using the electrical conductivity of aqueous solutions of each form. Aragonite is proved to be the high pressure modification. From the determined equilibrium curve, various thermodynamic quantities are obtained in a more accurate fashion than previously possible. All normal natural occurrences of aragonite must be due to metastable formation rather than equilibrium, since the geothermal gradient lies completely in the calcite field.

Introduction

The direct determination of the actual equilibrium curve with respect to temperature and pressure, of polymorphic forms exhibiting an irreversible transition, is difficult if not impossible. Hence an indirect approach must be made in terms of fundamental thermodynamic quantities. At any point on the (P,T) equilibrium curve, the Gibbs free energies of the two forms must be equal, so a determination of the free energy surfaces from thermal data gives immediately the equilibrium curve. Equally, the determination of any other property of the two forms, which is a single-valued function of their free energies, will give the equilibrium curve.

Two of the forms of $CaCO_3$, calcite and aragonite, are among the earliest known examples of a polymorphic pair, both having wide-spread geologic occurrence, but their actual stability fields have not previously been determined beyond the fact that aragonite is unstable with respect to calcite at all temperatures and moderate pressures, except possibly at low temperatures.

The method used to obtain the equilibrium curve for this polymorphic pair is the measurement of the electrical resistance of aqueous solutions of each form at high pressures and several temperatures. Then from these measurements the curve is extrapolated with the aid of thermal data.

Theoretical Background

Let G be the Gibbs free energy of a pure phase, S its entropy, V its volume, c_p its heat capacity at constant temperature, all in units per mole.

+ A dissertation submitted to the Faculty of the Division of the Physical Sciences in candidacy for the Degree of Doctor of Philosophy, University of Chicago.

* Now Post Ph.D. Fellow, National Science Foundation, Department of Geology, University of Chicago.

Then

$$\left(\frac{\partial G}{\partial T}\right)_P = -S \qquad \text{and} \qquad S = \int_O^T \frac{c_p}{T}\, dT \qquad (1)$$

where there are no phase transitions in the interval (O, T), and the integral is taken at constant pressure. Then for $P = P_o$,

$$G(P_o, T) - G(P_o, O) = -\int_O^T S dT. \qquad (2)$$

If the expression for c_p is known, then the function $\frac{G(P_o, T) - G(P_o, O)}{T}$ may be evaluated. This gives the Gibbs free energy of a phase as a function of temperature for a given pressure, but contains an as yet undetermined constant, namely $G(P_o, O)$, the free energy at P_o and the absolute zero of temperature. For the case of polymorphism, it is obvious that if the difference in free energy of the various forms is known for any one given temperature, then the difference in free energy is known for all temperatures, at the given pressure, for which adequate c_p data are available.

Anderson[1] has determined c_p for calcite and aragonite over the range 55 - 294°K, and lately these data have been extended by Kobayashi[2,3] up to a little under 800°K. It is of interest to calculate a point for calcite-aragonite equilibrium from these data first and then to compare it with the experimental results. It must be emphasized that these calculations bear only on the relative stability of the two forms and say nothing about the possibility of a third phase being the actual stable form of $CaCO_3$. This possibility must be taken care of by additional knowledge of the system.

Anderson[1] gives the two following expressions for the respective c_p:

$$c_p \text{ (calcite)} = D\left(\frac{180}{T}\right) + 2E\left(\frac{370}{T}\right) + 2E\left(\frac{1210}{T}\right)$$

$$c_p \text{ (aragonite)} = D\left(\frac{244}{T}\right) + 2E\left(\frac{342}{T}\right) + 2D\left(\frac{1897}{T}\right)$$

Kelley and Anderson[4] give $\Delta G(1,298.1) = G_c(1,298.1) - G_a(1,298.1) = -273$ cal/mole. The pressure is in kg/cm^2, the temperature in °K, the subscript "c" denotes calcite, and "a" denotes aragonite. (The calculations done before experimentation were based on these data.) More recently Kobayashi[2,3] has given values of $\frac{G(1,T) - G(1,O)}{T}$ obtained from his c_p measurements and those of Anderson[1] as reproduced partially in Table I. Kobayashi[2,3] also gives $\Delta G(1,298.1) = -311$ cal/mole, and $\Delta G(1,O) = -16$ cal/mole. From these data the equilibrium curve for calcite-aragonite could be calculated as in the following paragraphs.

For a pure phase $\left(\frac{\partial G}{\partial P}\right)_T = V(P,T)$, hence $G(P,T) - G(1,T) = \int_1^P V(P,T)\, dP$, where $V(P,T)$ is the mole volume. For calcite-aragonite we have $\Delta G(P,T) - \Delta G(1,T) = \int_1^P \Delta V(P,T)\, dP$. For the two forms to be in equilibrium at (P,T), $\Delta G(P,T) = 0$, hence $-\Delta G(1,T) = \int_1^P \Delta V(P,T)\, dP$. (3)

This equation when solved for P at a given T gives the (P,T) point at

TABLE I

Free Energy Data for Calcite-Aragonite at 1 kg/cm^2

T °K	$\frac{1}{T}(G_c - G_{co})$	$G_c - G_{co}$ cal/mole	$\frac{1}{T}(G_a - G_{ao})$	$G_a - G_{ao}$ cal/mole
298.1	- 10.68	- 3184	- 9.69	- 2889
300	- 10.75	- 3225	- 9.76	- 2928
320	- 11.53	- 3690	-10.53	- 3370
340	- 12.28	- 4175	-11.27	- 3832
360	- 13.02	- 4687	-12.00	- 4320

which aragonite and calcite are in equilibrium. To solve the equation, it is necessary to know the mole volume of each form as a function of pressure and temperature.

Birch, et al[5] give $\frac{\Delta V}{V_o}$ for calcite as follows: (The pressure has been converted from bars to kg/cm^2)

$$-\frac{\Delta V}{V_o} = 1.319\,(10)^{-6}\,P - 4.08(10)^{-12}\,P^2 \qquad \text{at } 303.1\ ^oK$$

$$-\frac{\Delta V}{V_o} = 1.344\,(10)^{-6}\,P - 4.30(10)^{-12}\,P^2 \qquad \text{at } 348.1\ ^oK$$

and for aragonite

$$-\frac{\Delta V}{V_o} = 1.52\,(10)^{-6}\,P \qquad \text{at } 273.1\ ^oK$$

The former was determined by Bridgman,[6] while the latter was determined from measurements by Madelung and Fuchs[7] only to a few hundred atmospheres. The change in compressibility of aragonite with temperature may be approximated by using Bridgman's[6] value for celestite ($SrSO_4$), which is orthorhombic as is aragonite, and possesses a compressibility of the same order of magnitude as that of aragonite. It seems better to use these more modern values rather than values such as are given by Voigt[8] which are calculated from elastic moduli, since the former are from actual measurements made under hydrostatic pressure. Thermal expansion data are given by Kozu and Kani[9] and Kozu, et al.[10] for atmospheric pressure. The values for the specific gravities may be found in Dana[11] as $\rho_c = 2.7102 \pm .0002$ at 20°C, $\rho_a = 2.947 \pm .002$, no temperature given. Thus from the above, plus Kobayashi's[2,3] value of $\Delta G(1, 298.1) = -311$ cal/mole, we obtain the equilibrium pressure of 4660 kg/cm^2 for 298.1°K. Calcite is the low pressure modification and aragonite is the high pressure modification of $CaCO_3$. This compares with an actually determined value of 3880 kg/cm^2, an error of 20 per cent. The major contribution to the error in this calculation is the uncertainty in the value of $\Delta G(1, 298.1)$, due to lack of knowledge of $\Delta G(O, O)$, which may be of the order of 10 - 15 per cent, hence this figure gives only a clue to the order of magnitude of pressure required, rather than a quantitative

result. However, in many situations, especially when dealing with substances of geologic interest, such a value may be the best obtainable. In the present case, similar calculations were carried out before experimental work was begun, in order to ascertain what range of pressure equipment would be needed.

Experimental Procedure

In order to determine experimentally the equilibrium curve between calcite and aragonite, the indirect approach of measuring the resistance of aqueous solutions of each form was used. This method can succeed only when the rate of transition from one form to the other is extremely slow, so that the unstable form can actually come to "equilibrium" with its solution. This point will be mentioned later in the description of the experimental results. At equilibrium of the two phases, the solubilities of each in water are equal, and hence, making the plausible assumption that the ions released by each are the same, with the same mobilities, the electrical conductivity of a solution of calcite is equal to that of a solution of aragonite at their (P,T) point of equilibrium. Since the conductivity is a function of the mobility of the ions, their charge, and number, it is possible that the conductivities should be equal at more than one pressure on each isotherm. However, for slightly soluble salts, the mobilities should be independent of which solid phase is present. In this case, the difference of the conductivities is a function only of the number of ions which are present.

It is to be noted that this method involves equilibrium of the two solid phases of $CaCO_3$ in a different thermodynamic environment, hence this equilibrium curve is not necessarily the same as that of the system without water. There are two factors to be taken into consideration, one is the possibility of H_2O entering into the calcite and aragonite lattices, and the other is the effect of a change in amount of CO_2 present in the H_2O. It is easily shown that for the case of H_2O entering into the solid phase in ideal solution, $P - P_o = \frac{RT}{\Delta\bar{V}} \ln \frac{C_c}{C_a}$, where P is the equilibrium pressure of the transition with H_2O in the respective lattices, P_o is the transition pressure of the two phases in the absence of H_2O, $\Delta\bar{V}$ is the difference in fictive mole volume between calcite and aragonite, C_c is the concentration of $CaCO_3$ in the calcite phase, C_a is the concentration of $CaCO_3$ in the aragonite phase, and the temperature is constant. Numerically we have for 300°K, $P - P_o = 8500 \ln \frac{C_c}{C_a}$ kg/cm^2, so even if there exists, say, 2 per cent of H_2O in the calcite phase and 1 per cent H_2O in the aragonite phase, the equilibrium pressure is changed only 85 kg/cm^2. It is estimated that the effect is actually much smaller than this.

In studying the second factor, Gibbs' Phase Rule informs us that with undersaturated CO_2 present in the liquid phase there are two degrees of freedom, i.e., the equilibrium curve is affected, while for CO_2 in excess, a fourth phase forms and there is a unique (P,T) equilibrium curve, but no necessarily that of the system in the absence of CO_2. However, the equilibrium curve is affected only to the extent that CO_2 is dissolved in the two $CaCO_3$ solid phases, which is governed by the amount of CO_2 in the H_2O. The change in equilibrium pressure for a constant temperature is again $P - P_o = \frac{RT}{\Delta\bar{V}} \ln \frac{C_c}{C_a}$ with the notation as previously defined except that P is

the equilibrium pressure with CO_2 in the lattices. This effect is negligible in the present case, since the amount of CO_2 in the H_2O is quite small.

The pressure was applied by the typical Bridgman apparatus for the range up to 15,000 atmospheres as has been described elsewhere by Kurnick,[12] except that an oil bath surrounding the bomb was used to maintain the temperature. The pressure was measured with a manganin gauge which has been calibrated against the freezing point of Hg, and a Wheatstone bridge to an absolute accuracy of .2 per cent. The temperature was measured with a Leeds & Northrup type K potentiometer, using a chromel P - alumel thermocouple inserted into a 3/4" deep hole drilled in the top of the bomb. The thermocouple was calibrated against the boiling point of H_2O. A calibration run, using an experimental plug with a thermocouple mounted in a hole drilled in the experimental plug to 1/4" of the experimental cavity, plus another junction in series with the first, extending to the middle of the chamber (Kurnick, 1952), gave agreement to 0.1°C with the bomb couple when the system was in thermal equilibrium. Hence an absolute accuracy of 0.5°C was obtained. The oil bath was regulated by a thermostat. At equilibrium, the temperature of the bomb was held $\pm$ 0.1°C, however there was as much as a degree difference from run to run even with the thermostat setting untouched. This was ascribed to the change in temperature of the tap water circulating in the connecting pipe, which served to keep the manganin pressure gauge at a uniform temperature.

The cell (Figure 1) was machined entirely from white virgin Teflon (polytetrafluoroethylene). It was constructed in the style of a hypodermic syringe, with a sliding section to separate the hexane, used as a pressure transmitting fluid, from the carbonate solutions, and to compensate for the differential compressibilities of the two fluids. The electrodes were supported by screwed-in plugs, which once in place were never removed. The tapped hole, in the top of the slide, was for a threaded chrome steel rod used in filling and handling the cell. The Pt electrodes were platinized. The theory of the cell was that at equal pressures, solutions of calcite and aragonite would have the same compressibility and hence have the same "cell constant" for a given pressure. The slide was always started out from the same position. Reproducibility of results and smoothness of curves were used as the proof of this hypothesis. After two early runs the cell gave results reproducible to 1 per cent. Since the isothermal curves were made up of points from several runs, their smoothness attested to no great variation in the cell itself from run to run. No effect was noted from the possible phase transition in Teflon at these pressures. By using difference plots the water correction cancelled out.

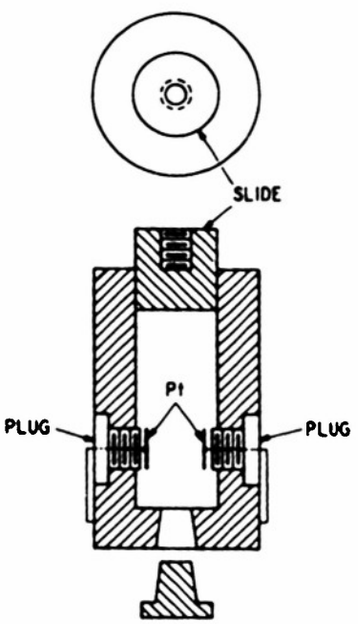

Figure 1. Conductivity cell for use at high pressures.

After platinization, several attempts were made to clean the cell by

boiling in HNO_3. The cell was found to be still contaminated and a steady fall in conductivity of a given solution with time was noticed. Alternate boilings of the cell in Methanol and double distilled water for a few days, followed by placing the cell under a 2 micron vacuum at room temperature for 12 hours and then at 90°C for 12 hours, prepared the cell for use. After each run, the cell was cleaned by soaking in Methanol for an hour, and then boiled in double distilled water for 1 to 2 hours.

The cell was supported on the experimental plug by two thin brass pieces and a phosphor-bronze spring which also made electrical connections.

The water used was prepared by double distillation in a Pyrex still and was stored in Pyrex flasks sealed with Parafilm. The specific conductivity of the water was about $2(10)^{-6}$ mhos. A check of the pH of the water was maintained, measurements being made with a Beckman pH meter immediately preceding the filling of the cell. The pH was maintained at 6.3 ± 0.1, indicating a fairly constant CO_2 percentage in the water. Unfortunately, there did not seem to be any way of maintaining a really rigorous control of CO_2 pressure in this series of experiments.

The calcite was prepared from freshly cleaned and ground Iceland Spar, sieved through 100-mesh screen, with the fine dust left in to compensate for the fineness of the aragonite. The aragonite was prepared by slowly dropping 1N $CaCl_2$ into 1N Na_2CO_3 (both C.P. grade) at 100°C after the method of de Keyser and Dequeldre.[13] Analysis by X-ray spectrometer failed to show any trace of calcite in this preparation.

Analysis by X-ray spectrometer of the end products of several runs of both aragonite and calcite at various temperatures and pressures showed traces of vaterite. This was regarded as being only incidentally due to the pressure applied. Since these carbonates become more soluble at high pressures, when pressure is released they precipitate partially in metastable forms. For this reason measurements were made only after increases in pressure, minor fluctuations in the apparatus of course being tolerated.

Electrical measurements were made on a Brown Electro-Measurement Corporation Universal Impedance Bridge, Model 250-C, using a General Radio Corporation Null Detector, type 1231B, for the balance. The bridge was isolated from the 1000 cps generator by a General Radio Corporation Transformer, type 578-A. The absolute accuracy of the bridge readings was 0.5 per cent, however for these experiments the important accuracy of the bridge was that of duplication, namely 0.02 per cent. This figure was established by checking the bridge against a resistance box on several occasions. Capacitance was balanced out with a 500 $\mu\mu$F variable air condenser in shunt. No correction was made for this capacitance since against the important consideration was duplication.

Each run on one filling of the cell lasted from 2 to 4 days. In that time 3 or 4 points were set on an isothermal curve as a function of pressure. Time for equilibrium after a pressure change varied from 7 to 24 hours. In general the higher the pressure, the longer the time to reach equilibrium. Readings of the bridge were made as a function of time until a constant value of the resistance was obtained. No disturbance of the system by the readings was noticed. No signs were found during measurements of an actual transition proceeding.

Experimental Results

Runs were made at four temperatures, 29.0, 38.1, 52.6, and 77.1°C. Two runs were made with aragonite in the cell at 103°C and 2900 kg/cm^2, but no signs of reaching an equilibrium were observed in 26 hours on either and the runs were abandoned. It is not known whether this lack of equilibrium is to be attributed to the slowness of solution of the aragonite, to some other factor, or to the cell itself, which had not been seasoned to that temperature (see above).

The data were corrected for minor temperature deviations, plotted as the reciprocals of the measured resistance, fitted to smooth curves, and then the differences between the calcite curve and the aragonite curve for the same temperature were noted at several pressures. These differences are plotted as in Figure 2, and the intersection of the isothermal curve with

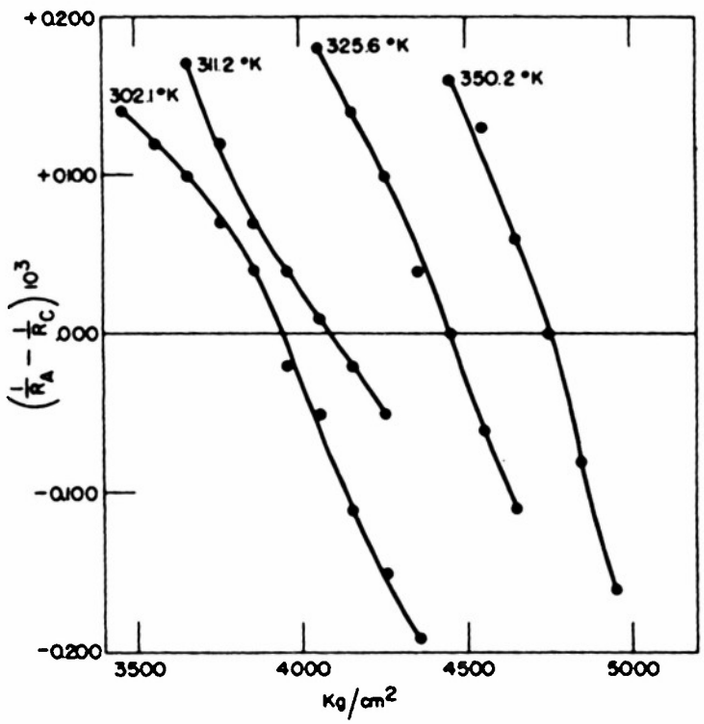

Figure 2. Difference plot to determine equilibrium pressures as a function of temperature.

the zero axis gives the equilibrium pressure. Table II gives the results of this plot. R_A is the resistance of the cell containing H_2O and aragonite, R_C that of H_2O and calcite.

In order to obtain other thermodynamic quantities, the data from Table II were fitted by the method of least squares to the following equation:

$$P = 17.548T - 1347 \qquad (P \text{ in kg/cm}^2,\ T \text{ in } ^\circ\text{K}) \qquad (4)$$

The fit is accurate to 2 per cent. In Table III and Table IV are collected the thermal data which may be derived from this equilibrium curve. ($\Delta X = X_c - X_a$) The Clapeyron Relation (5) was used to

TABLE II

Experimentally Determined Equilibrium Points for Calcite-Aragonite

T °K	P kg/cm^2
302.1	3940
311.2	4090
325.6	4450
350.1	4750

TABLE III

Derived Thermal Data along the Equilibrium Curve

T °K	$\Delta H(P,T)$ cal/mole	$\Delta S(P,T)$ cal/mole	ΔC_p cal/mole
302.1	+ 367	+ 1.21	- 0.13
311.2	377	1.21	- 0.13
325.6	392	1.20	- 0.17
350.2	417	1.19	- 0.19

TABLE IV

Derived Thermal Data at 1 kg/cm^2

T °K	$\Delta G(1,T)$ cal/mole	$\Delta G(1,O)$	$\Delta H(1,T)$ cal/mole
302.1	- 275	+ 24.2	+ 70
311.2	- 286	24.5	72
325.6	- 302	25.0	76
350.2	- 328	28.8	85

$$\frac{dP}{dT} = \frac{\Delta H}{T\,\Delta V} = \frac{\Delta S}{\Delta V} \qquad (5)$$

obtain $\Delta H(P,T)$ and $\Delta S(P,T)$. In Table IV, $\Delta G(1,T)$ was computed from (3) using the values for the thermal expansion and compressibility, referred to previously. These values for $\Delta G(1,T)$ together with Kobayashi's[2,3] values for $\Delta G(1,T) - \Delta G(1,O)$ give the next column $\Delta G(1,O)$. ΔC_p was obtained from (6) and finally $\Delta H(1,T)$ was derived from (7).

$$\Delta C_p(P,T) = \frac{d(\Delta H)}{dT} - \Delta S(P,T) \qquad (6)$$

$$\Delta H(P,T) - \Delta H(1,T) = - \Delta G(1,T) + T\Delta S(P,T) - T\Delta S(1,T) \qquad (7)$$

Discussion and Conclusions

For all practical purposes $\Delta G(1,O) = \Delta G(0,O)$. From Table IV, the average $\Delta \overline{G(0.O)} = \Delta G_o = + 25.6$ cal/mole, with an accuracy of $\pm$ 3 cal/mole. This value, together with Kobayashi's[2,3] free energy data, leads to a value of - 269.5 $\pm$ 3 cal/mole for $\Delta G(1,298.1)$. This value is in excellent agreement with Kelley and Anderson's[4] older value of $\Delta G(1,298.1) = 0.273$ cal/mole. It is in fair agreement with Kobayashi's[2,3] value of - 311 $\pm$ 23 cal/mole, the most recent determination by calorimetric means. Other older values of $\Delta G(1,298.1)$ are discussed by these authors. The only disagreement with Kobayashi's[2,3] value is in the determination of ΔG_o. Again in the case of $\Delta H(1,T)$, the only disagreement with Kobayashi's[2,3] value is in the determination of ΔG_o. The negative sign for ΔC_p signifies that the heat capacities of the two forms have interchanged in magnitude, since at room pressure, calcite has the higher heat capacity. The increase in $\Delta S(P,T)$ from $\Delta S(1,T)$, namely about 0.1 E.U., is of the right order of magnitude to satisfy Maxwell's Equation $\left(\frac{\partial S}{\partial P}\right)_T = - aV$, where a is the coefficient of thermal expansion.

Using the value $\Delta G_o = + 25.6$ cal/mole and Anderson's free energy data, we can extrapolate the measured curve of equilibrium as shown in Figure 3.

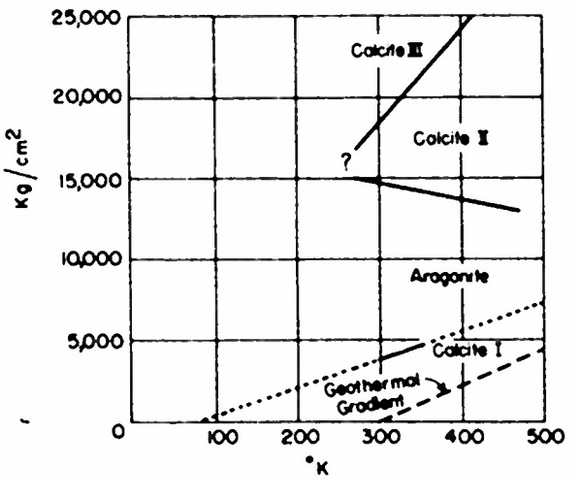

Figure 3. Phase diagram of $CaCO_3$.

The other phases of $CaCO_3$ in the diagram are the other two forms of calcite observed by Bridgman.[14] Also indicated is the geothermal gradient for this range. Preliminary investigations on aragonite with a shearing apparatus as described by Bridgman[15] gave inconclusive results over the range up to 30,000 kg/cm^2. The best that can be said is that there are possibly two transitions at 30°C, one at about 20,000 kg/cm^2, the other at 26,000 kg/cm^2. Further investigation with more sensitive apparatus is needed at this point. For this reason these data have not been included.

It will be noted from Figure 3 that the usually accepted values of the geothermal gradient (e.g., Yoder[16]) lie completely in the calcite$_I$ phase of $CaCO_3$ with the possible exception that if the temperature of disassociation is raised sufficiently high by pressure. calcite$_{II}$ or aragonite may become

stable. Thus probably, except for peculiar local conditions of high hydrostatic pressure and moderate temperatures, the only known form of $CaCO_3$ which is stable under natural geologic conditions is that of calcite. This fact has been widely accepted for many years, but this is the first time that a physico-chemical proof has been offered. In order to explain the occurrence of aragonite, both organic and inorganic, the conditions for metastable precipitation must be considered rather than those of equilibrium. Backström's[17] hypothesis that aragonite has a low temperature stability field seems to be verified since the extrapolated curve intersects the $P = 0$ axis at about $75^{\circ}K$. The actual stability field (if any) of vaterite, the third atmospheric pressure form of $CaCO_3$, is still undetermined.

The experimental method of determining $\Delta G(1,298.1)$ seems to have certain advantages. Since the measurement of the conductivity of a solution can be considerably refined, the value of this standard free energy change for polymorphic forms may be obtained quite precisely as compared to that obtained by calorimetric methods. The value for $\Delta G(1,298.1)$ is less dependent on pressure errors than on heat measurements, while the values for compressibility and thermal expansion can be made very precise. The main uncertainty lies in the frequent lack of determination of compressibility and thermal expansion, and in the case of most minerals the variation in reported densities creates a major difficulty. Of course, the method is not suited for any transitions which are at all rapid. These are capable of being directly determined.

The use of a cell constructed from Teflon for conductivity work seems quite feasible, at least for moderate temperatures. The temperature limits of this type of cell have not as yet been explored. The work of calibrating the cell to determine conductivities and solubilities at high pressure is at present in progress. The intention is to explore the possibilities of obtaining the solubilities of silicates at high pressures. There is data in existence at present from Zisman[18] by which the cell could be calibrated, but it has been decided that an independent check would be desirable.

Acknowledgments

The author wishes to express his thanks to Dr. H. Ramberg, Dr. A. W. Lawson, and Dr. J. R. Goldsmith for their encouragement, suggestive questions, and constructive criticism throughout the course of this research. Dr. N. H. Nachtrieb and Dr. A. H. Smith made many helpful suggestions. Mr. N. D. Nachtrieb constructed the cell and did much other machine work. Thanks are due to the Geology Department for its grant of an R. D. Salisbury Memorial Fellowship for the course of this work, and to the staff of the Institute for the Study of Metals, where the work was performed, for the interest they have shown.

This work was supported in part by funds from the Office of Naval Research.

References

1. C. T. Anderson, J. Am. Chem. Soc. 56, 340 (1934).
2. K. Kobayashi, Sci. Rept. Ser. I, Tôhoku Univ. 35, 103 (1951).
3. K. Kobayashi, Sci. Rept. Ser. I, Tôhoku Univ. 35, 111 (1951).
4. K. K. Kelley and C. T. Anderson, U. S. Bur. Mines, Bull. 384 (1935).

5. F. Birch, J. F. Schairer, and H. C. Spicer, Geol. Soc. Am., Special Paper 36 (1942).
6. P. W. Bridgman, Am. J. Sci. Ser. 5, 10, 483 (1925).
7. E. Madelung and R. Fuchs, Ann. Phys. 65, 289 (1921).
8. W. Voight, Lehrbuch der Kristallphysik, Teubner, Berlin, 1928.
9. S. Kozu and K. Kani, Proc. Imp. Acad. Japan 10, 222 (1934).
10. S. Kozu, M. Masuda, and J. Veda, Sci. Rept. Ser. III, Tohoku Univ. 3, 247 (1929).
11. C. Palache, H. Berman, and C. Frondel, Dana's System of Mineralogy, Vol. 2, 7th ed., New York, John Wiley & Sons (1951).
12. S. W. Kurnick, J. Chem. Phys. 20, 218 (1952).
13. W. L. de Keyser and L. Dequeldre, Bull. Soc. Chim. Belg. 59, 40 (1950).
14. P. W. Bridgman, Am. J. Sci., Ser. 5, 237, 7 (1939).
15. P. W. Bridgman, Phys. Rev. 48, 825 (1935).
16. H. S. Yoder, Jr., Trans. Am. Geophys. Union 31, 827 (1950).
17. H. L. J. Backström, Z. physik. Chem. 97, 179 (1921).
18. W. A. Zisman, Phys. Rev. 39, 151 (1932).

VIII

THE PLASTIC DEFORMATION OF IRON BETWEEN 300 - 77.2°K

Donald F. Gibbons*
Submitted to Trans. A. I. M. E.

Introduction

This investigation was undertaken in order to gain further information on the mechanism of plastic deformation of iron, at temperatures between room temperature and 77.2°K, and also contribute to our understanding of the low temperature brittleness phenomenon which occurs in both the tensile test and impact test. It was decided to study as pure an iron as possible and to use the tensile test in order to simplify the problem as much as possible.

Materials and Treatment

Two series of iron were used throughout the investigation. First, that obtained from the National Research Corporation, supplied as gas free, high purity iron, hereafter referred to as iron A. Second, iron obtained from Dr. J. D. Fast[1] and produced by melting iron under purified hydrogen, hereafter referred to as iron B. Typical analyses of samples of both irons, after fabrication are given in Table I.

TABLE I

Analysis, Wt. %

	Al	Cu	Mg	Ni	Si	Ag	Mn	Co	Be	C	N	O
Iron A	.001	.001	--	.05+	.008	--	.001	--	--	.005	.0005*	.021*
Iron B	.005	.0008	.0005	.002	.005	ND	ND	ND	ND	.002	.0005*	.0034*

\+ wet analysis
* vacuum fusion analysis
All other determinations spectrographic

The main difference in composition of these irons is in their nickel and oxygen contents. Nickel has a very large solid solubility in iron. However, oxygen has an extremely small solid solubility. An attempt was made to reduce the oxygen content still further by remelting under purified hydrogen. This was successful in reducing the oxygen content to $\sim$ .0006%. However, no results on tests of this iron are included, since difficulty was encountered in fabricating the ingot.

Wire specimens 1 mm dia. were used for the investigation. The wires

* Now at Royal Military College, Kingston, Ont., Can.

were produced from the ingots, as supplied, by cold rolling and swaging, with intermediate vacuum anneals at 700°C. Care was taken to reduce preferred orientation in the wires to a minimum by keeping a % reduction in area between anneals of 30 - 40%. X-ray transmission photographs showed no indication of preferred orientation. The final grain size of iron A was 20-24 grains/linear mm and of iron B 16-18 grains/linear mm.

All specimens were tested in the decarburized and denitrided condition unless otherwise stated. The procedure was to pass hydrogen, saturated with water vapour at 26°C, over the specimens at 730°C for 2 hours. The specimens were quenched in iced water and then annealed in a vacuum of $\sim 5 \times 10^{-6}$ mm Hg for 1 day at 560°C to remove hydrogen. Higher temperatures were used for the vacuum anneal but this temperature was found to be quite satisfactory in removing hydrogen. The specimens were slow cooled after the vacuum anneal. Where it is stated that the specimens were carburized, the specimens were given an identical decarburizing treatment and then carburized by passing hydrogen, saturated with pure n-heptane vapour at 0°C, over the specimens at 730°C. The specimens were then homogenized at 730°C for 2 hrs in dry hydrogen. After the carburizing treatment the specimens were given the same vacuum anneal as for the decarburized specimens. The carbon content was determined from the maximum value of the internal friction carbon peak.[2]

Apparatus

Figure 1 shows a diagram of the tensile apparatus, with half the cooling coil removed. The cooling coil enabled temperatures from 200 - 77.2°K to be obtained. The apparatus was designed to fit onto a standard Tinius Olsen Universal tensile machine.

The apparatus consisted of the rigid plate A which carried two carefully machined hooks H. These hooks attached the plate firmly to the moving crosshead of the tensile machine. The lower grip B was rigidly suspended from the plate A by three stainless steel rods. The upper grip C was joined to the upper grip of the tensile machine by the stainless steel rod E. The lower part of the apparatus was surrounded by a dewar vessel, which was made a sliding fit inside the brass collar D. The specimen was held in a clamp which fitted into the grip, forming a ball and socket joint (see inset (a)). This was to attain as near pure tension in the specimen as possible. The stress was applied to the specimen by lowering the crosshead, and so the lower grip B, at a constant speed of .05"/min.

The temperature of the specimen was

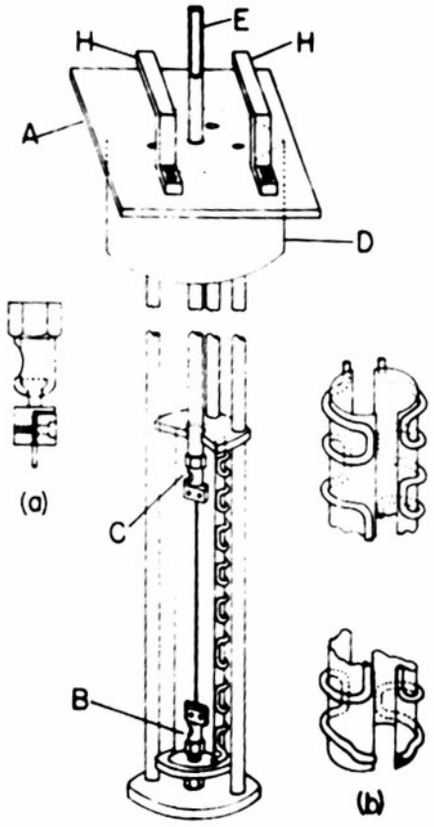

Figure 1. Arrangement of the tensile apparatus and cooling coil for the low temperature tests.

controlled by the coil assembly shown in inset (b). This was a split brass cylinder onto which 1/8" I.D. copper tube was soldered as shown. Cold evaporated nitrogen gas was passed through the assembly by immersing one end of the tube (this section of the tube was lagged) in liquid nitrogen. The other end of the coil was joined to the laboratory vacuum line via a Hooke valve. By setting this valve, the rate of gas flow and therefore the temperature could be controlled manually to within $\pm$ 1/2°K with ease.

The temperature gradient along the specimen was checked by placing a dummy specimen in position which had copper-constantan thermocouples soldered to it at 1" intervals. The gradient along the specimen was found to be 3°K with a maximum deviation from the mean of 1.75°K. This was regarded as being satisfactory for this investigation.

Experimental Results

Ductility

As the testing temperature of iron A specimens was decreased, the ductility, as measured by the % reduction in area of fracture, remained nearly constant, until between 127 and 119°K it suddenly dropped to zero. Curve A, Figure 2 shows the plot of % reduction of area versus testing temperature in this temperature range. Direct observation of the fractured surface

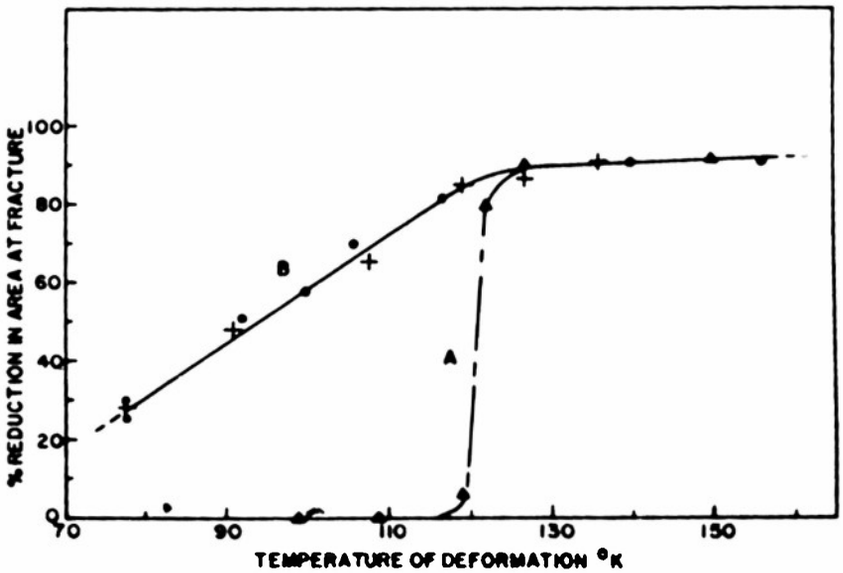

Figure 2. Variation of % reduction in area at fracture with temperature of test. Curve A - for specimens of Iron A. Curve B - for specimens of Iron B.

on a specimen deformed below 124°K showed apparently wholly cleavage type of fracture. However, if a longitudinal section was taken through the fracture, grain boundary failure as well as the cleavage failure could be seen. Figure 3 (a) shows the region adjoining a fractured surface in which fracture also started, it can be seen to follow the grain boundary. Figure 3 (b) shows a section through a fracture, which was nickel plated before sectioning, the intercrystalline as well as cleavage nature of the fracture

(a)

(b)

Figure 3. (a) Area near fracture in specimen of Iron A tested at 105°K. (b) Section through fracture in specimen of Iron A tested at 109°K.

can be seen clearly. This sudden onset of brittleness also occurred of the specimens were quenched from 700°C after the vacuum anneal instead of being slow cooled.

As the testing temperature of iron B specimens was decreased there

was no sudden loss in ductility corresponding to that in specimens of iron A. However, at approximately the same temperature the ductility started to decrease steadily. Curve B, Figure 2 shows a plot of % reduction in area versus temperature of deformation for iron B.

Neumann Lamellae. Below 125°K the stress-strain curve became serrated and the deformation during this serrated region was accompanied by a series of characteristic "sharp" sounds, similar to a sharp rifle "crack." Figure 4 curves (a), (b), and (c) show typical stress-strain curves in this

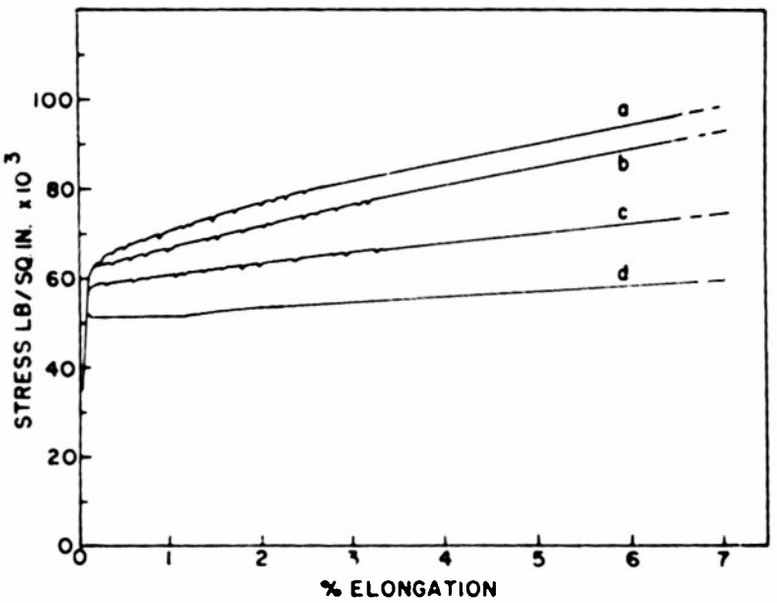

Figure 4. Stress-strain curves for specimens of Iron B tested at (a) 77.2°K, (b) 96.5°K, (c) 124°K, (d) 150°K.

temperature region. Metallographic examination of specimens after deformation revealed that below 125°K, decreasing the temperature of deformation increased the number of Neumann lamellae. The end of the serrated region of the stress-strain curve was found to coincide with the cessation of the characteristic sound of deformation and there was no discernable increase in the number of Neumann lamellae present in the specimen after the end of the serrated region of the stress-strain curve.

The rate of work hardening of a specimen was affected quite markedly by the temperature of deformation below 125°K. Figure 4 (a), (b), and (c) showed stress-strain curves for specimens deformed at 77.2°K, 96.5°K, and 124°K respectively. It can be seen that the lower the deformation temperature, and so the greater the amount of deformation occurring by the formation of Neumann lamellae, the greater is the rate of work hardening. It can also be seen from these curves that there is a change in the rate of work hardening coincident with the end of the serrated region. This change is more marked the lower the deformation temperature.

Figure 5 shows a plot of yield stress, as defined by a 0.1% proof stress, versus temperature of deformation. The curve shows a definite approach to a constant value of the yield stress below 120°K.

If iron A was carburized to a value as little as .004%C, it no longer

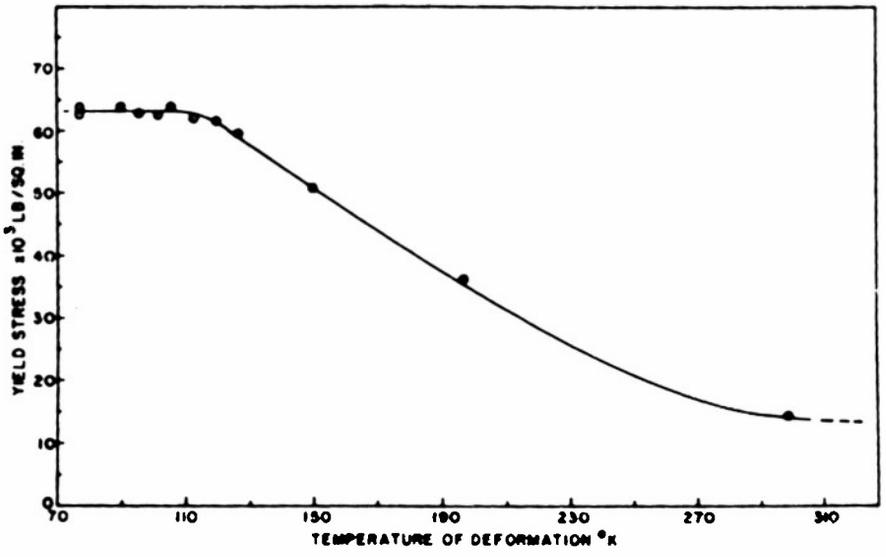

Figure 5. Variation of yield stress with temperature of deformation.

exhibited the sudden loss of ductility at 125°K. The curve of % reduction in area versus temperature of deformation followed that for iron B (curve B, Figure 2). The curve for lower yield stress versus temperature of deformation was of the same form as for iron B. However, the curve was displaced along the stress axis towards higher stress due to the carbon content. The removal of the sudden loss in ductility by carburizing occurred whether the carbon was retained in solid solution by quenching from 730°C, or precipitated as carbide, as determined by the disappearance of the carbon internal friction peak.

Lüders Bands. After complete decarburization a small yield point and yield point elongation could still be observed in specimens of both iron A and B tested at temperatures above 125°K. However, the yield point elongation was small, only ~1%, as compared with the carburized specimens which had a yield point elongation of 7-8% in this temperature range. This small yield point is attributed to oxygen in solid solution and confirms the observations of Boulanger.[3] Boulanger has since shown the existence of an internal friction peak in iron due to oxygen (private communication) which would also indicate that this yield point is due to oxygen in solid solution. No Lüders bands were detected in these specimens.

In specimens of iron A carburized to .006%C, the Lüders bands were very pronounced. Examination of specimens deformed above 125°K showed that a Lüders band was always initiated at each grip, the boundary between the deformed and undeformed regions being propagated towards the centre of the specimen. However, during deformation below 125°K (the temperature for the onset of Neumann lamellae formation) the number of Lüders bands formed increased. Many Lüders bands were formed along the length of the specimen, in addition to those initiating at each grip. The stress-strain curve during the yield point elongation was also serrated, as was the case in the initial part of the stress-strain curves of iron B tested in this temperature range.

All the Neumann lamellae were found to be produced during the yield point elongation; there was no change in the number of Neumann lamellae present in specimens whose deformation was stopped at the end of the yield point elongation and those which were deformed until fracture occurred. Secondary evidence to support this conclusion is that the characteristic sound accompanying Neumann lamellae formation also ceased at the end of the yield point elongation.

Below 125°K the magnitude of the yield point elongation of carburized wires was found to decrease with decreasing temperature of deformation. The % yield point elongation versus temperature of deformation is shown in Figure 6. The form of this curve is similar to that of Figure 2 (curve B)

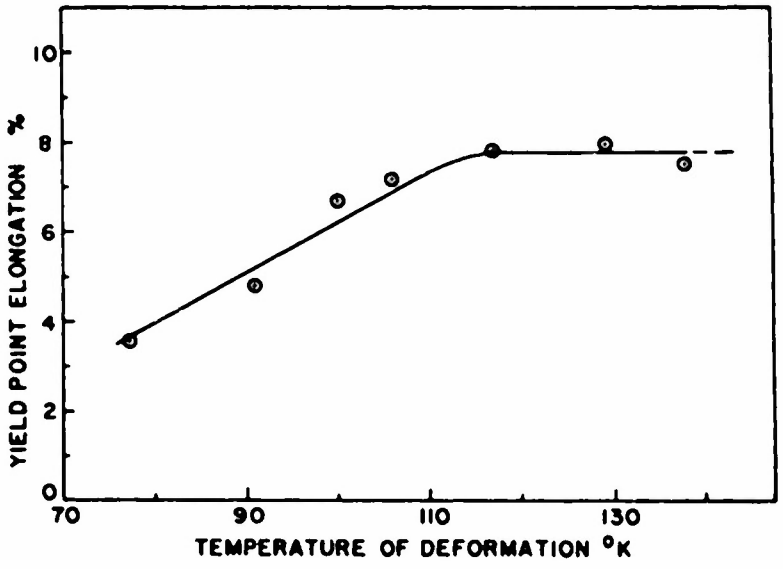

Figure 6. Variation of % yield point elongation with temperature of deformation for carburized specimens of Iron A.

where the % reduction in area versus temperature of deformation is plotted.

The yield point and yield point elongation occurring in decarburized specimens of iron B when tested above 125°K was completely removed when the specimens were tested below this temperature. This is illustrated by the stress-strain curves of Figure 4.

Deformation of Single Crystals. A number of single crystals, 3-4 cm long, were grown in specimens of iron A by the strain anneal method. The specimens tested, therefore, consisted of a number of single crystals in a "bamboo" type structure. In some cases the single crystals were separated by a large grained polycrystalline region approximately 1/2 cm in length.

After a standard decarburizing treatment the single crystals were found to be quite ductile down to 77.2°K and the stress-strain curve showed no evidence of a yield point. The fracture was a typical, single crystal wedge type fracture, the reduction in area at the fracture being $\sim$ 95%. The stress-strain curve was serrated and the characteristic sound was emitted during the early stages of the deformation, as was the case in the polycrystalline specimens of iron B. Figure 7 is a longitudinal section

through a single crystal after deformation showing the Neumann lamellae.

Crystallographic Relations of the Neumann Lamellae. The orientation and crystallographic relationship of Neumann lamellae has been studied in Silicon ferrite by Harnecker and Rassow[4] and Mathewson and Edmunds[5] by microscopic and X-ray reflection methods respectively. However, it was felt that their evidence was inconclusive.

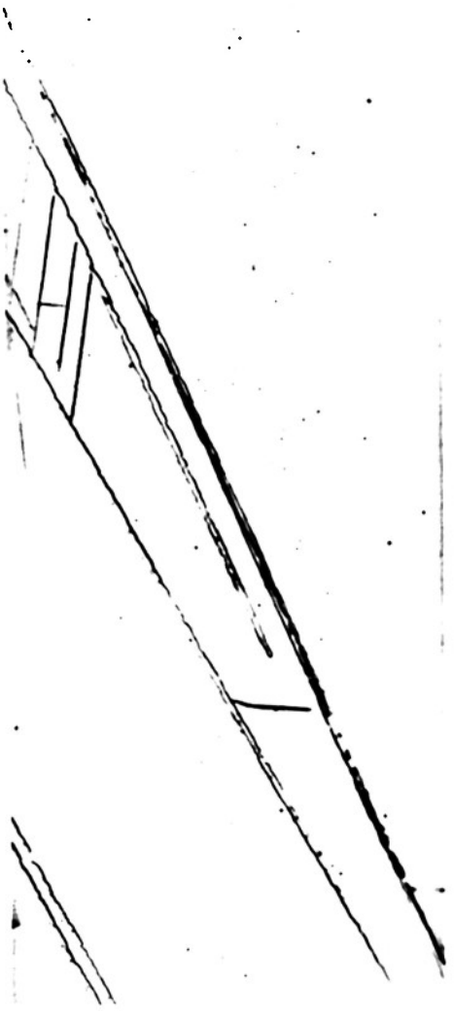

Figure 7. Photomicrograph of Neumann lamellae in single crystal of Iron A tested at 77.2°K.

The crystallographic plane and direction of glide of the lamellae was determined from the single crystal wires. The orientation of the crystal was determined before deformation from a Laue back reflection pattern. After deformation the pole of the Neumann lamellae was determined on an optical goniometer. On plotting the results stereographically the plane was found to coincide with the (112) plane of the crystal within $\pm$ 1/2° in the six determinations that were made. From the same crystals the glide direction was also determined from the optical goniometer and it coincided with the $\langle 111 \rangle \pm 4°$. It was much more difficult to determine the direction precisely on the goniometer and therefore the accuracy of the glide direction measurements is less than that in the determination of the plane. The glide plane and direction are therefore those which can result in either glide or twinning.

In order to determine if the lamellae were twins a back reflection Laue photograph was taken of a grain containing the lamellae. It was found impossible, however, to identify any spots positively as being from a twin orientation. It was decided, therefore, to measure the shear which occurs in a lamella in order to differentiate between the two mechanisms. The technique used was very similar to that used by Bowles[6] to determine the crystallographic relationships of Martensite.

A flat sheet tensile specimen was machined from a rolled sheet of iron B. After decarburization of the specimen both surfaces were polished electrolytically and the specimen then vacuum annealed. The orientation of 2 crystals was determined by X-rays and the specimen deformed approximately 1/2% at 114°K. The angle with which the lamellae intersect the polished reference surface was then determined by an optical goniometer. Very sharp reflections were obtained from the lamellae, which showed little or no angular spread. From this angle and the orientation of the crystal relative to the polished reference surface, the

angle of shear can be calculated by simple geometry. The angle of shear can also be calculated from twinning theory and so the theoretical and experimental angles can be compared.

The angle predicted by theory is 35° 16' and the angles determined in these two crystals were 38° and 34°. It can be seen that these agree with the predicted value within ± 3°, which is considered the accuracy of the experimental procedure. It is considered, therefore, that the Neumann lamellae are in fact deformation twins.

Effect of Prior Deformation at Room Temperature. A specimen of iron B was elongated by 4% at 300°K and then tested immediately at 109°K. The stress-strain curve was quite smooth with no serrations and the noise during deformation was absent. A micrograph of such a specimen showed complete absence of Neumann lamellae. This phenomenon has been previously observed by Pfeil.[7] After annealing such a specimen for several days at room temperature, no Neumann lamellae were produced on deformation below 125°K. However, if the specimen was annealed at 100°C for 14 hours, after 4% elongation at 300°K, and then tested below 125°K the Neumann lamellae formation partially returned. The serrations on the stress-strain curve and noise during deformation also returned.

A specimen of iron A was deformed at 300°K prior to testing at 109°K and the specimen exhibited some ductility, ~45%, as measured by the % reduction in area at the fracture. As in the case of iron B there was no evidence of Neumann lamellae formation.

Discussion

In Iron A, which exhibits the sudden onset of brittleness, fracture occurs by rupture, at least in part, along the grain boundaries. It has also been shown that a single crystal is completely ductile. It is evident, therefore, that the brittleness is intimately associated with the grain boundaries. As the two series of iron used only differ in their oxygen content, it seems justifiable to correlate the removal of this low temperature brittleness, in iron B, with the decrease in oxygen content. This agrees with the recent work of Rees and Hopkins[8] who found that intercrystalline failure started to occur if the oxygen concentration was greater than ~.003%. This leads us to the conclusion that the oxygen must be associated with the grain boundaries. One question to be decided, therefore, is whether the oxygen at the grain boundary is in solid solution or present as a second phase.

The most recent value for the solid solubility of oxygen in α iron at 700°C is given as ~ 0.01% by Ziegler.[9] This value may be expected to be an over estimate, however, because it was near the limit of accuracy of his experimental procedure. This value for the oxygen solubility indicates that the oxygen concentration in iron B is below and that in iron A above the solubility limit. Oxygen may be expected to be present at the grain boundary as an oxide phase, therefore, in iron A.

Examination of metallographic specimens by the light or electron microscope showed no evidence of the existence of a second phase at the grain boundary. This, however, cannot be regarded as positive evidence that it was not present. An examination under the microscope of the fractured surfaces with polarized light, showed regions, on exposed grain boundaries, which exhibited bi-refringence. These regions showed extinction at 90°

intervals, which would correspond to Fe_2O_3.[10] However, since it was impossible to view a relatively large flat field, this extinction could have been spurious and due to geometric factors.

Positive evidence of a difference in the grain boundary behaviour between the two irons was, however, given by internal friction measurements. The internal friction of the wires was determined using the torsion pendulum developed by Ke.[11] Curve (A), Figure 8 shows the grain boundary peak

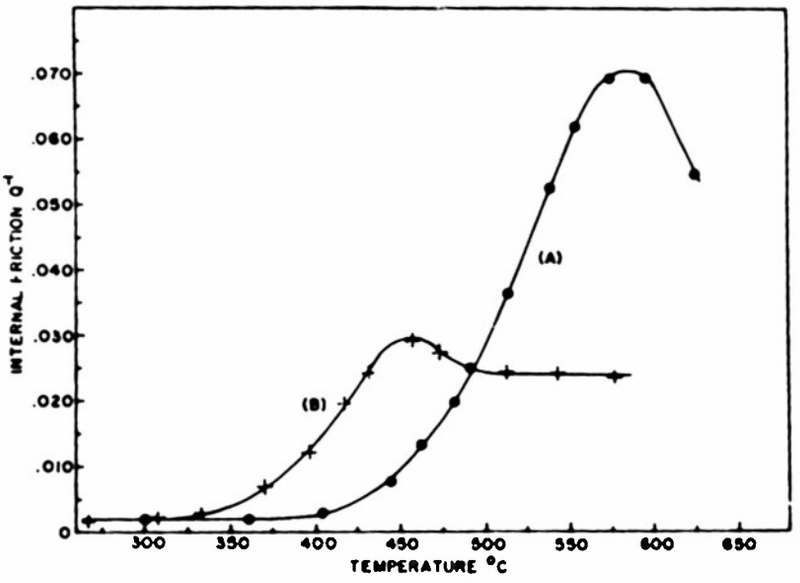

Figure 8. Variation of internal friction with temperature. Curve A - for specimen of Iron A. Curve B - for specimen of Iron B.

for a specimen of iron A which had been quenched from the decarburizing treatment. Curve (B), Figure 8 shows the peak obtained for iron B after an identical treatment. The temperature at which the maximum of the peak occurs has been shifted from 580°C in iron A to 460°C in iron B, and the magnitude of the peak lowered in the case of iron B. Due to the difference in grain size of the two irons, a small difference in the temperature at which the maximum of the peak occurs would be expected.[12] However, this change should only be $\sim$ 20-30°C and in the opposite direction to that in which it occurred.

The shift in the temperature at which the peak maximum occurs means that the time of relaxation for a shear stress across the grain boundary has been markedly altered. We have no means of calculating whether the shear stress relaxation time for an oxide-iron interface would be greater or less than that for an iron – iron interface; therefore, no quantitative deductions can be made from these internal friction measurements.

If the oxygen is present as an oxide at the grain boundary, there is no reason why the oxide alone should be responsible for the brittleness, because at temperatures down to 125°K the grain boundary has deformed "normally." The sudden onset of brittleness is, however, coincident with the beginning of deformation by twinning. It is suggested, therefore, that the

combination of an oxide at the grain boundary and deformation by twinning may be necessary for the brittleness. A possible reason for this may be the rapid rate of formation of the twins, which would involve a rapid rate of deformation at the oxide-iron interface and so permit the formation of "microcracks." Whereas, when deformation occurs by glide there may be sufficient time for the stresses at the interface to be accommodated in the iron matrix. There is some indication that this may be the case, since when twin formation is suppressed by prior deformation at room temperature, specimens of iron A do exhibit some ductility below 120°K.

The mechanism by which carburizing iron A removes the brittleness is uncertain. If an oxide is either directly or indirectly the cause of brittleness, there would have to be a solid state reaction between carbon and oxygen at the grain boundary at 730°, the carburizing temperature. Whatever the mechanism, however, it must be reversible, since decarburizing the specimen makes it brittle again.

It has been suggested[13,14] that, because of the similarity between the atom movements in slip and twinning, it is logical to expect twinning during deformation occurs by a dislocation mechanism also, for the same reasons that they were proposed for slip. Cottrell and Bilby[15] have postulated a dislocation mechanism for the growth of twins during deformation which involves the dissociation of a unit dislocation into two partial dislocations. This mechanism predicts that there should be a constant stress for the onset of twinning, being that stress required to form the initial interface. This has been shown to be the case, see Figure 5, which shows that below the temperature at which twinning starts the yield stress becomes constant. In the case of one single crystal it was possible to calculate the lower resolved critical shear stress for twinning, which was 37×10^3 lb/in^2.

The mechanism of Cottrell and Bilby also shows that twins could form in the order of microseconds, which has been shown to be the case experimentally for tin.[16] The serrations on the stress strain curve and the "sound" during deformation are considered to be caused by bursts of twins forming rapidly within the specimen.

The dislocation mechanism also gives an explanation for prior deformation at room temperature suppressing the formation of twins. During plastic deformation at room temperature many dislocation lines will intersect each other, forming "jogs" in the dislocation line.[17] Also, as is evident from the wavy nature of visible slip lines, dislocations move out of one glide plane into a neighbouring plane. Both of these factors inhibit the dissociation of a unit dislocation into partial dislocations. Therefore, the formation of twins, which requires this dissociation into partial dislocations, would be stopped. Annealing for 14 hours at 100°C would allow some recovery to occur and so permit the dislocations to dissociate once more. Since an anneal at 100°C for 14 hours only allows a partial return of twin formation it indicates that the activation energy for the process is much greater than would be expected by an interstitial atom diffusion, such as carbon.

Summary

A study was made of the tensile deformation, between 300°K and 77.2°K, of two samples of iron, containing .0034% and .021% oxygen respectively.

Iron containing .021% oxygen becomes completely brittle below 120°K, the fracture being a combined intercrystalline and cleavage type. Ductility

can be restored by carburizing to .006% carbon.

Iron containing .0034% oxygen remained ductile down to 77.2°K; however, the ductility slowly decreases between 125°K and 77.2°K. At 125°K deformation starts to occur by the formation of Neumann lamellae, the number of lamellae produced increases with decreasing temperature.

Single crystals of iron containing .021% oxygen are completely ductile down to 77.2°K.

Internal friction measurements on the grain boundary peak indicate a marked difference between iron containing .021% oxygen and that containing .0034% oxygen.

Deformation at 300°K prior to deformation below 125°K suppresses the formation of Neumann lamellae and restores ductility to iron containing .021% oxygen.

The Neumann lamellae produced by deformation below 125°K are shown to be deformation twins.

It is considered that the brittle failure of iron containing .021% oxygen is caused by a combination of the grain boundary oxide phase and deformation by twinning. The removal of twin formation by prior deformation can be explained by considering Cottrell and Bilby's mechanism for growth of deformation twins.

Acknowledgments

The author wishes to than Mr. K. K. Ikeuye for preparing the photomicrographs, Mr. E. D. Selmanoff for preparing the wire specimens, and Mr. A. Moskowitz for the vacuum analyses.

References

1. J. D. Fast, Philips Res. Rep. (1949), 4, 370.
2. L. J. Dijkstra, Philips Res. Rep. (1947), 2, 357.
3. C. Boulanger, Revue de Metallurgie (1950), 47, 547.
4. K. Harnecker and E. Rassow, Z. Metallkunde (1924), 16, 312.
5. C. H. Mathewson and G. H. Edmunds, Trans. A.I.M.M.E. (1928), 80, 311.
6. J. S. Bowles, Acta Crystallographica (1951), 4, 162.
7. L. B. Pfeil, J. Iron and Steel Inst. (1926), 15, 319.
8. W. P. Rees and B. E. Hopkins, J.I.S.I. (1952), 172, 403.
9. N. A. Ziegler, Trans. A. Soc. Steel Treatment (1932), 20, 73.
10. A.S.M. Metals Hand Book (1948), 449.
11. T. S. Kê, Phys. Rev. (1947), 71, 533.
12. T. S. Kê, Phys. Rev. (1947), 72, 41.
13. J. Frenkel and T. Kontorova, J. Phys. Chem. (1939), 1, 137.
14. F. Seitz and T. A. Read, J.A.P. (1941), 12, 470.
15. A. H. Cottrell and B. A. Bilby, Phil. Mag. (1951), 42, 573.
16. W. P. Mason, H. J. McSkimin and W. Shockley, Phys. Rev. (1948), 73, 1213.
17. F. Seitz, Advances in Physics, Quarterly Supp. Phil. Mag. (1952), Vol. 1, No. 1.